

Conformal invariance of double random currents and the XOR-Ising model I: identification of the limit

Hugo Duminil-Copin^{*†} Marcin Lis[‡] Wei Qian[§]

July 29, 2021

Abstract

This is the first of two papers devoted to the proof of conformal invariance of the critical double random current and the XOR-Ising models on the square lattice. More precisely, we show the convergence of loop ensembles obtained by taking the cluster boundaries in the sum of two independent currents with free and wired boundary conditions, and in the XOR-Ising models with free and plus/plus boundary conditions. Therefore we establish Wilson’s conjecture on the XOR-Ising model [81]. The strategy, which to the best of our knowledge is different from previous proofs of conformal invariance, is based on the characterization of the scaling limit of these loop ensembles as certain local sets of the Gaussian Free Field. In this paper, we identify uniquely the possible subsequential limits of the loop ensembles. Combined with [28], this completes the proof of conformal invariance.

1 Introduction

1.1 Motivation and overview

The rigorous understanding of Conformal Field Theory (CFT) and Conformally Invariant random objects via the developments of the Schramm-Loewner Evolution (SLE) and its relations to the Gaussian Free Field (GFF) has progressed greatly in the last twenty-five years. It is fair to say that once a discrete lattice model is proved to be conformally invariant in the scaling limit, most of what mathematical physicists are interested in can be exactly computed using the powerful tools in the continuum.

A large class of discrete lattice models are conjectured to have interfaces that converge in the scaling limit to SLE_κ type curves for $\kappa \in (0, 8]$. Unfortunately, such convergence results are only proved for a handful of models, including the loop-erased random walk [68] and the uniform spanning tree [49] (corresponding to $\kappa = 2$ and 8), the Ising model [19] and its FK representation [77] (corresponding to $\kappa = 3$ and $16/3$), Bernoulli site percolation on the triangular lattice [76] (corresponding to $\kappa = 6$). Known proofs involve a combination of

^{*}Institut des Hautes Études Scientifiques

[†]Université de Genève

[‡]Universität Wien

[§]CNRS and Laboratoire de Mathématiques d’Orsay, Université Paris-Saclay

exact integrability¹ enabling the computation of certain discrete observables, and of discrete complex analysis to imply the convergence in the scaling limit to holomorphic/harmonic functions satisfying certain boundary value problems that are naturally conformally covariant.

To upgrade the result from conformal covariance of these “witness” observables to the convergence of interfaces in the system, one needs an additional ingredient. In some cases, when properties of the discrete models are sufficiently nice (typically tightness of the family of interfaces, mixing type properties, etc), a clever martingale argument introduced by Oded Schramm enables to prove convergence of interfaces to SLEs and CLEs. This last step involves the *spatial Markov properties* of the discrete model in a crucial fashion. We refer to the proofs of conformal invariance of interfaces in Bernoulli site percolation, the Ising model, the FK Ising model, or the harmonic explorer for examples. Unfortunately, the discrete properties of the model are sometimes not sufficiently nice to implement this martingale argument and there are still many remaining examples for which the scaling limit of the interfaces cannot be easily deduced from the conformal invariance of certain observables – most notably for the case of the double dimer model, for which an important breakthrough was performed by Kenyon in [46], followed by a series of impressive papers [9, 23].

In [81], Wilson discussed conjectures concerning the critical XOR-Ising model obtained by taking the product of two independent Ising models (see below for a formal definition). While he did not provide any proof of conformal invariance in his paper, Wilson performed advanced numerics and made a number of predictions for the behaviour of the interfaces in the model. We point out that unlike the aforementioned models, the XOR-Ising model does *not* satisfy any obvious spatial Markov property at the discrete level, thus making the classical martingale argument unlikely to offer a convenient road to prove conformal invariance. This makes it even more remarkable that its scaling limit does satisfy the spatial Markov property (see the end of Section 1.2 for a more detailed discussion). In this paper, we prove convergence of the critical XOR-Ising interfaces on the square lattice in the scaling limit to SLE_4 type curves. In the process of proving conformal invariance of XOR interfaces, we also obtain similar results for the double random current model. The double random current model also lacks spatial Markov property in the discrete (at the outer boundaries of the clusters: see end of Section 1.3 for a more detailed discussion).

Convergence to SLE_4 type curves were previously proved for the harmonic explorer [72], contour lines of the discrete GFF [69], and cluster boundaries of a random walk loop-soup with the critical intensity [12, 54]. Nevertheless, all these models are discrete approximations of objects defined in the continuum which are already known to be SLE_4 type curves. In this respect, the XOR-Ising and the double random current models are the first discrete lattice models not having any a priori connection to SLE_4 whose interfaces are proved to converge to SLE_4 type curves.

As mentioned above, our proof does not follow the martingale strategy. Instead, it relies on a coupling between the XOR Ising model and a naturally associated height function and can be decomposed into three main steps (see the next sections for more details):

- (i) Proving the joint tightness of the family of critical XOR interfaces and the height function, as well as certain properties of the joint coupling.
- (ii) Proving convergence of the height function to the GFF.

¹Only approximately for site percolation on the triangular lattice.

- (iii) In the continuum, identifying the scaling limit of XOR interfaces using properties of the GFF.

Each of the three previous steps involves quite different branches of probability. The first one extensively uses percolation-type arguments for dependent percolation models. The second one concerns a height function studied already by Dubédat [22], and Boutilier and de Tilière [11]. However, unlike in [11, 22], it harvests a link between a percolation model (the double random current) and dimers. Moreover, it uses techniques introduced by Kenyon to prove convergence of the dimer height function, but with a new twist as the proof relies heavily on fermionic observables introduced by Chelkak and Smirnov to prove conformal invariance of the Ising model, as well as a delicate result on the double random current model (see below) helping identifying the boundary conditions. Finally, the last step relies on a deep understanding of the so-called local sets of the GFF introduced by Schramm and Sheffield [70], and follows a rather intricate strategy. It makes use of the two-valued sets introduced by Aru, Sepúlveda and Werner [8], and further establishes new results on local sets including a characterization of local sets with three values. A primary difficulty of this step is to find the right strategy, in particular to single out a set of properties satisfied by every subsequential limit of the discrete model which are both obtainable using techniques in the discrete and also sufficient for proving the final results using techniques in the continuum. Interestingly, some properties which seem inaccessible using discrete techniques can be cleanly established using arguments from the continuum.

Part (i) of the proof is postponed to the second paper [28]. In this paper, we focus on (ii) and (iii).

Let us finish this motivational part by mentioning that our proof is made possible by the introduction of a new coupling between the XOR-Ising model and the double random current model. We therefore also obtain conformal invariance results for this model.

The random current model has proved to be a very powerful tool to understand the Ising model. Its applications range from correlation inequalities [36], exponential decay in the off-critical regime [2, 29, 33], classification of Gibbs states [65], continuity of the phase transition [5], etc. Even in two dimensions, where a number of other tools are available, new developments have been made possible via the use of this representation [6, 27, 55]. For a more exhaustive account of random currents, we refer the reader to [26].

We note that the coupling with the double random current extends to the family of Ashkin-Teller models [51], and it is likely that our argument may generalize to other models as well. More generally, we believe that invoking the connections between discrete height function and loop-ensemble types models is a very promising tool to obtain conformal invariance of other planar models at criticality.

In the remainder of this introduction, we will state our main results on the convergence of the models. For simplicity, we first present results on each model individually, and not on the related height function. In Section 2, we will describe our proof road-map and reveal the role of the height function. In particular, we will present a range of further results on the joint convergence of the interfaces and the height function. In the continuum, the height function converges to the GFF, and the interfaces to its level lines. One feature of this work is that we make use of couplings between various models in the discrete. A particularly nice consequence of our approach is that the couplings in the discrete can be carried through to the continuum limit:

- The limits of interfaces of four models (the XOR-Ising models with free and plus/plus boundary conditions and the double random currents models with free and wired boundary conditions) can all be coupled with the same GFF as its level loops at different heights. In particular, they do not cross each other and we fully understand their interaction (i.e., nesting and intersecting behavior). The Edwards–Sokal type coupling between the double random currents and XOR-Ising in the discrete also transforms to a coupling in the continuum similar to CLE percolation [61].
- We naturally obtain a coupling between SLE_3 type loops (which are the limit of Ising interfaces) and SLE_4 type loops (which are the limit of XOR-Ising interfaces). From the Brownian loop-soup construction of CLE [75], we know that the union of two independent copies of CLE_3 gives rise to a CLE_4 . In comparison, our coupling comes from the XOR operation acting in the discrete (it seems complicated to define such an operation directly in the continuum).

While parts of Section 2 involve some background on continuum objects such as the GFF and its local sets, the current section can be read without such knowledge.

Notation Consider a finite graph $G = (V, E)$ with vertex set V and edge set E . For a domain $D \subsetneq \mathbb{C}$ in the complex plane and $\delta > 0$, introduce the graph D^δ to be the subgraph of $\delta\mathbb{Z}^2$ induced by the vertices of $\delta\mathbb{Z}^2$ that are inside D .

Below, we will speak of convergence of random variables taking values in families of loops contained in D , and distributions (generalized functions). While the latter is classical and has a well-defined associated topology, we provide some details on the former. To this end, let $\mathfrak{C} = \mathfrak{C}(D)$ be the collection of locally finite families \mathcal{F} of non-self-crossing loops contained in D that do not intersect each other. Inspired by [3], we define a metric on \mathfrak{C} ,

$$\mathbf{d}(\mathcal{F}, \mathcal{F}') \leq \varepsilon \iff \left(\begin{array}{l} \exists f : \mathcal{F}_\varepsilon \rightarrow \mathcal{F}' \text{ one-to-one s.t. } \forall \gamma \in \mathcal{F}_\varepsilon, d(\gamma, f(\gamma)) \leq \varepsilon \\ \text{and similarly when exchanging } \mathcal{F}' \text{ and } \mathcal{F} \end{array} \right),$$

where, \mathcal{F}_ε is the collection of loops in \mathcal{F} with a diameter larger than ε , and for two loops γ_1 and γ_2 , we set

$$d(\gamma_1, \gamma_2) := \inf \sup_{t \in \mathbb{S}^1} |\gamma_1(t) - \gamma_2(t)|,$$

with the infimum running over all continuous bijective parametrizations of the loops γ_1 and γ_2 by \mathbb{S}^1 .

1.2 Results for the XOR-Ising model

The *Ising model with free boundary conditions* on a finite graph G is defined as follows. For a spin configuration $\sigma = (\sigma_v : v \in V) \in \{-1, +1\}^V$, introduce the nearest-neighbor ferromagnetic Ising Hamiltonian with *free boundary conditions*

$$H_G(\sigma) := - \sum_{\{v, v'\} \in E} J_{\{v, v'\}} \sigma_v \sigma_{v'},$$

where $J_{\{v,v'\}} \geq 0$ are *coupling constants*, and the associated Gibbs measure given by

$$\mu_{G,\beta}[X] := \frac{1}{Z_{G,\beta}^{\text{Ising}}} \sum_{\sigma \in \{\pm 1\}^V} X(\sigma) \exp[-\beta H_G(\sigma)] \quad \text{for every } X : \{-1, +1\}^V \rightarrow \mathbb{C},$$

where $Z_{G,\beta}^{\text{Ising}} := \sum_{\sigma \in \{\pm 1\}^V} \exp[-\beta H_G(\sigma)]$ is the *partition function* of the model.

Definition 1.1 (XOR-Ising model with free boundary conditions). *Let $\mathbf{P}_{G,\beta}^{\text{XOR}}$ be the law of $\tau := \sigma \times \sigma' = (\sigma_v \times \sigma'_v : v \in V)$, where σ and σ' are two independent copies of the Ising model spin configurations with free boundary conditions on G . The random variable τ is called an XOR-Ising configuration on G with free boundary conditions.*

We will always (except in Section 2.3 and Section 3 where we consider general Ising models) take $G = D^\delta$ to be a subgraph of the square lattice, and we will set $J_{\{x,y\}} = 1$ for every pair $\{x,y\}$ which is an edge of the lattice and 0 otherwise. Also, we fix β to be equal to the critical inverse temperature $\beta_c = \frac{1}{2} \log(1 + \sqrt{2})$ of the square lattice and drop it from the notation.

Define the dual graph $G^* = (U, E^*)$ as follows: the vertex set U is given by the set of faces of G and the edge set E^* is the set of unordered pairs $\{u, u'\}$ with $u, u' \in U$ two faces that are bordered by the same edge e of G . In this case, we often write $\{u, u'\} = e^*$. For every spin configuration $\sigma \in \{-1, +1\}^V$ on G , define the *contour configuration associated with σ* to be the collection of dual edges e^* for which $e = \{v, v'\}$ satisfies $\sigma_v \neq \sigma_{v'}$. These contours separate the pluses from the minuses. The decomposition of a contour configuration in terms of loops is non-canonical on subgraphs of the dual square lattice (it is on graphs of degree 3 such as the hexagonal lattice). We therefore consider a slightly different contour configuration, that we call the *(nested) outer boundaries contour configuration*, and that we denote by $\eta = \eta(\sigma)$, defined as follows. For a connected component of constant spin in σ , also called *cluster \mathcal{C}* , call its *outer boundary* the loop made of dual edges e^* where $e = \{v, v'\}$ with $v \in \mathcal{C}$ and $v' \notin \mathcal{C}$ is not encircled by \mathcal{C} in the graph (\mathcal{C} does not separate v' from infinity). Then, η is the set of all the loops corresponding to the outer boundaries of all clusters in σ (both negative and positive).

The first theorem of this paper describes the scaling limit of the collection of nested outer boundaries in the XOR-Ising model with free boundary conditions. To state it, we will need the notion of two-valued sets $\mathbb{A}_{-a,b}$ introduced in [8]. In a simply connected Jordan domain D in the complex plane, $\mathbb{A}_{-a,b}$ is the unique thin local set of the Gaussian free field in D with boundary values $-a$ and b . In this work, we use $\mathcal{L}_{-a,b}$ to denote the collection of outer boundaries (which are SLE₄-type simple loops and level loops of the Gaussian free field) of the connected components of $D \setminus \mathbb{A}_{-a,b}$. We refer to later parts (Sections 2.2.1 and 6) for more details on two-valued sets and related objects.

Theorem 1.2 (Convergence of XOR-Ising interfaces with free boundary conditions). *Let $D \subsetneq \mathbb{C}$ be a simply connected Jordan domain. Let η^δ be the nested outer boundaries contour configuration in the critical XOR-Ising model with free boundary conditions on D^δ . Then as $\delta \rightarrow 0$, η^δ converges in distribution to a limit whose law is invariant under all conformal automorphisms of D . More precisely, we have that (see Fig. 1.1 Left)*

- *The outer boundaries of the outermost negative clusters converge to $\mathcal{L}_{-(2\sqrt{2}+1)\lambda,\lambda}$ in D .*

- If the outer boundary of a cluster converges to γ , then the outer boundaries of the outermost clusters that are enclosed by this cluster with the opposite sign converge to $\mathcal{L}_{-2\lambda, 2\sqrt{2}\lambda}$ in the domain encircled by γ .

We are also able to prove convergence of the outer boundaries contour configuration in the XOR-Ising model obtained by taking the Ising model with monochromatic boundary conditions. To this end, for a graph G , let ∂G be the set of vertices of G that lie on the unbounded face of G . We define G^+ to be the graph with vertex set $V^+ := V \cup \{\mathfrak{g}\}$ where \mathfrak{g} is an additional vertex that lies in the unbounded face of G , and $E^+ := E \cup \{\{x, \mathfrak{g}\} : x \in \partial G\}$. Now consider the nearest-neighbor ferromagnetic Ising Hamiltonian with *plus boundary conditions* on G defined by

$$H_G^+(\sigma) := H_G(\sigma) + \sum_{\{v, \mathfrak{g}\} \in E^+} J_{\{v, \mathfrak{g}\}} \sigma_v$$

and the associated Gibbs measure

$$\mu_{G, \beta}^+[X] := \frac{1}{Z_{G, \beta}^{\text{Ising}, +}} \sum_{\sigma \in \{\pm 1\}^V} X(\sigma) \exp[-\beta H_G^+(\sigma)] \quad \text{for every } X : \{-1, +1\}^V \rightarrow \mathbb{C},$$

where $Z_{G, \beta}^{\text{Ising}, +} := \sum_{\sigma \in \{\pm 1\}^V} \exp[-\beta H_G^+(\sigma)]$ is the *partition function* of the model.

Definition 1.3 (XOR-Ising model with plus/plus boundary conditions). *Let $\mathbf{P}_{G, \beta}^{\text{XOR}, +/+}$ be the law of $\tau = \sigma \times \sigma'$, where σ and σ' are two independent copies of the Ising model spin configuration on G with plus boundary conditions. The random variable τ is called an XOR-Ising configuration on G with plus/plus boundary conditions.*

As before, when G is a subgraph of the square lattice, we fix $J_{\{x, y\}} = 1$ for all $\{x, y\} \in E^+$, set $\beta = \beta_c = \frac{1}{2} \log(1 + \sqrt{2})$, and drop it from the notation.

Remark 1.4. We will often consider the XOR-Ising model with free boundary conditions on a graph G coupled together with the dual XOR-Ising model with plus/plus boundary conditions on the dual graph G^* . To fit this setup into the definitions above, one can think of the dual graph as $G^* = (G^\dagger)^+$, where G^\dagger is the *weak dual* graph that does not contain the vertex corresponding to the unbounded face of G .

We are now in a position to state the second theorem of this section.

Theorem 1.5 (Convergence of XOR-Ising interfaces with plus/plus boundary conditions). *Let $D \subsetneq \mathbb{C}$ be a simply connected Jordan domain. Let η^δ be the nested outer boundaries contour configuration in the critical XOR-Ising model with plus/plus boundary conditions on D^δ . Then as $\delta \rightarrow 0$, η^δ converges in distribution to a limit whose law is invariant under all conformal automorphisms of D . More precisely, we have that (see Fig. 1.1 Right)*

- The outer boundaries of the outermost negative clusters converge to $\mathcal{L}_{-(\sqrt{2}+1)\lambda, (\sqrt{2}+1)\lambda}$ in D .
- If the outer boundary of a cluster converges to γ , then the outer boundaries of the outermost clusters that are enclosed by this cluster with the opposite sign converge to $\mathcal{L}_{-2\lambda, 2\sqrt{2}\lambda}$ in the domain encircled by γ .

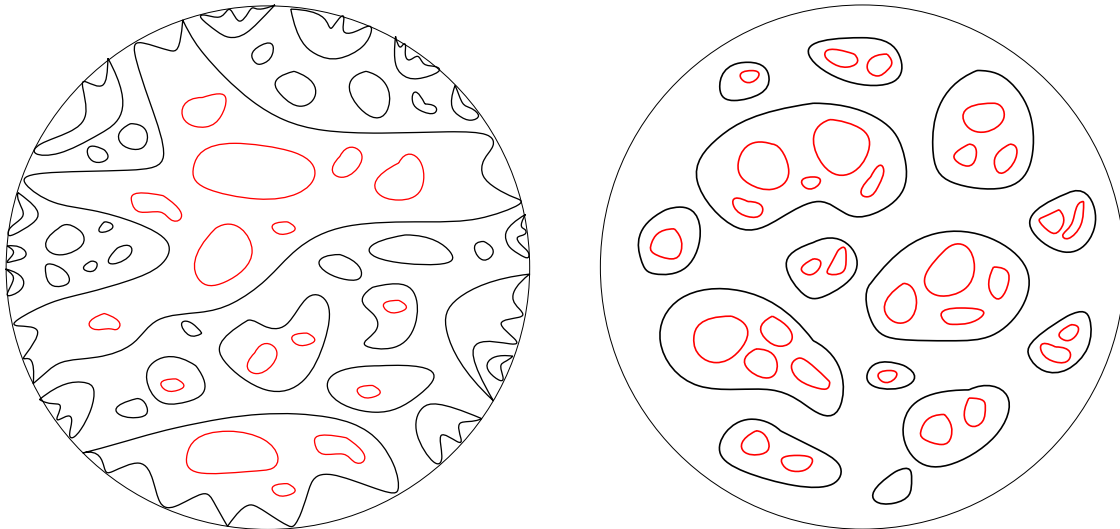


Figure 1.1: **Left:** XOR-Ising with free boundary conditions. The black loops represent the outer boundaries of the outermost negative clusters. Some touch the boundary and some stay in the interior. They are disjoint from each other. **Right:** XOR-Ising with plus/plus boundary conditions. The black loops represent the outer boundaries of the outermost negative clusters which all stay in the interior of the domain. **For both:** We depict in red the next layer of outer boundaries of outermost positive clusters encircled by the black loops. Given each black loop, the law of the red loops is the same for both pictures (up to conformal maps), and is equal to $\mathcal{L}_{-2\lambda, 2\sqrt{2}\lambda}$. One can iteratively sample the nested layers of loops.

Comparing Theorems 1.2 and 1.5, we see that the outermost layer of interfaces have different laws under different boundary conditions. However, the nested layers of interfaces are given by nested $\mathcal{L}_{-2\lambda, 2\sqrt{2}\lambda}$ in both models. If we let the domain D tend to the entire plane, then we obtain in the limit a full-plane version of $\mathcal{L}_{-2\lambda, 2\sqrt{2}\lambda}$ (this can be defined in a similar way the full-plane CLE is defined [42, 62]). The full-plane XOR-Ising model was studied by Boutillier and de Tilière [11] who showed, using the results of de Tilière [21], that the associated height function converges to the full-plane GFF in the scaling limit. Given this together with our results, it will not be difficult to prove that the full-plane XOR-Ising interfaces converge to the full-plane $\mathcal{L}_{-2\lambda, 2\sqrt{2}\lambda}$ (we leave the details to the interested reader). The latter consists of level loops of the full-plane GFF which is invariant under all Möbius transformations of the Riemann sphere.

In [81], Wilson predicted a few properties of the scaling limit of XOR-Ising loops in the bulk, i.e., when one zooms into the neighborhood of an interior point. Our results, together with properties of the nested $\mathcal{L}_{-2\lambda, 2\sqrt{2}\lambda}$, allow us to confirm these predictions:

- (Shape of the loops) The “shape” of each loop in the scaling limit of XOR-Ising interfaces in the bulk is the same as the loops in CLE_4 , since they are all level loops of the GFF. In [81], Wilson measured a few quantities of the XOR-Ising loops such as Hausdorff dimension, winding angle variance and electrical thickness, and found them to be equal to the same quantities for CLE_4 loops.
- (Difference in log conformal radii) The difference of log conformal radii between two

successive loops of the scaling limit of the XOR-Ising model surrounding the origin has the same law as the first time that a standard Brownian motion exits $[-\pi, \sqrt{2}\pi]$ (see [8, Proposition 20]).

- (Number of loops) Let $\mathbf{N}(\varepsilon)$ be the number of loops in the scaling limit of the XOR-Ising model in the unit disk surrounding the origin whose conformal radii with respect to the origin are at least ε . We will show in Lemma 8.6 that

$$\mathbf{N}(\varepsilon)/\log(\varepsilon^{-1}) \xrightarrow{\varepsilon \rightarrow 0} \frac{1}{\sqrt{2}\pi^2} \quad \text{a.s.} \quad (1.1)$$

The same quantity for CLE_4 loops is equal to $1/\pi^2$. This confirms Wilson's observation that the number of loops in the scaling limit of the XOR-Ising model is $\sqrt{2}$ times sparser than the CLE_4 loops.

- (Hausdorff dimension of a cluster) Since the dimension of $\mathbb{A}_{-a,b}$ is equal to $2 - 2\lambda^2/(a+b)^2$ by [67], the dimension of the scaling limit of an XOR-Ising cluster is equal to $\frac{1}{2} + \sqrt{2}$.

Let us conclude this section by discussing a conjecture that sheds light on the potential difficulties one may encounter when trying to prove the results of this paper. The previous statements imply that the scaling limit of the XOR-Ising interfaces satisfy the spatial Markov property, even though this does not hold in the discrete. Indeed, in the continuum limit, conditionally on the outer boundary γ of (the scaling limit of) an XOR-Ising cluster, the (scaling limit of) the next layer of outermost clusters of the opposite sign is distributed as $\mathcal{L}_{-2\lambda, 2\sqrt{2}\lambda}$ in the domain enclosed by γ , which is independent of the configuration outside of γ as well as the boundary conditions of the model.

It is then very tempting to guess that $\mathcal{L}_{-2\lambda, 2\sqrt{2}\lambda}$ is the law of the outermost negative XOR-Ising cluster boundaries in a domain with positive boundary condition (meaning that the XOR-Ising model with free boundary conditions is conditioned to be positive on the boundary, which is different from plus/plus boundary condition). Yet, we believe that this is not true. In [81], Wilson simulated an XOR-Ising model in a bounded domain, conditioned to have plus spin on one part of the boundary and minus spin on the other complementary part. He conjectured that the interface between the plus and minus spin is an $\text{SLE}_4(1/\sqrt{2}-1, 1/\sqrt{2}-1)$. This curve is not equal to SLE_4 , which is another evidence that *the plus or minus boundary conditions coming from an XOR-Ising interface in the interior of the domain act on the remaining XOR-Ising model differently from the plus or minus boundary conditions coming from the boundary of the domain*. This offers an explanation why it is difficult to prove Wilson's conjecture by using the traditional approach: intuition or strategies based on the spatial Markov property are very hard to implement.

We conjecture, based on Wilson's observation, that for an XOR-Ising model in a domain with positive boundary conditions, the outermost negative cluster boundaries are equal to $\mathcal{L}_{-(1/\sqrt{2}+1)\lambda, (3/\sqrt{2}+1)\lambda}$, and given the first layer of outermost negative clusters, the next layers of outer boundaries of clusters are again given by a nested $\mathcal{L}_{-2\lambda, 2\sqrt{2}\lambda}$.

1.3 Results for the double random current

As mentioned in Section 1.1, we will also obtain new results for the so-called double random current model. It will be a crucial step in our understanding of the XOR interfaces. Let

us note that the double random current model is an important model on its own, and that the following results are also of independent interest as they describe the scaling limit of a very natural representation of the Ising model. In particular, as mentioned at the end of this section, the scaling limit of the double random current gives access to the scaling limit of spin-spin correlations.

Definition of the random current and the double random current A *current* configuration \mathbf{n} on $G = (V, E)$ is an integer-valued function defined on the undirected edges $\{v, v'\} \in E$. The current's set of *sources* is defined as the set

$$\partial \mathbf{n} := \left\{ v \in V : \sum_{v' \in V: v' \sim v} \mathbf{n}_{\{v, v'\}} \text{ is odd} \right\}, \quad (1.2)$$

where $v' \sim v$ means that $\{v, v'\} \in E$.

Let Ω^B be the set of currents with the set of sources equal to B . When $B = \emptyset$, we speak of a *sourceless* current. For the nearest-neighbor ferromagnetic Ising model on G , we associate to a current configuration \mathbf{n} the *weight*

$$w_{G, \beta}(\mathbf{n}) := \prod_{\{v, v'\} \in E} \frac{(\beta J_{\{v, v'\}})^{\mathbf{n}_{\{v, v'\}}}}{\mathbf{n}_{\{v, v'\}}!}. \quad (1.3)$$

Again, for now we focus on the critical parameters on the square lattice $\beta = \beta_c$ and $J_{\{v, v'\}} = 1$ for every $\{v, v'\}$ which is an edge of G , and 0 otherwise, and drop them from the notation. General models will be considered in Section 2.3 and Section 3.

We introduce the probability measure on random currents with sources $B \subseteq V$ given by

$$\mathbf{P}_G^B(\mathbf{n}) := \frac{w_G(\mathbf{n})}{Z^B(G)}, \quad \text{for every } \mathbf{n} \in \Omega^B, \quad (1.4)$$

where $Z^B(G)$ is the partition function. The random variable \mathbf{n} is called a *random current configuration on G with free boundary conditions and source-set B* .

For future reference, let $\mathbf{P}_{G, H}^{A, B}$ be the law of $(\mathbf{n}_1, \mathbf{n}_2)$, where \mathbf{n}_1 and \mathbf{n}_2 are two independent currents with respective laws \mathbf{P}_G^A and \mathbf{P}_H^B . We call a *cluster* of \mathbf{n} a connected component of the graph with vertex set V and edge set $E(\mathbf{n}) := \{e \in E : \mathbf{n}_e > 0\}$. For a given cluster \mathcal{C} , we associate a loop configuration made of the edges e^* where $e = \{v, v'\}$ is such that $v \in \mathcal{C}$ and $v' \notin \mathcal{C}$. Note that this loop configuration is made of loops on the dual lattice corresponding to the different connected components of $\mathbb{Z}^2 \setminus \mathcal{C}$. The loop corresponding to the unbounded component is called the *outer boundary* of the cluster, and the loops corresponding to the boundaries of the bounded ones (sometimes referred to as holes) are called the *inner boundaries*. Like for the XOR-Ising model, define the (*nested*) *boundaries contour configuration* $\eta(\mathbf{n})$ by considering the collection of outer and inner boundaries of the clusters in \mathbf{n} .

As before, we fix a simply connected Jordan domain $D \subsetneq \mathbb{C}$ and consider the double random current on D^δ .

Theorem 1.6 (Convergence of double random current clusters with free boundary conditions). *Fix a simply connected Jordan domain $D \subsetneq \mathbb{C}$, and let η^δ be the nested boundaries*

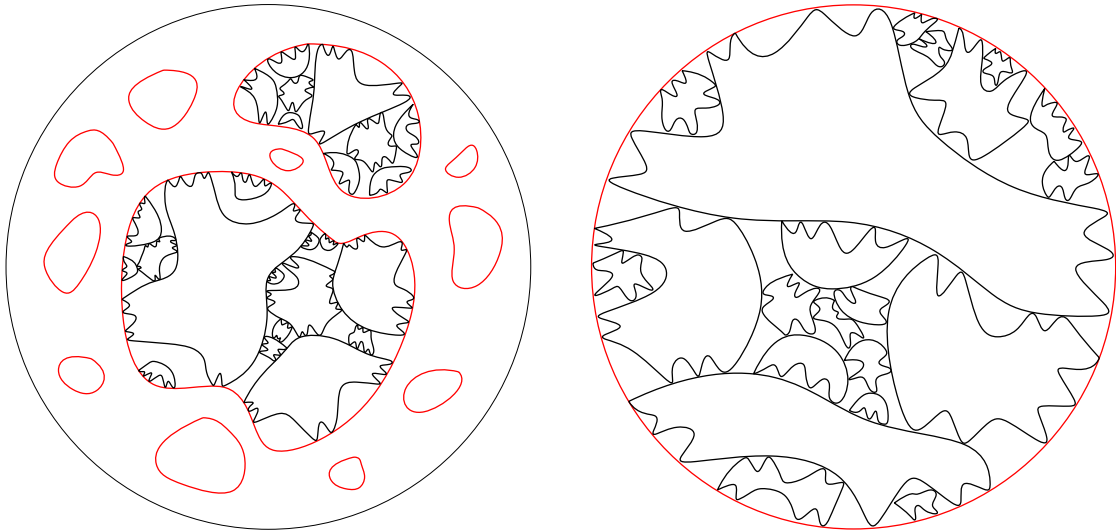


Figure 1.2: **Left:** We depict the outermost clusters in a double random current with free boundary conditions. The outer boundaries of these clusters are in red (they form a CLE_4). The inner boundaries of the clusters are in black. **Right:** We depict the unique outermost cluster in a double random current with wired boundary conditions. The inner boundaries of this cluster are in black. **For both:** In each domain encircled by an inner boundary loop, one has (the scaling limit of) an independent double random current with free boundary conditions. This allows us to iteratively sample the nested interfaces.

contour configuration of $\mathbf{n}_1^\delta + \mathbf{n}_2^\delta$ where $(\mathbf{n}_1^\delta, \mathbf{n}_2^\delta) \sim \mathbf{P}_{D^\delta, D^\delta}^{\theta, \theta}$. Then as $\delta \rightarrow 0$, η^δ converges in distribution to a limit whose law is invariant under all conformal automorphisms of D (see Fig. 1.2 Left). More precisely, we have that

- The outer boundaries of the outermost clusters converge to a CLE_4 in D .
- If the outer boundary of a cluster converges to γ , then the inner boundaries of this cluster converge to $\mathcal{L}_{-2\lambda, (2\sqrt{2}-2)\lambda}$ in the domain encircled by γ .
- If a loop in the inner boundary of a cluster converges to γ , then the outer boundaries of the outermost clusters enclosed by γ converge to a CLE_4 in the domain encircled by γ .

We will also work with the *random current model with wired boundary conditions* on G defined simply as the random current model on the augmented graph G^+ (with free boundary conditions on this graph). Accordingly, we introduce the measures $\mathbf{P}_{G^+}^B$ and $\mathbf{P}_{G^+, H^+}^{A, B}$ as before.

For technical reasons that will be discussed later, we focus on simply connected domains D such that ∂D is C^1 .

Theorem 1.7 (Convergence of double random current clusters with wired boundary conditions). *Fix a simply connected domain $D \subsetneq \mathbb{C}$ such that ∂D is C^1 , and let η^δ be the nested boundaries contour configuration of $\mathbf{n}_1^\delta + \mathbf{n}_2^\delta$ where $(\mathbf{n}_1^\delta, \mathbf{n}_2^\delta) \sim \mathbf{P}_{(D^\delta)^+, (D^\delta)^+}^{\theta, \theta}$. Then as $\delta \rightarrow 0$, η^δ converges in distribution to a limit whose law is invariant under all conformal automorphisms of D (see Fig. 1.2 Right). More precisely, we have that*

- *The inner boundaries of the unique outermost cluster converge to $\mathcal{L}_{-\sqrt{2}\lambda, \sqrt{2}\lambda}$ in D .*
- *If the inner boundary of a cluster converges to γ , then the outer boundaries of the outermost clusters enclosed by γ converge to a CLE_4 in the domain encircled by γ .*
- *If the outer boundary of a cluster converges to γ , then the inner boundaries of this cluster converge to $\mathcal{L}_{-2\lambda, (2\sqrt{2}-2)\lambda}$ in the domain encircled by γ .*

Theorems 1.6 and 1.7 have the following applications.

- The Hausdorff dimension of a double random current cluster in the scaling limit (for both free and wired boundary conditions) is $7/4$ ([67]).
- (Difference in log conformal radii) The difference of log conformal radii between two successive loops that encircle the origin in the scaling limit of double random current interfaces is equal to $T_1 + T_2$, where T_1 is the first time that a standard Brownian motion exits $[-\pi, (\sqrt{2} - 1)\pi]$ and T_2 is the first time that a standard Brownian motion exits $[-\pi, \pi]$ (see [8, Proposition 20]).
- (Number of clusters) Let $N(\varepsilon)$ be the number of double random current clusters in the unit disk surrounding the origin such that their outer boundaries have a conformal radius w.r.t. the origin at least ε . We will show in Lemma 8.7 that almost surely,

$$N(\varepsilon)/\log(\varepsilon^{-1}) \xrightarrow{\varepsilon \rightarrow 0} \frac{1}{\sqrt{2}\pi^2}.$$

It seems a coincidence to us that this quantity is the same as (1.1), because this does not result from any direct bijection between cluster of the double random current and the XOR Ising interfaces (the coupling between the two is quite complicated and is presented later in Section 2.3).

- (Scaling limit of the magnetization in domains) With a little bit of additional work, one may derive from our results the conformal invariance of the n -point spin-spin correlations of the critical Ising model already obtained in [18] as these correlations are expressed in terms of connectivity properties of $\mathbf{n}_1^\delta + \mathbf{n}_2^\delta$ (see for instance the proof of Theorem 2.6). The additional technicalities would consist in relating the point-to-point connectivity in $\mathbf{n}_1^\delta + \mathbf{n}_2^\delta$ to the probabilities that the ε -neighborhoods of the points are connected. Such reasonings have been implemented repeatedly when proving conformal invariance, and we omit the details here as it would lengthen the paper even more. We still wished to mention this corollary even though the result is already known as our paper mostly uses the convergence of certain fermionic observables to obtain convergence of the nesting field height function to the GFF (see Section 2). Such fermionic observables convergence has been obtained for the Ashkin-Teller model (which is a combination of two interacting Ising models) in [35] via renormalization arguments using the crucial fact that the observables in question are local observables of the Grassmann representation of the model. Notoriously, the spin-spin correlations are not of this kind, which makes renormalization arguments much more difficult to implement. We believe that the strategy of this paper may be of use to extend the universality results from [35] to non-local Grassmann observables.

We point out that the double random current model does *not* satisfy any obvious spatial Markov property in the discrete at the *outer* boundaries of the clusters (it does satisfy spatial Markov property at the *inner* boundaries of the clusters, namely inside each hole of a cluster, one has an independent double random current configuration with free boundary conditions). For example, for the double random current with free boundary conditions, given the outer boundary γ of a cluster, the inner boundaries of this cluster is distributed as $\mathcal{L}_{-2\lambda, (2\sqrt{2}-2)\lambda}$. On the other hand, for the outermost cluster of a double random current model with free boundary conditions, its inner boundaries are distributed as $\mathcal{L}_{-\sqrt{2}\lambda, \sqrt{2}\lambda}$. This suggests that *the wired boundary condition coming from a double random current interface in the interior of the domain act on the remaining model differently from the wired boundary condition coming from the boundary of the domain itself.*

2 Further results and proof road-map

In this section, we discuss further results, as well as our proof road-map. In particular, we present results which are stronger than those in Section 1. Since the statements require more background both from the discrete and continuous sides, we have postponed them here to facilitate the reading. As we have mentioned in the introduction, our argument is based on three pillars. The first one, which is the tightness of the models, is mainly dealt with in our second paper [28]. We will focus on the other two pillars in this paper.

We start by discussing results and proofs for the double random current model. In Section 2.1, we present the convergence of the associated height function, called the nesting field, to the GFF. In Section 2.2, we state stronger results (and present their proof strategy) on the joint convergence of double random current interfaces and the nesting field, which will imply Theorems 1.6 and 1.7.

Then we will turn to the XOR-Ising model. In Section 2.3, we discuss a new coupling between the double random current and the XOR-Ising model. It turns out that they are related in the same way the FK-Ising model is related to the Ising model, meaning via an Edwards–Sokal type coupling. The coupling also associates both the double random current and XOR-Ising models with corresponding dual models, as well as a height function H . In Section 2.4, we will state stronger results (and present their proof strategy) on the joint convergence of XOR-Ising interfaces and the height function, which imply Theorems 1.2 and 1.5.

We stress that our proof is a complex combination of discrete and continuous arguments. In Sections 2.2 and 2.4, we explain how the different pieces from the discrete and the continuum are assembled together. In later sections of the paper, we have regrouped inputs from the discrete and continuous sides separately so that they can be read independently.

A more detailed and complete strategy for the proofs of the main results can be found in Sections 7 and 8. Indeed, the properties obtained on the discrete side that we single out in the current section serve as inputs to the proofs of the main results in Sections 7 and 8. In this section, we at some point include a brief introduction to the GFF and its local sets to help the reader understand the statements in the continuum. However, the core of the continuum part of the proofs, which heavily involves the GFF and local sets, is postponed to Sections 7 and 8 – once we have made a more detailed review of the continuum background in Section 6.

In Section 2.5, we highlight the fact that our proofs allow us to carry the discrete coupling established in Section 2.3 (between the primal and dual double random current and XOR-Ising models) through to the continuum limit. The coupling in the continuum is similar to CLE percolation, which is itself the continuum analogue of the Edwards–Sokal coupling [61].

Finally, in Section 2.6 we gather results from [28] that we will extensively use in this paper.

2.1 Convergence of the nesting field of the double random current to the Gaussian free field

As mentioned above, a central piece in our strategy is a new convergence result dealing with the so-called nesting field of the double random current introduced by two of the authors in [27]. Let $G = (V, E)$ be a generic planar graph. Let \mathbf{n}_{odd} be the set of edges that have an odd current in \mathbf{n} . A nontrivial connected component of the graph $(V, \mathbf{n}_{\text{odd}})$ will be called a *contour*. In particular, each contour C is contained in a unique cluster of \mathbf{n} , and each cluster \mathcal{C} is associated to a contour configuration $\mathcal{C} \cap \mathbf{n}_{\text{odd}}$. Each contour configuration gives rise to a ± 1 spin configuration on the faces of G , where the external unbounded face is assigned spin $+1$, and where the spin changes whenever one crosses an edge of a contour. We call a cluster \mathcal{C} *odd around a face u* if the spin configuration associated with the contour configuration $\mathcal{C} \cap \mathbf{n}_{\text{odd}}$ assigns spin -1 to u .

For a current \mathbf{n} , let $\mathfrak{C}(\mathbf{n})$ be the collection of all clusters of \mathbf{n} , and let $(\epsilon_{\mathcal{C}})_{\mathcal{C} \in \mathfrak{C}(\mathbf{n})}$ be i.i.d. random variables equal to $+1$ or -1 with probability $1/2$ indexed by $\mathfrak{C}(\mathbf{n})$. These random variables are called the *labels* of the clusters. The *nesting field with free boundary conditions* of a current \mathbf{n} on G evaluated at a face u of G is defined by

$$h_G(u) := \sum_{\mathcal{C} \in \mathfrak{C}(\mathbf{n})} \mathbf{1}\{\mathcal{C} \text{ odd around } u\} \epsilon_{\mathcal{C}}. \quad (2.1)$$

Analogously, the *nesting field with wired boundary conditions* of a current \mathbf{n} on G^+ (recall the definition from Section 1.2) evaluated at a face u of G^+ is defined by

$$h_{G^+}^+(u) := (\mathbf{1}\{\mathcal{C}_{\mathfrak{g}} \text{ odd around } u\} - 1/2) \epsilon_{\mathcal{C}_{\mathfrak{g}}} + \sum_{\mathcal{C} \neq \mathcal{C}_{\mathfrak{g}}} \mathbf{1}\{\mathcal{C} \text{ odd around } u\} \epsilon_{\mathcal{C}}, \quad (2.2)$$

where $\mathcal{C}_{\mathfrak{g}}$ is the cluster containing the external vertex \mathfrak{g} , and where the sum is taken over all remaining clusters of \mathbf{n} . Here, whether $\mathcal{C}_{\mathfrak{g}}$ is odd around a face of G or not depends on the embedding of the graph G^+ . However, one can see that the distribution of $h_{G^+}^+(u)$ is independent of this embedding.

Note that due to the term corresponding to $\mathcal{C}_{\mathfrak{g}}$, the nesting field with wired boundary conditions takes half-integer values, whereas the one with free boundary conditions is integer-valued. Such definition is justified by the next result, and by the joint coupling of h_G and $h_{G^*}^+$ via a dimer model described in Section 3.1.3. The global shift of $1/2$ between h_G and $h_{G^*}^+$ (which is the same as in the work of Boutilier and de Tilière [11]) is also the reason why the level loops of the GFF corresponding to the outermost interfaces of the XOR-Ising model with free boundary conditions (Theorem 1.2) have different height than those for the plus/plus boundary conditions (Theorem 1.5): they are given by $\mathcal{L}_{-(2\sqrt{2}+1)\lambda, \lambda}$ and $\mathcal{L}_{-(\sqrt{2}+1)\lambda, (\sqrt{2}+1)\lambda}$ respectively. Indeed, the shift of $\sqrt{2}\lambda$ in the continuum corresponds to the shift of $1/2$ in the discrete as will become clear later on.

The following is the main result of this part of the argument. We identify the function h_{D^δ} defined on the faces of D^δ with a distribution on D in the following sense: extend h_{D^δ} to all points in D by setting it to be equal to $h_{D^\delta}(u)$ at every point strictly inside the face u , and 0 on the complement of the faces in D . Then, we view h_{D^δ} as a distribution (generalized function) by setting

$$h_{D^\delta}(f) := \int_D f(x) h_{D^\delta}(x) dx,$$

where f is a *test function*, i.e. a smooth compactly supported function on D . We proceed analogously with the field $h_{(D^\delta)^*}^+$ and extend it to all points within the faces of $(D^\delta)^*$.

The *Gaussian free field (GFF)* h_D with zero boundary conditions in D is a random distribution such that for every smooth function f with compact support in D , we have

$$\mathbb{E} \left[\left(\int_D f(z) h_D(z) dz \right)^2 \right] = \int_D \int_D f(z_1) f(z_2) G_D(z_1, z_2) dz_1 dz_2, \quad (2.3)$$

where G_D is the Green's function on D with zero boundary conditions satisfying $\Delta G_D(x, \cdot) = -\delta_x(\cdot)$, where δ_x denotes the Dirac mass at x . This normalization means e.g. that for the upper half plane \mathbb{H} , we have $G_{\mathbb{H}}(x, y) = \frac{1}{2\pi} \log |(x - \bar{y})/(x - y)|$.

Theorem 2.1 (Convergence of the nesting field). *Let $D \subsetneq \mathbb{C}$ be a bounded simply connected Jordan domain and let $D^\delta \subsetneq \delta\mathbb{Z}^2$ converge to D as $\delta \rightarrow 0$ in the Carathéodory sense. Denote by h_{D^δ} the nesting field of the critical double random current model on D^δ with free boundary conditions, and by $h_{(D^\delta)^\dagger}^+$ the nesting field of the critical double random current model on the weak dual graph $(D^\delta)^\dagger$ with wired boundary conditions. Then*

$$\lim_{\delta \rightarrow 0} h_{D^\delta} = \lim_{\delta \rightarrow 0} h_{(D^\delta)^\dagger}^+ = \frac{1}{\sqrt{\pi}} h_D,$$

where h_D is the GFF in D with zero boundary conditions, and where the convergence is in distribution in the space of generalized functions.

Moreover, h_{D^δ} and $h_{(D^\delta)^\dagger}^+$ can be coupled together as one random height function H_{D^δ} defined on the faces of a planar graph C_{D^δ} (whose faces correspond to both the faces of D^δ and $(D^\delta)^\dagger$; see Fig. 3.1) in such a way that

$$\lim_{\delta \rightarrow 0} H_{D^\delta} = \frac{1}{\sqrt{\pi}} h_D.$$

More properties of the coupling of h_{D^δ} and $h_{(D^\delta)^\dagger}^+$ are described in Section 2.3.

Our proof is based on the relationship between the nesting field of double random currents on a graph G and the height function of a dimer model on decorated graphs G^d and C_G established in [27]. We will first explicitly identify the inverse Kasteleyn matrix associated with these dimer models with the correlators of real-valued Kadanoff–Ceva fermions in the Ising model [39]. This is valid for arbitrary planar weighted graphs, and can also be derived from the bozonization identities of Dubédat [22]. For completeness of exposition, we choose to present an alternative derivation that uses arguments similar to those of [27]. Compared to [22], rather than using the connection with the six-vertex model, we employ the double random current model. We then express the real-valued observables on general graph in terms

of the complex-valued observables of Smirnov [77], Chelkak and Smirnov [19] and Hongler and Smirnov [38]. This is a well-known relation that can be e.g. found in [17]. We also state the relevant scaling limit results for the critical observables on the square lattice obtained in [19, 38, 77].

All in all, we identify the scaling limit of the inverse Kasteleyn matrix on graphs C_{D^δ} as $\delta \rightarrow 0$. This is an important ingredient in the computation of the limit of the moments of the height function which is done by modifying an argument of Kenyon [43]. Another crucial and new ingredient is a class of delicate estimates on the critical random current model from [28] that allow us to do two things:

- to identify the boundary conditions of the limiting GFF to be zero boundary conditions;
- to control the behaviour of the increments of the height function between vertices at small distances.

The first item is particularly important as handling boundary conditions directly in the dimer model is notoriously difficult. Here, the identification of the limiting boundary conditions is made possible by the connection with the double random current as well as the main result of [28] stating that large clusters of the double random current with free boundary conditions do not come close to the boundary of the domain (see Theorem 2.14 below). We see this observation and its implication for the nesting field as one of the key innovation of our paper.

We stress the fact that Theorem 2.1 does not follow from the scaling limit results of Kenyon [43, 44] as the boundary conditions considered in these papers are related to Temperley's bijection between dimers and spanning trees [47, 48, 79], whereas those considered in this paper correspond to the double Ising model [11, 22, 27]. Moreover we note that the infinite volume version of Theorem 2.1 was obtained by de Tilière [21]. Finally it can also be shown that the hedgehog domains of Russkikh [66] are a special case of our framework, where the boundary of D^δ makes turns at each discrete step.

2.2 Convergence of the double random current interfaces

Let us now present the proof strategy of our main results on the convergence of double random current interfaces (Theorems 1.6 and 1.7).

In this subsection, we focus on the interplay between the discrete and continuous sides and refer the reader to Section 7 for a proof road-map involving more details in the continuum. Let us briefly mention that among other things we will prove a result (Theorem 7.8) on the characterization of thin local sets with boundary values in $\{-\mu, 0, \mu\}$ for $\mu \geq 2\lambda$ (where $\lambda = \sqrt{\pi/8}$). This is purely a result about local sets and GFF which is interesting in its own right. Even though it is a crucial ingredient in the proof, we postpone its statement to Section 7 since it is not the main purpose of this work.

In order to explain further results and strategy, we first recall some background in Section 2.2.1. Throughout, let $D \subsetneq \mathbb{C}$ be a simply connected domain.

2.2.1 Background on SLE, CLE, Gaussian free field and two-valued sets

This is a short preliminary section aimed at giving a brief account of the continuous objects involved in this work, while conveying as much intuition as possible. We refer to Section 6 for more detailed preliminaries.

The Schramm-Loewner evolution (SLE) was introduced by Schramm in [68]. It is a family of non self-crossing random curves which depend on a parameter $\kappa > 0$. For many discrete models, free or wired/monochromatic boundary conditions force the interfaces to take the form of loops. The loop interfaces are conjectured (and sometimes proved) to converge to a conformal loop ensemble (CLE) in the continuum, which is a random collection of loops contained in D that do not cross each other. The family of CLE was introduced by Sheffield in [74] and further studied by Sheffield and Werner in [75]. It depends on a parameter $\kappa \in (8/3, 8)$ and can be constructed using variants of SLE_κ .

In [69, 70], Schramm and Sheffield made the important discovery that level lines of the discrete Gaussian free field (GFF) converge in the scaling limit to SLE_4 curves, and that the limiting SLE_4 curves are coupled with the continuum GFF as its *local sets* (i.e., a set with a certain spatial Markov property, see Section 6.2). More generally, the theory of local sets developed in [70] allows one to couple SLE_κ with the GFF for all $\kappa \in (0, 8)$. The coupling between SLE_κ and GFF was further developed in [24, 57–60] (also, see references therein).

In this work, we are only concerned with the case $\kappa = 4$. It was shown in [70] that SLE_4 -type curves are coupled with the GFF with a height gap 2λ in such a way that they are local sets of the GFF with boundary values respectively $a - \lambda$ and $a + \lambda$ on the left- and right-hand sides of the curve (see Section 6.2 for more details). A crucial property shown in [70] is that such SLE_4 -type curves are deterministic functions of the GFF. We call these curves level lines, to keep the same terminology as in the discrete. The value $a \in \mathbb{R}$ is called the *height* of the level line. The coupling between SLE_4 and GFF was extended to CLE_4 and GFF by Miller and Sheffield [56] (a more general coupling between CLE_κ and GFF for all $\kappa \in (0, 8)$ was established in [61]; a proof for the case $\kappa = 4$ was also provided in [8]).

Let us fix some notation that will be used throughout this work. For any simply connected domain U , we say that its boundary ∂U is a *contour*. If γ is a simple loop, then let $O(\gamma)$ denote the domain encircled by γ , which is equal to the unique bounded connected component of $\mathbb{C} \setminus \gamma$. Every simple loop is a contour, but a contour need not be a loop or a curve.² Let h be a zero boundary GFF in D . For every simply connected domain $U \subseteq D$, let $h|_U$ denote the restriction of h to the domain U . If $h|_U$ is equal to a GFF in U with constant boundary conditions, say equal to c , then let $h^0|_U$ be the zero boundary GFF so that $h|_U$ is equal to $h^0|_U$ plus c . This constant c is also called the *boundary value* of U , or the *inner boundary value* of ∂U when it is a simple loop.³ Let Γ denote a collection of simple loops which do not cross each other. Let $\text{gask}(\Gamma)$ denote the *gasket* of Γ , which is equal to $\overline{D} \setminus \cup_{\gamma \in \Gamma} O(\gamma)$. Given a connected set $A \subseteq \overline{D}$ such that $\partial D \subseteq A$, let $\mathcal{L}(A)$ denote the collection of outer boundaries of the connected components of $D \setminus A$.

The Miller-Sheffield coupling between the GFF and CLE_4 states that h a.s. uniquely determines a random collection Γ of simple loops which do not cross each other and satisfy the following property (see Fig. 2.1, left): conditionally on $\text{gask}(\Gamma)$, for each loop $\gamma \in \Gamma$, there exists $\epsilon(\gamma) \in \{-1, 1\}$ such that $h|_{O(\gamma)}$ is equal to $\epsilon(\gamma)2\lambda$ plus a zero-boundary GFF.

²In this paper, we in fact only deal with contours which are or turn out in the end to be simple loops. However, we distinguish the notions of *contour* and *loop*, because we will later prove general results about local sets whose boundaries are not *a priori* known to be curves.

³We do not use the notion of “outer boundary value”. However, we emphasize “inner” in this terminology, because we will often consider contours which are level loops (they are part of level lines) and each level line has different boundary values at its two sides (with a height gap 2λ). The inner boundary value of a level loop is also equal to the boundary value of this level line on the inner side.

In addition, the fields $h|_{O(\gamma)}$ for different γ 's are (conditionally) independent of each other. In other words, $\text{gask}(\Gamma)$ is a *local set* of h with boundary values in $\{-2\lambda, 2\lambda\}$. It turns out that Γ has the law of a CLE_4 . In addition, $\text{gask}(\Gamma)$ carries no mass of the GFF: for all test function f on D , we have

$$\int_D f(x)h(x)dx = \sum_{\gamma \in \Gamma} \int_{O(\gamma)} f(x)h|_{O(\gamma)}(x)dx. \quad (2.4)$$

Each loop γ in CLE_4 is a level line (we also call it a level loop) of the GFF with boundary value $\epsilon(\gamma)2\lambda$ on the inner side of the loop and 0 on the outer side of the loop (so it is at height $\epsilon(\gamma)\lambda$).

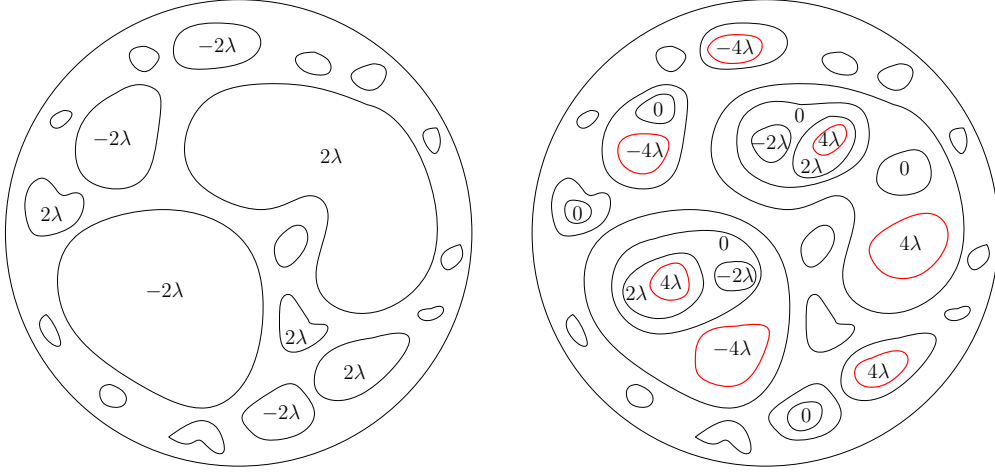


Figure 2.1: **Left:** A sketch of CLE_4 coupled with the GFF. The loops have inner boundary values -2λ or 2λ . **Right:** We depict a few layers of the nested CLE_4 coupled with the same GFF. We mark in red the outermost loops that have boundary values -4λ or 4λ , which belong to $\mathcal{L}_{-4\lambda, 4\lambda}$.

It is also natural to consider level loops of h at other heights than those of CLE_4 . For example, the previous coupling can be extended to the nested CLE_4 (by sampling the CLE_4 coupled to $h^0|_{O(\gamma)}$ for each $\gamma \in \Gamma$), so that the further layers of CLE_4 loops are at heights $(2k+1)\lambda$ for $k \in \mathbb{Z}$. For $a \in (-\lambda, \lambda)$, the outermost level loops of h at height a are given by boundary conformal loop ensembles (BCLE) [61] (a certain random collection of loops that touch the boundary, see Section 6.3 for more details), and one can then also consider nested versions of BCLE to obtain level loops of h at a continuum range of heights.

The gaskets of CLEs and BCLEs belong to a particular class of local sets called *two-valued sets* introduced in [8]: a two-valued set is a *thin local set* (a terminology in [71] meaning that the local set carries no mass of the GFF, described e.g. by (2.4)) with two boundary values in $\{-a, b\}$, denoted by $\mathbb{A}_{-a, b}$. For example, the gasket of CLE_4 is equal to $\mathbb{A}_{-2\lambda, 2\lambda}$, and the gaskets of BCLEs correspond to $\mathbb{A}_{-a, b}$ with $a+b=2\lambda$. It was shown in [8] that the sets $\mathbb{A}_{-a, b}$ exist for $a, b > 0$ with $a+b \geq 2\lambda$, and are a.s. unique and determined by h . Let us use $\mathcal{L}_{-a, b}$ to denote $\mathcal{L}(\mathbb{A}_{-a, b})$. Throughout, we denote by $\mathcal{L}_{-a, b}^+$ (resp. $\mathcal{L}_{-a, b}^-$) the set of loops in $\mathcal{L}_{-a, b}$ with inner boundary value b (resp. $-a$). We will also use notations like $\text{CLE}_4(h)$

and $\mathcal{L}_{-a,b}(h)$ to represent these sets coupled to h (especially when there are different GFFs involved).

The loops in $\mathcal{L}_{-a,b}$ are composed of SLE₄-type curves which are level lines of h , hence are a.s. simple and do not cross each other (but can intersect each other). The law of $\mathcal{L}_{-a,b}$ is invariant under all conformal automorphisms from D onto itself, since h is invariant under those conformal maps. The geometric properties of the loops in $\mathcal{L}_{-a,b}$ are well understood (see e.g. [7, 8, 67] and Section 6.4).

Let us now give a simple and intuitive explanation of the two-valued sets, and postpone more details to Section 6.4. As pointed out in [8], $\mathbb{A}_{-a,b}$ is a 2D analogue for GFF of the stopping time of a 1D Brownian motion upon exiting $[-a, b]$, and is intuitively the set of points that are connected to the boundary by a path on which the values of h remain in $[-a, b]$. Let us illustrate this by the following construction of $\mathbb{A}_{-2n\lambda, 2n\lambda}$ via iterated CLE₄s (see Fig. 2.1, right). For each point $z \in D$, the inner boundary values of the successive loops that encircle z in the nested CLE₄ perform a symmetric random walk with steps $\pm 2\lambda$. The loops in $\mathcal{L}_{-2n\lambda, 2n\lambda}$ correspond to the first time that we obtain a nested CLE₄ loop with inner boundary value equal to $-2n\lambda$ or $2n\lambda$.

2.2.2 Scaling limit of outermost double random current clusters

To identify the scaling limit of double random current clusters (for both the free and wired boundary conditions), the essential part is to understand the scaling limit of the outermost clusters. From there, the law of the nested layers of interfaces can be identified thanks to the spatial Markov property of the model at the inner boundaries of each cluster.

In this subsection, we state Theorem 2.2 below, which implies the statements of Theorem 1.6 regarding the outermost double random current clusters. We emphasize that Theorem 2.2 contains much more information, in particular since it states the joint convergence of the double random current clusters, their labels and the height function, as well as it specifies the joint law of their limits.

More precisely, let us consider the coupling \mathbb{P}_{D^δ} between two independent copies \mathbf{n}_1^δ and \mathbf{n}_2^δ of sourceless currents on D^δ , i.e., $(\mathbf{n}_1^\delta, \mathbf{n}_2^\delta) \sim \mathbf{P}_{D^\delta, D^\delta}^{\theta, \theta}$, the labels ϵ^δ associated to the clusters of $\mathbf{n}_1^\delta + \mathbf{n}_2^\delta$, and the nesting field h^δ . Let B^δ be the collection of outer boundaries of the outermost double random current clusters on D^δ . For each loop $\ell \in B^\delta$, let $\epsilon^\delta(\ell)$ be the label of the double random current cluster $\mathcal{C}(\ell)$ with outer boundary ℓ , and $A^\delta(\ell)$ be the collection of loops corresponding to the inner boundary of $\mathcal{C}(\ell)$. Let $A^\delta := \cup_{\ell \in B^\delta} A^\delta(\ell)$. For each $\gamma \in A^\delta(\ell)$, we say that it is the boundary of an *odd hole* if $\mathcal{C}(\ell)$ is odd around every face encircled by γ (see definition in Section 2.1). Otherwise we say that γ is the boundary of an *even hole*. We will prove the following theorem.

Theorem 2.2. *Let $D \subsetneq \mathbb{C}$ be a simply connected Jordan domain; As $\delta \rightarrow 0$, the quadruple $(B^\delta, A^\delta, h^\delta, \epsilon^\delta)$ defined above converges in distribution to a limit (B, A, h, ϵ) satisfying (see Fig. 2.2):*

- h is a GFF with zero boundary conditions in D .
- The collection of loops B is equal to $CLE_4(h)$. For each $\ell \in B$, $h|_{O(\ell)}$ is equal to an independent zero-boundary GFF $h^0|_{O(\ell)}$ plus the constant $\epsilon(\ell)2\lambda$.

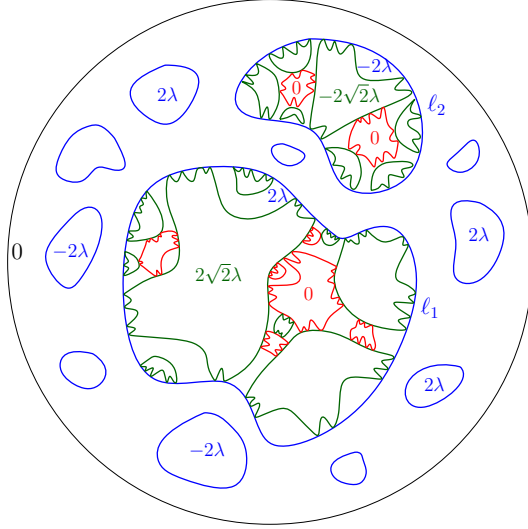


Figure 2.2: We depicted the loops in B in blue. For each $\ell \in B$, the loops in $A(\ell)$ have inner boundary value either 0 or $\epsilon(\ell)2\sqrt{2}\lambda$. For two loops ℓ_1 and ℓ_2 in B with labels $\epsilon(\ell_1) = 1$ and $\epsilon(\ell_2) = -1$, we depict the loops in $A(\ell_1)$ and $A(\ell_2)$. For $i = 1, 2$, we draw the loops in $A(\ell_i)$ with inner boundary value 0 (resp. $\epsilon(\ell_i)2\sqrt{2}\lambda$) in red (resp. green). Each green (resp. red) loop is the limit of the boundary of an odd (resp. even) hole. We say two loops are connected if they touch each other. Then, loops of the same color are always connected to the outer boundary of the cluster (i.e., a blue loop in B) via a chain of loops of the same parity. In particular, only green loops can touch the outer boundary of the cluster, and loops of the same color never touch each other.

- Every loop in A is encircled by a loop in B . For each loop $\ell \in B$, let $A(\ell)$ denote the collection of loops in A that are encircled by ℓ .

- If $\epsilon(\ell) = 1$, then $A(\ell)$ is equal to $\mathcal{L}_{-2\lambda, (2\sqrt{2}-2)\lambda}(h^0|_{O(\ell)})$.
- If $\epsilon(\ell) = -1$, then $A(\ell)$ is equal to $\mathcal{L}_{-(2\sqrt{2}-2)\lambda, 2\lambda}(h^0|_{O(\ell)})$.

Moreover, for each loop $\gamma \in A$, if γ has inner boundary value 0, then it is the limit of the boundary of an even hole, otherwise if it has inner boundary value in $\{-2\sqrt{2}\lambda, 2\sqrt{2}\lambda\}$, then it is the limit of the boundary of an odd hole.

The proof of Theorem 2.2 combines ingredients from both the discrete and the continuous sides. We first need to gather the following geometric properties of the discrete system.

Proposition 2.3. Fix a simply connected Jordan domain $D \subsetneq \mathbb{C}$ and consider the double random current on D^δ with free boundary conditions. The family $(B^\delta, A^\delta, \epsilon^\delta, h^\delta)_{\delta>0}$ is tight for the topology of weak convergence and for every subsequential limit (B, A, ϵ, h) , a.s.

1. h is a GFF with zero boundary conditions in D .
2. The sets A and B consist of simple loops which do not cross each other. Every loop in A is encircled by some loop in B . The set A is not equal to $\{\partial D\}$.

3. (Local set) The set $\text{gask}(A)$ is a thin local set of h , with boundary values in $[-2\sqrt{2}\lambda, 2\sqrt{2}\lambda]$. More precisely, for each loop $\ell \in B$, for all $\gamma \in A(\ell)$, h restricted to $O(\gamma)$ is equal to an independent GFF with boundary condition $\epsilon(\ell)c(\gamma)$ with $c(\gamma) \in [0, 2\sqrt{2}\lambda]$. Furthermore, if there exists a finite sequence $\gamma_1, \dots, \gamma_k$ of loops in $A(\ell)$ such that γ_1 and γ_k respectively intersect ℓ and γ , then $c(\gamma) \in \{0, 2\sqrt{2}\lambda\}$. If one can find such a sequence with k even, then $c(\gamma) = 2\sqrt{2}\lambda$ and γ is the limit of the boundary of an odd hole; otherwise if k is odd, then $c(\gamma) = 0$ and γ is the limit of the boundary of an even hole.
4. The loops in A that have inner boundary value 0 do not touch the loops in B .
5. The loops in B are more exterior than CLE_4 loops.

Let us make a few remarks about Proposition 2.3 and how it is used to prove Theorem 2.2.

- As usual, the first step is to establish the tightness of the quadruple $(B^\delta, A^\delta, h^\delta, c^\delta)$, and this is based on the results of [28]. Property 1 is a reformulation of Theorem 2.1. Property 4 can be obtained from a theorem in [28]. Property 5 is a consequence of the convergence of interfaces in the Ising model to CLE_3 obtained in [10].
- Property 3 follows from the analysis of the structure of the discrete coupling together with the joint convergence to (B, A, ϵ, h) . The fact that $\text{gask}(A)$ is a thin local set is a consequence of the fact that the loops of A^δ satisfy the spatial Markov property in the discrete. However, since $\text{gask}(A)$ takes boundary values in a continuous range $[-2\sqrt{2}\lambda, 2\sqrt{2}\lambda]$, this property is far from enough to determine A .

In order to pin down the law of A , we rely on the additional geometric properties of A and B stated in Properties 4 and 5 and we prove new results on local sets of the GFF. In particular, we crucially use a result (Theorem 7.8) characterizing all thin local sets with boundary values in $\{-\mu, 0, \mu\}$ for $\mu \geq 2\lambda$ (as indicated by Theorem 2.2, $\text{gask}(A)$ turns out in the end to take boundary values in $\{-2\sqrt{2}, 0, 2\sqrt{2}\}$).

- Contrarily to A^δ , the loops of B^δ do not satisfy spatial Markov property at the discrete level. The proof that B is the CLE_4 coupled to h – hence in particular it does satisfy the spatial Markov property in the continuum – relies on the previously proved properties of A and the interaction between the loops in A and B .

We now turn to wired boundary conditions. Fix a simply connected domain $D \subset \mathbb{C}$ and consider the double random current \mathbf{n} with wired boundary conditions in D^δ . Let \widehat{A}^δ be the collection of loops in the inner boundary of the cluster \widehat{C} of the outer boundary of D^δ in \mathbf{n} . For each $\gamma \in \widehat{A}^\delta$, we say that it is the boundary of an odd hole if \widehat{C} is odd around every face encircled by γ . Otherwise we say that γ is the boundary of an even hole. We will prove the following result on the joint convergence of $(\widehat{A}^\delta, h^\delta)_{\delta > 0}$.

Below, we focus on simply connected domains D with C^1 -smooth boundary. The restriction to such domains comes from a technical condition from Remark 7.3 of [28] which could possibly be removed modulo some additional work.

Theorem 2.4. *Consider a simply connected domain $D \subset \mathbb{C}$ and such that ∂D is C^1 . Then as $\delta \rightarrow 0$, $(\widehat{A}^\delta, h^\delta)$ converges in distribution to a limit (\widehat{A}, h) , where h is a GFF in D with zero boundary conditions and $\widehat{A} = \mathcal{L}_{-\sqrt{2}\lambda, \sqrt{2}\lambda}(h)$. Moreover, if γ is the limit of the boundary*

of an even hole, then γ has inner boundary value $-\sqrt{2}\lambda$; if γ is the limit of the boundary of an odd hole, then γ has inner boundary value $\sqrt{2}\lambda$.

To prove Theorem 2.4, we need to collect the following input from the discrete.

Proposition 2.5. *Consider a simply connected domain $D \subsetneq \mathbb{C}$ and such that ∂D is C^1 . Then the family $(\widehat{A}^\delta, h^\delta)_{\delta>0}$ is tight for the topology of weak convergence defined above. Moreover, for every subsequential limit (\widehat{A}, h) :*

1. h is a GFF with zero boundary conditions in D ,
2. (Local set) The set $\text{gask}(\widehat{A})$ is a thin local set of h , with boundary values in $[-\sqrt{2}\lambda, \sqrt{2}\lambda]$. More precisely, for all $\gamma \in \widehat{A}$, h restricted to $O(\gamma)$ is equal to an independent GFF with boundary condition $c(\gamma) \in [-\sqrt{2}\lambda, \sqrt{2}\lambda]$. Furthermore, if there exists a finite sequence $\gamma_1, \dots, \gamma_k$ of loops in \widehat{A} such that γ_1 and γ_k respectively intersect ∂D and γ , then $c(\gamma) \in \{-\sqrt{2}\lambda, \sqrt{2}\lambda\}$. If one can find such a sequence with k even, then $c(\gamma) = \sqrt{2}\lambda$ and γ is the limit of the boundary of an odd hole; otherwise if k is odd, then $c(\gamma) = -\sqrt{2}\lambda$ and γ is the limit of the boundary of an even hole.

For both the free and wired double random currents models, when one conditions on the outermost cluster(s), the picture inside the holes of each outermost cluster is an independent free boundary double random currents model. This spatial Markov property remains true in the scaling limit (see Section 5.4). This, combined with Theorems 2.2 and 2.4 will allow us to deduce the scaling limit of the nested interfaces, as stated in Theorems 1.6 and 1.7, as well as their couplings with the limiting GFF.

2.3 A coupling between the double random current and the XOR-Ising model

In this section we discuss one of the central constructions of this article, namely the joint coupling of the double random current model and the XOR-Ising model (both their primal and dual versions) together with a height function that restricts to both the nesting field of the primal and the dual random current. In this coupling, the double random current and the XOR-Ising models are related together in the same way the Fortuin–Kasteleyn percolation with cluster-weight $q = 2$ is coupled to the Ising model in the Edwards–Sokal coupling [34]. Here, we state the results for a general inverse temperature β and coupling constants J . We start with the Edwards–Sokal property of the coupling.

Theorem 2.6. *Consider a finite (not necessarily planar) graph $G = (V, E)$ and the coupling $\mathbb{P}_{G,\beta}$ between two independent currents \mathbf{n}_1 and \mathbf{n}_2 , both with law $\mathbf{P}_{G,\beta}^\emptyset$, and a spin configuration obtained by sampling independently ± 1 -valued spins $(\tau_C : C \in \mathfrak{C}(\mathbf{n}_1 + \mathbf{n}_2))$, where $\mathfrak{C}(\mathbf{n}_1 + \mathbf{n}_2)$ is the collection of clusters of $\mathbf{n}_1 + \mathbf{n}_2$. Define $\tau = (\tau_v : v \in V)$, where $\tau_v = \tau_C$ and $C \in \mathfrak{C}(\mathbf{n}_1 + \mathbf{n}_2)$ the cluster containing v . Then, τ has the law of the XOR-Ising model $\mathbf{P}_{G,\beta}^{\text{XOR}}$.*

Proof. For every $A \subseteq V$, by definition of $\mathbb{P}_{G,\beta}$, we have

$$\mathbb{E}_{G,\beta} \left[\prod_{v \in A} \tau_v \right] = \mathbf{P}_{G,\beta}^\emptyset \otimes \mathbf{P}_{G,\beta}^\emptyset [\mathbf{n}_1 + \mathbf{n}_2 \in \mathcal{F}_A],$$

where $\mathbb{E}_{G,\beta}$ is the expectation with respect to $\mathbb{P}_{G,\beta}$, and where $\mathbf{n} \in \mathcal{F}_A$ is the event that each cluster of \mathbf{n} contains an even number of (possibly zero) vertices of A .

Now, the switching lemma [28, Lemma 2.1] gives that

$$\mathbf{P}_{G,\beta}^\emptyset \otimes \mathbf{P}_{G,\beta}^\emptyset[\mathbf{n}_1 + \mathbf{n}_2 \in \mathcal{F}_A] = \mu_{G,\beta} \left[\prod_{v \in A} \sigma_v \right]^2 = \mathbf{E}_{G,\beta}^{\text{XOR}} \left[\prod_{v \in A} \tau_v \right].$$

Since the spins are ± 1 -valued, this implies that the law of τ under $\mathbb{P}_{G,\beta}$ is the law of the XOR-Ising model at inverse temperature β (e.g. one can look at the characteristic function of the random vector τ and expand it into a finite sum of correlation functions as above). \square

An analogous coupling also holds for plus/plus boundary conditions, where this time one has to consider the random current model with wired boundary conditions and the cluster of the outer vertex \mathfrak{g} gets assigned spin $+$.

As mentioned, a stronger property, namely the following joint coupling of the primal and dual models can be established. We will provide a proof of this result at the end of Section 3.1.3 using a relation with the dimer model. In the statement we talk about the dual double random current and XOR-Ising models. These are the models defined on the dual graphs where the coupling constant $J_{e^*}^*$ on a dual edge e^* and the dual inverse temperature β^* are given by the Kramers–Wannier relation

$$\exp(-2\beta^* J_{e^*}^*) = \tanh(\beta J_e).$$

Recall that the critical inverse temperature β_c on the square lattice with coupling constants $J_e = 1$ for all $e \in E$ is self-dual, meaning that $\beta_c^* = \beta_c$.

Theorem 2.7 (Master coupling). *One can couple the following objects:*

1. a double random current model \mathbf{n} with free boundary conditions on the primal graph $G = (V, E)$, together with i.i.d. ± 1 -valued spins $(\tau_{\mathcal{C}} : \mathcal{C} \in \mathfrak{C}(\mathbf{n}))$ associated to each cluster of \mathbf{n} ,
2. the dual double random current model \mathbf{n}^\dagger with wired boundary conditions on the weak dual graph G^\dagger (equivalently with free boundary conditions on the full dual graph $G^* = (U, E^*)$) and with the dual coupling constants, together with i.i.d. ± 1 -valued spins $(\tau_{\mathcal{C}}^\dagger : \mathcal{C} \in \mathfrak{C}(\mathbf{n}^\dagger))$ associated with each cluster of \mathbf{n}^\dagger ,
3. a height function H defined on $V \cup U$,

in such a way that the following properties hold:

1. The spins $\tau = (\tau_v : v \in V)$, where $\tau_v = \tau_{\mathcal{C}}$, with \mathcal{C} being the cluster containing v , have the law of the XOR-Ising model $\mathbf{P}_{G,\beta}^{\text{XOR}}$.
2. The spins $\tau^\dagger = (\tau_u^\dagger : u \in U)$, conditioned on the spin of the outer vertex \mathfrak{g} being $+$, have the law of the dual XOR-Ising model $\mathbf{P}_{G^\dagger,\beta^*}^{\text{XOR},+}$.
3. The odd part of \mathbf{n} is equal to the collection of interfaces of τ^\dagger , and the odd part of \mathbf{n}^\dagger is equal to the collection of interfaces of τ .

4. For a face $u \in U$ and a vertex $v \in V$ incident on u , we have

$$H(u) - H(v) = \frac{1}{2}\tau_u^\dagger\tau_v.$$

It is clear that each cluster \mathcal{C} of \mathbf{n} (resp. \mathbf{n}^\dagger) can be assigned a well-defined dual spin $\tau_{\mathcal{C}}^\dagger$ (resp. $\tau_{\mathcal{C}}$). This is the spin assigned to any face of G (resp. G^*) incident on \mathcal{C} from the outside. With this definition, the height function H restricted to the faces of G (resp. G^*) has the law of the nesting field of \mathbf{n} with free boundary conditions (resp. \mathbf{n}^\dagger with wired boundary conditions) with labels associated to the clusters as in the definition (2.1) given by

$$\epsilon_{\mathcal{C}} = \tau_{\mathcal{C}}\tau_{\mathcal{C}}^\dagger. \quad (2.5)$$

5. The configurations \mathbf{n} and \mathbf{n}^\dagger are disjoint in the sense that $\mathbf{n}_e > 0$ implies $\mathbf{n}_{e^*}^\dagger = 0$ and $\mathbf{n}_{e^*}^\dagger > 0$ implies $\mathbf{n}_e = 0$, where e^* is the dual edge of e .

Recall that in the definition of the nesting field (2.1), the labels are independent given the current, and one can see that indeed the variables $(\epsilon_{\mathcal{C}})_{\mathcal{C} \in \mathfrak{C}(\mathbf{n})}$ as defined by (2.5) are independent given \mathbf{n} as $\tau_{\mathcal{C}}^\dagger$ is a deterministic function of \mathbf{n} , and $\tau_{\mathcal{C}}$ are independent by definition.

Although Property 5 will not be directly used in our arguments, it is an interesting feature of the coupling on its own. Indeed, from our scaling limit results we know that all the associated continuum interfaces do not cross, and Property 5 says that this holds already at the discrete level (and for arbitrary, not necessarily critical Ising models). We stress that the fact that the interfaces of τ and τ^\dagger are disjoint in the sense of Property 5 appears already in the works of Dubédat [22], and Boutilier and de Tilière [11]. However, Property 5 is a stronger statement as it concerns the full double random current, and not only its odd part.

Finally, an extension of this coupling to the Ashkin–Teller model can be found in the works [51, 52] that appeared before but were based on the current article. Here we will provide a different proof that uses the associated dimer model representation.

2.4 Scaling limit of the XOR-Ising interfaces

Let us now present the proof strategy of our main results on the convergence of XOR-Ising interfaces. Here we focus on the interplay between the discrete and continuous sides. A more detailed strategy in the continuum can be found in Section 8.

We first focus on the discussion of the proof for free boundary conditions (Theorem 1.2). In practice, we will prove a stronger result (Theorem 2.8 below) which states the joint convergence of the XOR-Ising model with free boundary conditions and the height function (coupled as in Theorem 2.7). Theorem 2.8 implies Theorem 1.2, and is also the main input for the proof of the scaling limit of the XOR-Ising interfaces with plus/plus boundary conditions.

Theorem 2.8. *Let $D \subsetneq \mathbb{C}$ be a simply connected Jordan domain. Let η_{XOR}^δ be the outer boundaries contour configuration of the XOR-Ising model with free boundary condition in D^δ . Then as $\delta \rightarrow 0$, $(\eta_{\text{XOR}}^\delta, h^\delta)$ (defined according to the coupling in Theorem 2.7) converges in distribution to a limit (η_{XOR}, h) . The collection of the outer boundaries of the outermost positive (resp. negative) XOR-Ising clusters in D^δ converges to $\mathcal{L}_{-(2\sqrt{2}+1)\lambda, \lambda}(h)$ (resp. $\mathcal{L}_{-\lambda, (2\sqrt{2}+1)\lambda}(h)$). More precisely, there are two types of outermost positive clusters 1, 3 and two types of outermost negative clusters 2, 4 as follows (see Fig. 2.3 for an illustration):*

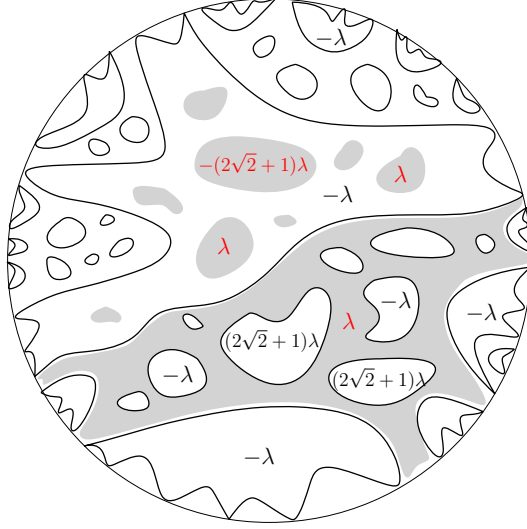


Figure 2.3: XOR-Ising with free boundary conditions. The black loops represent the outer boundaries of the outermost positive clusters. The black loops that touch the boundary correspond to those negative clusters of Type 2 (these loops all have inner boundary value $-\lambda$). The black loops that do not touch the boundary correspond to the negative clusters of Type 4 (these loops have inner boundary value $-\lambda$ or $(2\sqrt{2}+1)\lambda$). We also depict in grey a few (not all) outermost positive clusters. The grey cluster that touches the boundary belongs to Type 1. The other grey clusters are encircled by one of the black loops and belong to Type 3. We indicate the boundary values of these grey clusters in red.

1. The outermost positive clusters that are not encircled by any negative cluster.
2. The outermost negative clusters that are not encircled by any positive cluster.
3. The outermost positive clusters that are encircled by some negative cluster of Type 2.
4. The outermost negative clusters that are encircled by some positive cluster of Type 1.

The outer boundaries of the clusters of Types 1 and 2 respectively converge to $\mathcal{L}_{-\lambda,\lambda}^+(h)$ and $\mathcal{L}_{-\lambda,\lambda}^-(h)$.

For each limit γ of the outer boundary of an XOR-Ising cluster, γ is coupled with h in a way that $h|_{O(\gamma)}$ is equal to a constant plus a zero-boundary GFF. Conditionally on γ , the next layer of outermost clusters with the opposite sign in $O(\gamma)$ are distributed as $\mathcal{L}_{-2\lambda,2\sqrt{2}\lambda}$ in $O(\gamma)$.

In order to prove Theorem 2.8, we will first collect a number of results summarized in Proposition 2.9. The proof of Theorem 2.8 crucially relies on the convergence of the double random current (Theorem 2.2) and the coupling given in Theorem 2.7. Recall the notation from Section 2.2.2. To each double random current cluster with outer boundary $\ell \in B^\delta$ we assign a spin $s^\delta(\ell)$ which is equal to $\epsilon^\delta(\ell)$. Let C^δ denote the collection of the outer boundaries of the outermost XOR-Ising clusters (i.e., none of them is surrounded by any other XOR-Ising cluster). For each $\gamma \in C^\delta$, the XOR-Ising cluster corresponding to γ is associated with a spin $s^\delta(\gamma) \in \{-1, 1\}$ and let $S^\delta(\gamma)$ be the collection of loops in B^δ that intersect and are encircled

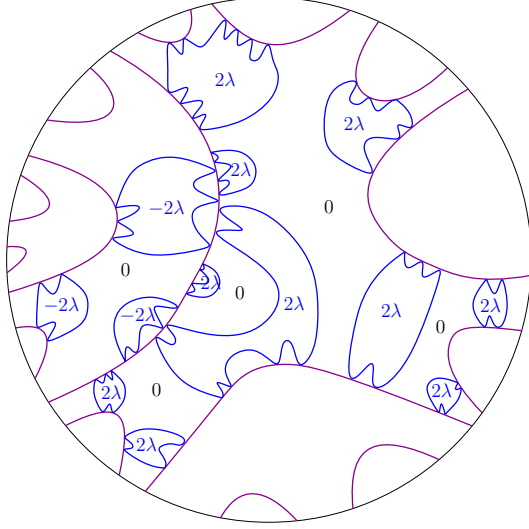


Figure 2.4: We draw the boundary-touching XOR-Ising interfaces in purple. These interfaces can be connected into loops in C . We also draw in blue the loops in S which are the loops in B which touch the loops in C . By Theorem 2.2, we know that h restricted to the blue loops have boundary conditions $\pm 2\lambda$. The loops in \tilde{S} are boundaries of the blank regions (not encircled by a blue loop) marked with 0, meaning that h restricted to a loop in \tilde{S} has 0 boundary condition.

by γ . For each $\ell \in S^\delta(\gamma)$, the double random current cluster corresponding to ℓ has the label $\epsilon^\delta(\ell) = s^\delta(\gamma)$. The connected components of $O(\gamma) \setminus \cup_{\ell \in S^\delta(\gamma)} O(\ell)$ are all simply connected, and we let $\tilde{S}^\delta(\gamma)$ be the collection of loops which consists of the outer boundaries of these connected components. Let S^δ (resp. \tilde{S}^δ) be the union of the $S^\delta(\gamma)$ (resp. $\tilde{S}^\delta(\gamma)$) for $\gamma \in C^\delta$. See Fig. 2.4 for an illustration of these objects in the scaling limit (the next proposition states that there exists a subsequential limit).

Proposition 2.9. *Fix a simply connected domain $D \subsetneq \mathbb{C}$ and consider the measure \mathbb{P}_{D^δ} . Then the family $(C^\delta, s^\delta, S^\delta, \tilde{S}^\delta, \epsilon^\delta, B^\delta, A^\delta, h^\delta)_{\delta > 0}$ is tight for the topology of weak convergence. Moreover, for every subsequential limit $(C, s, S, \tilde{S}, \epsilon, B, A, \epsilon, h)$:*

1. (B, A, ϵ, h) satisfies the properties of Proposition 2.3. The sets S, \tilde{S}, C consist of simple loops. The set C is not equal to $\{\partial D\}$.
2. $S \subseteq B$ and every loop in $S \cup \tilde{S}$ is encircled by a loop in C . For each $\gamma \in C$, let $S(\gamma)$ be the collection of loops in S which are encircled by γ . Then $S(\gamma)$ coincides with the set of loops in B that intersect γ . In addition to this, for every loop $\ell \in S(\gamma)$,

$$\epsilon(\ell) = s(\gamma). \quad (2.6)$$

3. (Thin local set) For any test function f , we have

$$\int f(z)h(z)dz = \sum_{\ell \in S \cup \tilde{S}} \int_{O(\ell)} f(z)h|_{O(\ell)}(z)dz,$$

where the $h|_{O(\ell)}$ are random distributions with support in $O(\ell)$. Furthermore, the $h|_{O(\ell)}$ with $\ell \in \tilde{S}$ are independent GFF with boundary value 0.

4. For any loop in C , if we parametrize it as a curve in a continuous and injective way, then its intersection with B does not contain any sub-curve of positive time length.

Let us make some comments on Proposition 2.9 and how it is used to prove Theorem 2.8.

- Again, tightness is a direct consequence of the second paper [28] and the first item is simply Proposition 2.3. The second item is fairly straightforward, while the third follows from the properties of the discrete coupling together with the joint convergence. The fourth item on the other hand follows from delicate crossing estimates in fractal domains that are obtained in [28].

- We remark that the interfaces of C do not satisfy the spatial Markov property in the discrete. As we have mentioned earlier, this is also the main difficulty in identifying the scaling limits of the XOR-Ising interfaces using conventional methods.

To identify C , the key lies in the set $S^\delta \cup \tilde{S}^\delta$. The loops in \tilde{S}^δ satisfy the spatial Markov property in the discrete. The loops in $S \subseteq B$ are proved to be part of $\text{CLE}_4(h)$ in Theorem 2.2. Combined with Property 3, we can deduce that the gasket of $S \cup \tilde{S}$ is a thin local set with boundary values in $\{-2\lambda, 0, 2\lambda\}$. We are then in a position to apply the characterization of thin local sets with boundary values in $\{-\mu, 0, \mu\}$ (Theorem 7.8). Again, we need to combine the properties of such local sets with the geometric properties of the interfaces in C, S, B to pin down the joint law of $(C, s, S, \tilde{S}, \epsilon, B, A, \epsilon, h)$.

- Proposition 2.9 only addresses the outermost double random current clusters. To understand the scaling limit of XOR-Ising interfaces (even just the outermost ones), we need to look at the nested double random current clusters, in order to do so we rely on the spatial Markov property of the loops in $A(\gamma)$ for every $\gamma \in S$.

For the XOR-Ising on the dual graph which has plus/plus boundary conditions, we will prove the following result.

Theorem 2.10. *Let $D \subsetneq \mathbb{C}$ be a simply connected domain such that ∂D is C^1 . Let $\hat{\eta}_{\text{XOR}}^\delta$ be the outer boundaries contour configuration of the dual XOR-Ising model on $(D^\delta)^\dagger$ with plus/plus boundary conditions. Then as $\delta \rightarrow 0$, $(\hat{\eta}_{\text{XOR}}^\delta, h^\delta)$ converges in distribution to a limit $(\hat{\eta}_{\text{XOR}}, h)$ where h is a GFF in D with zero boundary conditions and the outermost loops in η is equal to $\mathcal{L}_{-(\sqrt{2}+1)\lambda, (\sqrt{2}+1)\lambda}(h)$. If the outer boundary of a cluster converges to γ , then the outer boundaries of the outermost clusters that are enclosed by this cluster with the opposite sign converge to $\mathcal{L}_{-2\lambda, 2\sqrt{2}\lambda}$ in $O(\gamma)$.*

Theorem 2.10 implies Theorem 1.5. The proof of Theorem 2.10 combines Theorem 2.4, Property 2 in Theorem 2.7 and Theorem 2.8.

2.5 Coupling of various models in the continuum limit

We have described a coupling between four models (the double random current and XOR-Ising models on the primal and dual lattices) and one height function in Theorem 2.7. A remarkable consequence is that this coupling can be carried through to the continuum limit.

More precisely, Theorems 2.2, 2.4, 2.8 and 2.10 imply that the four coupled models and the height function converge jointly, and the joint limit is described by these theorems where we use the same height function which converges to the same GFF h . Therefore, the interfaces of the double random current and XOR-Ising models on the primal and dual graphs converge jointly to level loops at different heights of the same GFF. For simplicity, we have focused in Theorems 2.2, 2.4, 2.8 and 2.10 on the description of the coupling of the outermost interfaces of the corresponding models with h . However, it is not difficult to work out the coupling of the nested interfaces with h , using the spatial Markov property of certain loops. Consequently, we fully understand how the nested interfaces of the four models interact with each other. A more detailed description is postponed to Section 8.2. Among other properties, the interfaces of different models a.s. do not cross each other (since level loops of a GFF do not cross each other), like in the discrete (Property 5 from Theorem 2.7).

As the discrete coupling is similar in spirit to the Edwards–Sokal coupling, the continuum picture also bears similarities to that of CLE percolation [61]. For example, given the scaling limit of the outermost double random current clusters with free boundary conditions (whose outer boundaries are distributed as a CLE_4) and i.i.d. labels in $\{-1, 1\}$ for each cluster, the first layer of the scaling limit of the XOR-Ising interfaces with free boundary conditions should be the interfaces between the aggregated $+$ and $-$ clusters. However, unlike in the discrete, it is not possible to define such an aggregation directly in the continuum, since none of the CLE_4 loops touch each other. There is nevertheless a notion of *continuous percolation interface* (CPI) in the CLE carpet [61]. For a CLE_4 where each loop receives an i.i.d. and symmetric sign, its associated CPI is the unique interface which satisfies a certain conformal invariance, a spatial Markov property, and which explores the CLE_4 carpet in a way that leaves $+$ loops on its left and $-$ loops on its right (see [61] for more details). This interface is distributed as $\mathbb{A}_{-\lambda, \lambda}$ [61, Proposition 5.3]. This is indeed the same as the interfaces stated in Theorem 2.8. However, we point out that we *a priori* did not know the conformal invariance and the spatial Markov property of the limiting interfaces, so CPI cannot be used to prove our results, but constitutes an *a posteriori* explanation of the continuum picture.

2.6 Input from the second paper of the series

In this section we briefly recap some inputs from [28] that are used in this paper. We refer to [28] for the proofs. We only mention the main tools from [28] that we will use and refer, later in the proof, to the precise statements of [28] when they were not mentioned in this section.

Results for the double random current model As mentioned above, we need tightness results for several families of loops, notably for the outer boundaries of the double random current clusters. This is done using an Aizenman–Burchard-type criterion for the double random current. Below, for a subset A of vertices, a A -cluster is a cluster for the (current or XOR-Ising) configuration restricted to A . A *domain* D is a subgraph of \mathbb{Z}^2 whose boundary is a self-avoiding polygon in \mathbb{Z}^2 . Let $\Lambda_r := [-r, r]^2$ and $\text{Ann}(r, R) := \Lambda_R \setminus \Lambda_{r-1}$. Call an $\text{Ann}(r, R)$ -cluster *crossing* if it intersects both $\partial\Lambda_r$ and $\partial\Lambda_R$. For an integer $k \geq 1$, let $A_{2k}(r, R)$ be the event⁴ that there are k distinct $\text{Ann}(r, R)$ -clusters in $\mathbf{n}_1 + \mathbf{n}_2$ crossing $\text{Ann}(r, R)$.

⁴The subscript $2k$ instead of k is meant to illustrate that there are k $\text{Ann}(r, R)$ -clusters from inside to outside separated by k dual clusters separating them.

Theorem 2.11 (Aizenman–Burchard criterion for the double random current model). *There exist sequences $(C_k)_{k \geq 1}, (\lambda_k)_{k \geq 1}$ with λ_k tending to infinity as $k \rightarrow \infty$, such that for every domain D , every $k \geq 1$ and all r, R with $1 \leq r \leq R/2$,*

$$\mathbf{P}_{D,D}^{\emptyset,\emptyset}[A_{2k}(r, R)] \leq C_k \left(\frac{r}{R}\right)^{\lambda_k}. \quad (2.7)$$

We will also need some a priori properties of possible subsequential scaling limits. These will be obtained using estimates in the discrete on certain four-arm type events. We list them now. Let

$$A_4^\square(r, R) := \{\text{there exist two } \Lambda_R\text{-clusters crossing } \text{Ann}(r, R)\}$$

and let $A_4^\square(x, r, R)$ be the translate of $A_4^\square(r, R)$ by x .

Theorem 2.12. *There exists $C > 0$ such that for all r, R with $1 \leq r \leq R$,*

$$\mathbf{P}_{\mathbb{Z}^2, \mathbb{Z}^2}^{\emptyset,\emptyset}[A_4^\square(r, R)] \leq C(r/R)^2. \quad (2.8)$$

Furthermore, for every $\varepsilon > 0$, there exists $\eta = \eta(\varepsilon) > 0$ such that for all r, R with $1 \leq r \leq \eta R$ and every domain $\Omega \supset \Lambda_{2R}$,

$$\mathbf{P}_{\Omega, \Omega}^{\emptyset,\emptyset}[\exists x \in \Lambda_R : A_4^\square(x, r, R)] \leq \varepsilon. \quad (2.9)$$

The result is coherent with the fact that the scaling limit of the outer boundary of large clusters in $\mathbf{n}_1 + \mathbf{n}_2$ is given by CLE_4 , which is known to be made of simple loops that do not touch each other. Interestingly, to derive the convergence to the continuum object it will be necessary to first prove this property at the discrete level.

We turn to a second result of the same type. For a current \mathbf{n} , let \mathbf{n}^* be the set of dual edges e^* with $\mathbf{n}_e = 0$. For a dual path $\gamma = (e_1^*, e_2^*, \dots, e_k^*)$, call the \mathbf{n} -flux through γ the sum of the \mathbf{n}_{e_i} . Call an $\text{Ann}(r, R)$ -hole in $\mathbf{n}_1 + \mathbf{n}_2$ a connected component of $(\mathbf{n}_1 + \mathbf{n}_2)^*$ restricted to $\text{Ann}(r, R)^*$ (note that it can be seen as a collection of faces). An $\text{Ann}(r, R)$ -hole is said to be *crossing* $\text{Ann}(r, R)$ if it intersects $\partial\Lambda_r^*$ and $\partial\Lambda_R^*$. Consider the event

$$A_4^\blacksquare(r, R) := \left\{ \begin{array}{l} \text{there exist two } \text{Ann}(r, R)\text{-holes crossing } \text{Ann}(r, R) \text{ and the} \\ \text{shortest dual path between them has even } (\mathbf{n}_1 + \mathbf{n}_2)\text{-flux} \end{array} \right\}$$

(see Fig. 2.5). Denote its translate by x by $A_4^\blacksquare(x, r, R)$.

Theorem 2.13. *There exists $C > 0$ such that for all r, R with $1 \leq r \leq R$,*

$$\mathbf{P}_{\mathbb{Z}^2, \mathbb{Z}^2}^{\emptyset,\emptyset}[A_4^\blacksquare(r, R)] \leq C(r/R)^2. \quad (2.10)$$

Furthermore, for every $\varepsilon > 0$, there exists $\eta = \eta(\varepsilon) > 0$ such that for all r, R with $1 \leq r \leq \eta R$ and every domain $D \supset \Lambda_{2R}$,

$$\mathbf{P}_{\Omega, \Omega}^{\emptyset,\emptyset}[\exists x \in \Lambda_R : A_4^\blacksquare(x, r, R)] \leq \varepsilon. \quad (2.11)$$

Let us mention that the previous results are obtained using the following key statement, which is of independent interest and is also directly used in this paper. For a set D , let $\partial_r D$ be the set of vertices in D that are within a distance r from ∂D .

Theorem 2.14 (Connection probabilities close to the boundary for double random current). *There exists $c > 0$ such that for all r, R with $1 \leq r \leq R$ and every domain D containing Λ_{2R} but not Λ_{3R} ,*

$$\frac{c}{\log(R/r)} \leq \mathbf{P}_{D,D}^{\emptyset,\emptyset}[\Lambda_R \xrightarrow{\mathbf{n}_1 + \mathbf{n}_2} \partial_r D] \leq \epsilon\left(\frac{r}{R}\right),$$

where $x \mapsto \epsilon(x)$ is an explicit function tending to 0 as x tends to 0.

We predict that the upper bound should be true for $\epsilon(x) := C/\log(1/x)$ but we do not need such a precise estimate here. Again, the result is coherent with the fact that the scaling limit of the outer boundary of large clusters in $\mathbf{n}_1 + \mathbf{n}_2$ is given by CLE_4 .

The lower bound is to be compared with recent estimates [31, 32] obtained for another dependent percolation model, namely the critical Fortuin–Kasteleyn random cluster model with cluster-weight $q \in [1, 4)$. There, it was proved that the crossing probability is bounded from below by a constant $c = c(q) > 0$ uniformly in r/R . We expect that the behaviour of the critical random cluster model with cluster weight $q = 4$ on the other hand is comparable to the behaviour presented here: large clusters do not come close to the boundary of domains when the boundary conditions are free.

Results for the XOR Ising model Of course, as for the double random current we need tightness for the XOR-Ising interfaces which, again, is obtained via an Aizenman–Burchard-type criterion. For an integer $k \geq 1$, let $A_{2k}^{\text{XOR}}(r, R)$ be the event⁵ that there are k clusters of pluses in $\text{Ann}(r, R)$ that are crossing.

Theorem 2.15 (Aizenman–Burchard criterion for the XOR-Ising model). *There exist sequences $(C_k)_{k \geq 1}$, $(\lambda_k)_{k \geq 1}$ with λ_k tending to infinity as $k \rightarrow \infty$, such that for every domain D , every $k \geq 1$ and all r, R with $1 \leq r \leq R$,*

$$\mathbf{P}_{\Omega}^{\text{XOR}}[A_{2k}^{\text{XOR}}(r, R)] \leq C_k \left(\frac{r}{R}\right)^{\lambda_k}. \quad (2.12)$$

We will also need the following result similar to the results obtained recently in [32] for random-cluster models (however, the techniques to obtain the two results are very different). Let (D, a, b, c, d) be a *quad*, meaning a domain D with four distinct vertices a, b, c, d found on its outer boundary in counter-clockwise order. The *extremal distance* $\ell_D[(ab), (cd)]$ between (ab) and (cd) inside D is defined as the unique $\ell > 0$ such that there exists a conformal map from the continuous domain⁶ naturally associated with D to the rectangle $(0, \ell) \times (0, 1)$, with a, b, c, d being mapped (by the continuous extension of the conformal map) to the corners of $[0, \ell] \times [0, 1]$, in counterclockwise order, starting with the lower-left corner.

Corollary 2.16 (Crossing estimates for the XOR-Ising model). *For every $\kappa \in (0, \infty)$, there exists $c = c(\kappa) > 0$ such that for every quad (D, a, b, c, d) with $\kappa \leq \ell_D[(ab), (cd)] \leq 1/\kappa$,*

$$c \leq \mathbf{P}_{\Omega}^{\text{XOR}}[(ab) \xrightarrow{+} (cd)] \leq 1 - c. \quad (2.13)$$

⁵The subscript $2k$ instead of k is meant to illustrate that there are k disjoint paths of pluses from inside to outside separated by k paths of minuses separating them (the paths of minuses only need to be $*$ -connected).

⁶The quad D can be seen as a continuous domain of the plane by considering the counter-clockwise loop γ around D (up to cyclic permutation this loop is unique) and identifying it to a continuous piecewise linear curve in \mathbb{R}^2 by seeing all its edges as segments of length 1. Then, the continuous domain associated to D is obtained by taking the bounded connected component of $\mathbb{R}^2 \setminus \gamma$.

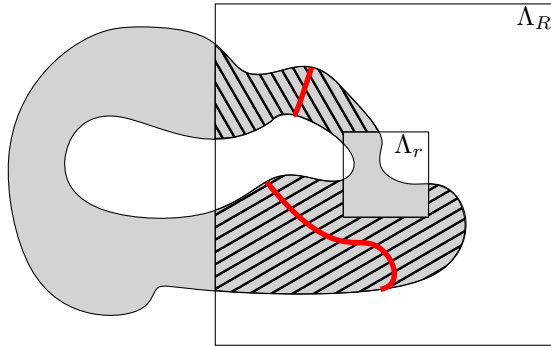


Figure 2.5: A depiction of the event $A_4^{\blacksquare}(r, R)$.

Organization The paper is organized as follows. In Section 3 we recall the relationship between different discrete models and derive a connection between the inverse Kasteleyn matrix and complex-valued fermionic observables. While some (but not all) of these results are not completely new, they are scattered around the literature and we therefore review them here. In Section 4 we derive Theorem 2.1. Section 5.1 is composed of the arguments leading to Propositions 2.3, 2.5, and 2.9. Sections 6, 7 and 8 are dedicated to the continuum part of the proof. Section 6 presents more preliminaries on the continuum objects. Section 7 is devoted to the identification of the limit of double random currents. Section 8 is devoted to the identification of the limit of the XOR-Ising models.

Acknowledgements The first author was supported by the NCCR SwissMap from the FNS. This project has received funding from the European Research Council (ERC) under the European Union’s Horizon 2020 research and innovation program (grant agreement No. 757296). The beginning of the project involved a number of people, including Gourab Ray, Benoit Laslier, and Matan Harel. We thank them for inspiring discussions. The project would not have been possible without the numerous contributions of Aran Raoufi to whom we are very thankful. We also thank Pierre Nolin for useful comments on an earlier version of this article.

3 Preliminaries on discrete models

3.1 Mappings between discrete models

In this section we recall the combinatorial equivalences between double random currents, alternating flows and bipartite dimers established in [27, 53]. We will later use them to derive a version of Dubédat’s bosonization identity [22]. An additional black-white symmetry for correlators of monomer insertions is established that is not apparent in [22]. The results here are stated for general Ising models on arbitrary planar graphs $G = (V, E)$ and with arbitrary coupling constants $(J_e)_{e \in E}$. We focus on the free boundary conditions case and the wired boundary conditions can be treated analogously, replacing G with G^+ . We will actually mostly consider wired boundary conditions on the dual graph G^* which, as mentioned in Remark 1.4, one can think of as $(G^\dagger)^+$, where G^\dagger is the weak dual of G whose vertex set does

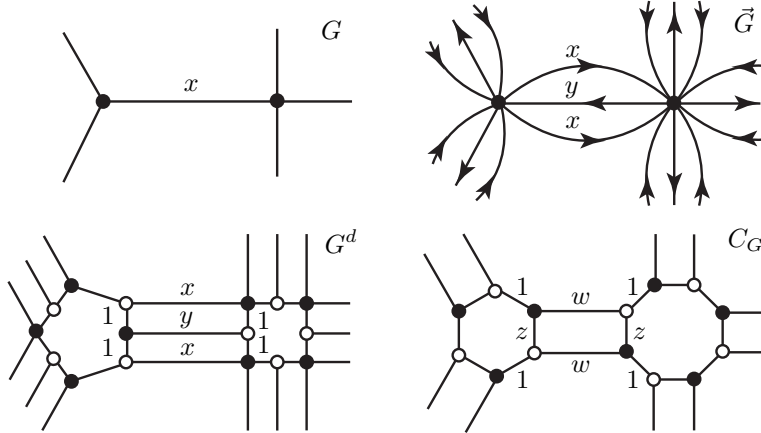


Figure 3.1: One can construct the graphs \vec{G} , G^d and C_G locally around each vertex of G . The weights satisfy $y = \frac{2x}{1-x^2}$, $w = \frac{2x}{1+x^2}$, $z = \frac{1-x^2}{1+x^2}$. Here $x = x_e$ is the high-temperature weight equal to $\tanh(\beta J_e)$. The edges carrying weight 1 in G^d (resp. in C_G) are called short (resp. roads), and the remaining edges are called long (resp. streets).

not contain the unbounded faces of G .

We start by describing the relevant decorated graphs: the double random current model on a graph G will be related to the alternating flow model on a directed graph \vec{G} , and the dimer model on two bipartite graphs G^d and C_G . All these graphs are weighted, and their local structure together with the corresponding edge weights are shown in Fig. 3.1. We now describe their construction in detail.

Given G , \vec{G} is obtained by replacing each edge e of G by three parallel directed edges e_{s1} , e_m , e_{s2} such that the orientation of the side (or outer) edges e_{s1} and e_{s2} is opposite to the orientation of the middle edge e_m . The orientation of the middle edge can be chosen arbitrarily.

To obtain G^d from \vec{G} , we replace each vertex v of \vec{G} by a cycle of vertices of even length which is given by the number of times the orientation of edges in \vec{G} incident on v changes when going around v . We colour the new vertices black if the corresponding edges are incoming into v and white otherwise. We then connect the white vertices in a cycle corresponding to v with the appropriate black vertices in a cycle corresponding to v' , where v and v' are adjacent in \vec{G} . We call *long* all the edges of G^d that correspond to an edge of \vec{G} , and *short* the remaining edges connecting the vertices in the cycles.

The last graph C_G can be constructed directly from G by replacing each edge of G by a quadrangle of edges, and then connecting two quadrangles by an edge if the corresponding edges of G share a vertex and are incident to the same face (see Fig. 3.1). Following [22], we call *streets* the edges in the quadrangles and *roads* those connecting the quadrangles (which represent cities).

We note that the set of faces U (resp. vertices V) of G naturally embeds into the set of faces of \vec{G} , G^d and C_G (resp. G^d and C_G). We therefore think of U and V as subsets of the set of faces of the respective decorated graphs (e.g., when we talk about equality in distribution of the height function on C_G and the nesting field on G).

In the remainder of this section we describe the mappings between the different models in the following order: In Section 3.1.1, Alternating flows on \vec{G} are mapped by an application θ to the image by a map ϑ of double random currents on G . In Section 3.1.2, dimers on G^d are mapped by an application π to alternating flows on \vec{G} . In Section 3.1.3, dimers on G^d are mapped to dimers on C_G . The corresponding statements for wired boundary conditions can be recovered by replacing G with G^+ .

The first two maps yield relations between configurations of the associated models, and the last map is described as a sequence of local transformations (urban renewals) of the graphs C_G or G^d that does not change the distribution of the height function on a certain subset of the faces of these two graphs.

We first describe relations on the level of distributions on configurations where no sources or disorders are imposed. Later on (in Section 3.2) we increase the complexity by introducing sources.

3.1.1 Double random currents on G and alternating flows on \vec{G}

A *sourceless alternating flow* F is a set of edges of the directed graph \vec{G} satisfying the *alternating condition*, i.e., for each vertex v , the edges in F that are incident to v alternate between being oriented towards and away from v when going around v (see Fig. 3.2). In particular, the same number of edges enters and leaves v . We denote the set of sourceless alternating flows on \vec{G} by \mathcal{F}^\emptyset , and following [53], we define a probability measure on \mathcal{F}^\emptyset by the formula, for every $F \in \mathcal{F}^\emptyset$,

$$\mathbf{P}_{\text{flow}}^\emptyset(F) := \frac{1}{Z_{\text{flow}}^\emptyset} \mathbf{w}_{\text{flow}}(F), \quad (3.1)$$

where $Z_{\text{flow}}^\emptyset$ is the partition function of sourceless flows and, if $V(F)$ denotes the set of vertices in the graph (V, F) that have at least one incident edge,

$$\mathbf{w}_{\text{flow}}(F) := 2^{|V|-|V(F)|} \prod_{e \in F} x_e, \quad (3.2)$$

with the weights x_e as in Fig. 3.1. We also define the *height function* of a flow F to be a function $h = h_F$ defined on the faces of \vec{G} in the following way:

- (i) $h(u_0) = 0$ for the unbounded face u_0 ,
- (ii) for every other face u , choose a path γ connecting u_0 and u , and define $h(u)$ to be total flux of F through γ , i.e., the number of edges in F crossing γ from left to right minus the number of edges crossing γ from right to left.

The function h is well defined, i.e., independent of the choice of γ , since at each $v \in V$, the same number of edges of F enters and leaves v (and so the total flux of F through any closed path of faces is zero).

We are ready to state the correspondence between double random currents and alternating flows. Consider the map ϑ from Ω^B to the set Ω^B of pairs $(E_{\text{odd}}, E_{\text{even}})$ of subsets of E with E_{odd} of even degree at every vertex in $V \setminus B$, and odd degree at every vertex in B , obtained as follows:

$$\vartheta(\mathbf{n}) := (\mathbf{n}_{\text{odd}}, \mathbf{n}_{\text{even}}) \text{ where } \begin{array}{l} \mathbf{n}_{\text{odd}} \text{ is the set of edges } e \text{ with } \mathbf{n}_e \text{ odd,} \\ \mathbf{n}_{\text{even}} \text{ is the set of edges with } \mathbf{n}_e \text{ even and strictly positive.} \end{array}$$

In what follows we will often identify a current \mathbf{n} with the pair $(\mathbf{n}_{\text{odd}}, \mathbf{n}_{\text{even}})$ as it carries all the relevant information for our considerations.

Also define a map $\theta : \mathcal{F}^\emptyset \rightarrow \Omega^\emptyset$ as follows. For every $F \in \mathcal{F}^\emptyset$ and every $e \in E$, consider the number of corresponding directed edges e_m, e_{s1}, e_{s2} that are present in F . Let $\mathbf{n}_{\text{odd}} \subseteq E$ be the set with one or three such present edges, and $\mathbf{n}_{\text{even}} \subseteq E$ the set with exactly two such edges, and set

$$\theta(F) := (\mathbf{n}_{\text{odd}}, \mathbf{n}_{\text{even}}).$$

Denote by $\theta_* \mathbf{P}_{\text{flow}}^\emptyset$ the pushforward measure on Ω^\emptyset . The following result was proved in [27, 53].

Lemma 3.1 ([27]). *We have $\theta_* \mathbf{P}_{\text{flow}}^\emptyset = \vartheta_* \mathbf{P}_{\text{dcur}}^\emptyset$. Moreover, under this identification the restrictions to U of the nesting field of double random currents and the height function of the alternating flows have the same distribution.*

Proof. This is a consequence of the fact that the total weight of all alternating flows corresponding to a cluster in the double random current, and whose outer boundary is oriented clockwise is the same as those oriented counterclockwise (see also the proof of Lemma 3.7). This corresponds to the fact that the nesting field is defined using symmetric coin flip random variables $\epsilon_\mathcal{G}$. Moreover, the sum of these two weights is the same as the weight of the cluster in the double random current model. The details are provided in [27]. \square

3.1.2 Alternating flows on \vec{G} and dimers on G^d

Consider a weighted graph G . Recall that a *dimer cover* (or *perfect matching*) M of G is a subset of edges such that every vertex of the graph is incident to exactly one edge of M . We write $\mathcal{M}(G)$ for the set of all dimer covers of G . The *dimer model* is a probability measure on $\mathcal{M}(G)$ which assign a probability to a dimer cover that is proportional to the product of the edge-weights over the dimer cover.

To each dimer cover M on a bipartite planar finite graph G (implicitly colored in black and white in a bipartite fashion, one can associate a *1-form* f_M (i.e. a function defined on directed edges which is antisymmetric under a change of orientation) satisfying $f_M((v, v')) = -f_M((v', v)) = 1$ if $\{v, v'\} \in M$ and v is white, and $f_M((v, v')) = 0$ otherwise. For a 1-form f and a vertex v , let $df(v) = \sum_{v' \sim v} f((v, v'))$ be the *divergence* of f at v . Note that for a dimer cover M , $df_M(v) = 1$ if v is white, and $df_M(v) = -1$ if v is black. Fixing a reference 1-form f_0 with the same divergence, we define the *height function* $h = h_M$ by

- (i) $h(u_0) = 0$ for the unbounded face u_0 ,
- (ii) for every other face u , choose a dual path γ connecting u_0 and u , and define $h(u)$ to be the total flux of $f_M - f_0$ through γ , i.e., the sum of values of $f_M - f_0$ over the edges crossing γ from left to right.

The height function is well defined, i.e. independent of the choice of γ , since $f_M - f_0$ is a divergence-free flow, i.e. $d(f_M - f_0) = 0$.

We will write $\mathbf{P}_{G^d}^\emptyset$ for the dimer model measure on G^d with weights as in Fig. 3.1. We also fix a reference 1-form f_0 on G^d given by

- $f_0((w, b)) = -f_0((b, w)) = 1/2$ if $\{w, b\}$ is a short edge and w is white,

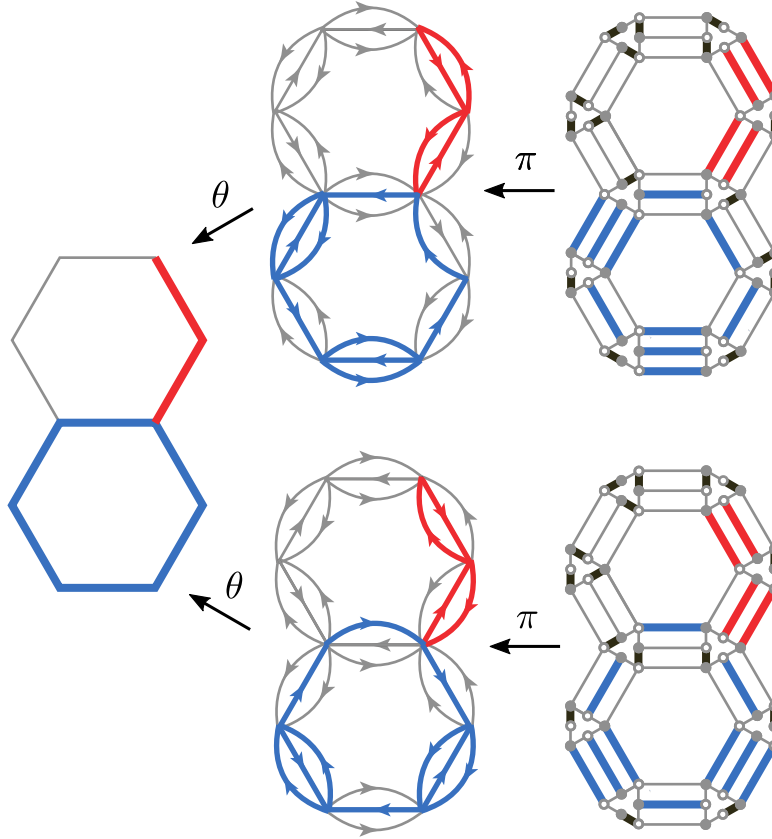


Figure 3.2: Left: A configuration $\vartheta(\mathbf{n}) = (\mathbf{n}_{\text{odd}}, \mathbf{n}_{\text{even}})$ on a piece of the hexagonal lattice G . The blue edges represent \mathbf{n}_{odd} and the red edges represent \mathbf{n}_{even} . The blue and red edges together form one cluster \mathcal{C} . Middle: Two alternating flow configurations on \vec{G} mapped to $\vartheta(\mathbf{n})$ under θ . The two clusters have opposite orientations of the outer boundary. Depending on this orientation the height function either increases or decreases by one when going from the outside to the inside of the lower hexagon. This corresponds to two different outcomes for the label $\epsilon_{\mathcal{C}}$ in the definition of the nesting field (2.1). Right: Two dimer configurations on G^d that map to the corresponding alternating flows under π . Note that the parity of the height function on G^d restricted to the vertices of \mathcal{C} and shifted by $1/2$ changes whenever the sign of $\epsilon_{\mathcal{C}}$ changes. This can be seen from the placement of the dimers on the short edges. This property is used in the proof of Theorem 2.7. On the other hand the parity of the height function on the faces of G is independent of $\epsilon_{\mathcal{C}}$.

We also note that both π and θ are many-to-one maps.

- $f_0((w, b)) = f_0((b, w)) = 0$ if $\{w, b\}$ is a long edge.

We now describe a straightforward map π from the dimer covers on G^d to alternating flows on \vec{G} that preserves the law of the height function. We note that one could carry out the same discussion and make a connection with double random currents directly, without introducing alternating flows. However, we find the language of alternating flows particularly convenient to express some of the crucial steps discussed later on (especially Lemmata 3.7 and 3.8). To this end, to each matching $M \in \mathcal{M}(G^d)$, associate a flow $\pi(M) \in \mathcal{F}^\emptyset$ by replacing each long edge in M by the corresponding directed edge in \vec{G} . One can check that this always produces an alternating flow. Indeed, assuming otherwise, there would be two consecutive edges in $F(M)$ of the same orientation, and therefore the path of short edges connecting them in a cycle would be of odd length and therefore could not have a dimer cover, which is a contradiction. Let $\pi_*\mathbf{P}_{G^d}^\emptyset$ be the pushforward measure on \mathcal{F}^\emptyset under the map π .

Lemma 3.2 ([27]). *We have $\pi_*\mathbf{P}_{G^d}^\emptyset = \mathbf{P}_{\text{flow}}^\emptyset$. Moreover, under this identification, the restriction to U of the height functions of the dimer model and alternating flows have the same distribution.*

Proof. This is a consequence of the fact that the reference 1-form vanishes on long edges, and hence its contribution to the increment of the height function across a long edge of G^d is equal to zero, and the fact that the weights of the edges of \vec{G} and the long edges of G^d are the same. Moreover, if a vertex v has zero flow through it, i.e. $v \in V \setminus V(F)$, then there are exactly 2 dimer covers of the cycle of short edges of G^d corresponding to v . Since both of these covers have total edge-weight 1, this accounts for the factor $2^{|V|-|V(F)|}$ in (3.2). \square

3.1.3 Dimers on G^d and on C_G

We will write $\mathbf{P}_{C_G}^\emptyset$ for the dimer model measure on C_G with weights as in Fig. 3.1. The dimer models on G^d and $(G^*)^d$ are closely related to the dimer model on C_G (as was described in [27]) using standard dimer model transformations called the vertex splitting and urban renewal, see Fig. 3.3.

Lemma 3.3 ([27]). *One can transform G^d and $(G^*)^d$ to C_G (and the other way around) using urban renewals and vertex splittings.*

Proof. We will describe how to transform G^d to C_G . The second part follows since C_G is symmetric with respect to G and G^* .

To this end, note that to each edge e in G , there corresponds one quadrilateral in C_G , and two quadrilaterals in G^d . Given e , choose for the internal quadrilateral of urban renewal the quadrilateral in G^d with the opposite colors of vertices. Then, split each vertex that the chosen quadrilateral shares with a quadrilateral corresponding to a different edge of G . In this way we find ourselves in the situation from the upper left panel in Fig. 3.3. After performing urban renewal and collapsing the doubled edge, we are left with one quadrilateral as desired. One can check that the weights that we obtain match those from Fig. 3.1. We then repeat the procedure for every edge of G . The resulting graph is C_G . \square

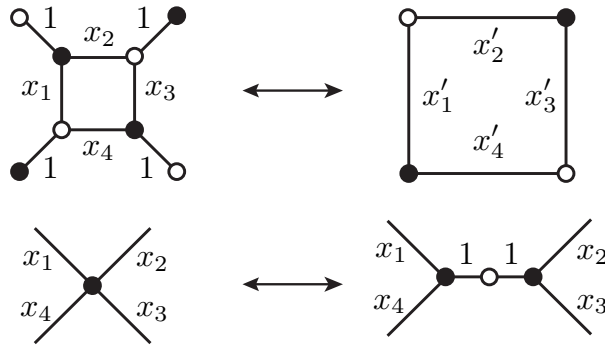


Figure 3.3: Urban renewal and vertex splitting are transformations of weighted graphs preserving the distribution of dimers and the height function outside the modified region. The weights in urban renewal satisfy $x'_1 = \frac{x_3}{x_1x_3+x_2x_4}$, $x'_2 = \frac{x_4}{x_1x_3+x_2x_4}$, $x'_3 = \frac{x_1}{x_1x_3+x_2x_4}$, $x'_4 = \frac{x_2}{x_1x_3+x_2x_4}$.

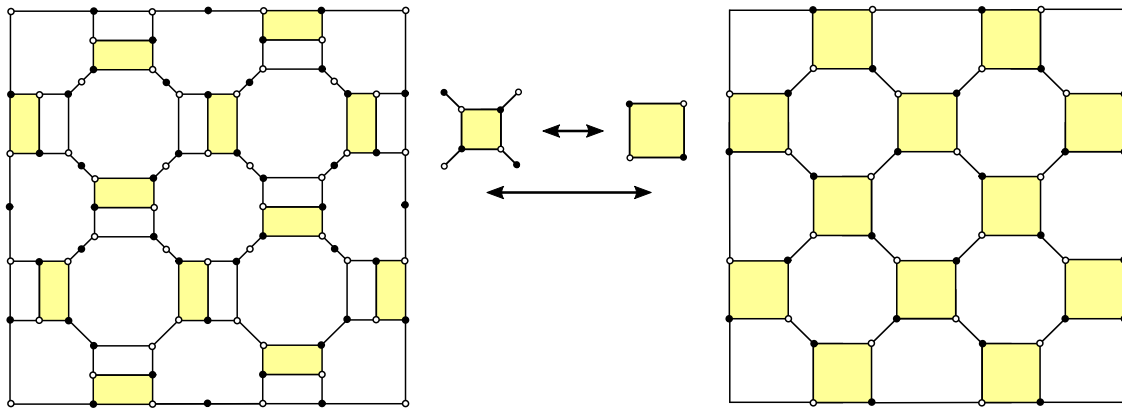


Figure 3.4: An example of the correspondence between dimer models on G^d and C_G . The yellow quadrilaterals are transformed using urban renewal moves. The underlying graph G is a 3×3 piece of the square lattice.

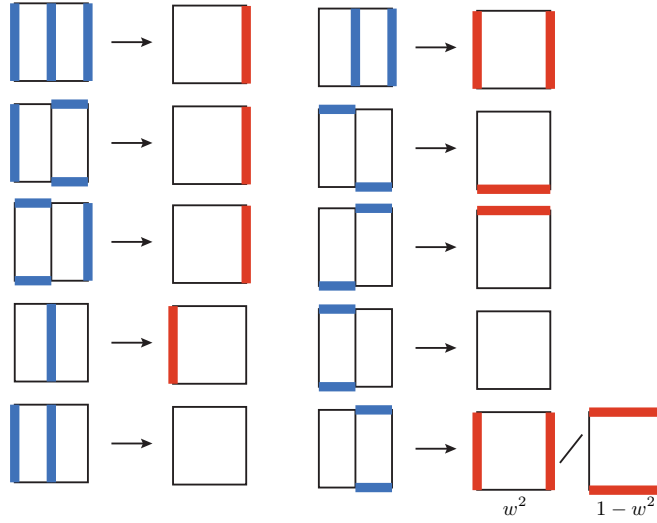


Figure 3.5: The figure shows the measure preserving mapping of local configurations on G^d (corresponding to a single edge e of G) to local configurations on the streets of C_G under urban renewal performed on the left-hand side quadrilateral in G^d . The last case involves additional random choice between two possible configurations. These choices are independent for local configurations corresponding to different edges of G and the probabilities are as in the figure with $w = 2x/(1 + x^2)$.

A choice of quadrilaterals where urban renewals are applied for a rectangular piece of the square lattice is depicted in Fig. 3.4. In this way, the XOR-Ising model on the square lattice is related to a (weighted) dimer model on the square-octagon lattice. In Fig. 3.5, we illustrate the behaviour of local dimer configurations under one urban renewal performed in the construction described in the lemma above.

As the reference 1-form for the dimer model on C_G we choose the canonical one given by

$$f_0((w, b)) = -f_0((b, w)) = \mathbf{P}_{C_G}^\emptyset(\{w, b\} \in M), \quad (3.3)$$

where w is a white vertex. Note that this makes the height function centered as all its increments become centered by definition. This is the same 1-form as used in [11] on the infinite square-octagon lattice $C_{\mathbb{Z}^2}$. In [45], two crucial properties of f_0 were established when G is an infinite isoradial graph and the Ising model on G is critical. In the next lemma we show that both of these properties hold for arbitrary Ising weights on general finite planar graphs.

Lemma 3.4. *We have*

- $\mathbf{P}_{C_G}^\emptyset(e \in M) = 1/2$, if e is a road, i.e., e corresponds to a corner of G ,
- $\mathbf{P}_{C_G}^\emptyset(e \in M) = \mathbf{P}_{C_G}^\emptyset(e' \in M)$, if e and e' are two parallel streets corresponding to the same edge of G (or of the dual G^*).

In the proof, which is postponed to the end of Section 3.2, we actually compute the probability from the second item in terms of the underlying Ising measure. However, the exact value will not be important for our considerations. We note that the first bullet of the lemma above is the reason why the nesting field with free boundary conditions on G is defined to be integer-valued and the one with wired boundary conditions on G^* to be half-integer valued.

A crucial observation now is that the height function on the faces of G^d corresponding to the faces and vertices of G is not modified by vertex splitting and urban renewal. This follows from basic properties of these transformations, and the fact that the reference 1-form on the short edges of G^d is the same as the one on the roads of C_G (by the first item of the lemma above). Indeed, one can compute the height function on the faces of G^d and C_G corresponding to the faces and vertices of G using only increments across short edges and roads respectively. This means that the resulting height function on these faces of C_G has the same distribution as the one on G^d . Since C_G plays the same role with respect to G^* as to G , we immediately get the following corollary.

Corollary 3.5. *The height function on C_G restricted to the faces and vertices of G is distributed as the the height functions on G^d and $(G^*)^d$ restricted to the faces and vertices of G . In particular, the height function on C_G restricted to the faces of G has the law of the nesting field of the double random current with free boundary conditions on G , and restricted to the vertices of G has the law of the nesting field of the double random current with wired boundary conditions on G^\dagger (or free boundary conditions on G^*).*

This observation is at the heart of the proof of the master coupling for double random currents and the XOR-Ising model from Theorem 2.7. However, one has to be careful since there is loss of information between the dimer model on G^d and the one on C_G . Indeed, a dimer configuration on C_G does not contain information on where the even nonzero values of the double random current are. To recover it, one needs to add additional randomness in the form of independent coin flips for each edge of G with a proper success probability.

Proof of Theorem 2.7. We will use a procedure reverse to that from the proof of Lemma 3.3. This procedure induces a measure preserving mapping between local configurations on C_G and G^d , see Fig. 3.6, where in certain cases additional randomness is used to decide on the exact configuration on G^d .

As mentioned, the graph C_G plays a symmetric role with respect to G and G^* . Hence, taking the Kramers–Wannier dual parameters $x_e^* = (1 - x_e)/(1 + x_e)$ and rotating the local configuration on C_G by $\pi/2$, one can use the same mapping from Fig. 3.6 to generate local dimer configurations on $(G^*)^d$ that will correspond to dual random current configurations. Recall that part of our aim is to couple the double random current on G with its dual on G^* so that no edge and its dual are open at the same time. The idea is to first sample a dimer configuration on C_G , and then using the rules from Fig. 3.6 choose, possibly introducing additional randomness, the dimer configurations on both G^d and $(G^*)^d$. The desired property of the coupling will follow from the way we use the additional randomness for G^d and $(G^*)^d$.

We now explain this in more detail. In the coupling between double random currents and dimers on G^d , an edge in the current is closed (or has value zero) if and only if there is no long edge present in the corresponding local dimer configuration. From Fig. 3.6, we see that the only possibility to have nonzero values of double currents for both a primal edge e and its

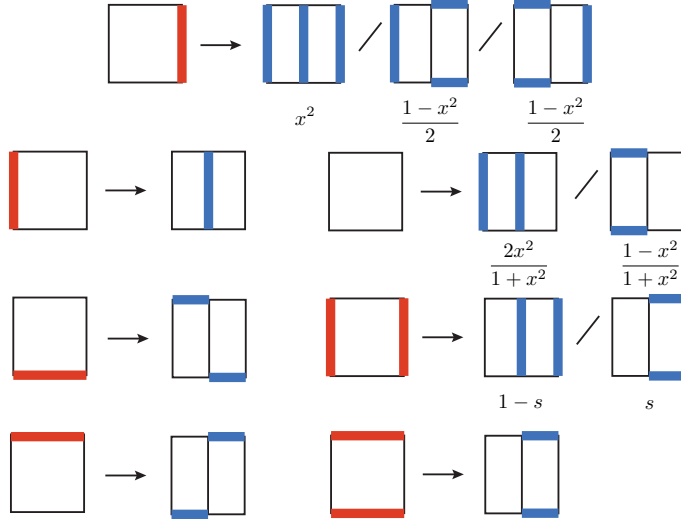


Figure 3.6: The reverse mapping to that in Fig. 3.5. Again, urban renewal is performed on the left-hand side quadrangle of the local configuration on G^d . Whenever there is ambiguity, we use additional randomness which is independent for each local configuration and with probabilities as in the figure with $s = \frac{2(1-x^2)}{3+x^4}$. These probabilities are simply obtained from Fig. 3.5 using the definitions of the weights in both dimer models on C_G and G^d and elementary conditional probability computations.

dual e^* is when the quadrangle in C_G that corresponds to both e and e^* has no dimer in the dimer cover. In that case we have a probability of $2x_e^2/(1+x_e^2)$ to get a non-zero (and even) value of the primal double current and a probability of $2(x_e^*)^2/(1+(x_e^*)^2)$ to get a non-zero (and even) value of the dual double current. However, since these choices are independent of the possible choices for other local configurations, and since

$$\frac{2x_e^2}{1+x_e^2} + \frac{2(x_e^*)^2}{1+(x_e^*)^2} = 1 - \frac{2x_e(1-x_e)}{1+x_e^2} < 1$$

we can couple the results so that the primal and dual currents are never both open (nonzero) at e . Together with Theorem 2.6, this establishes Properties 1, 2 and 5 from the statement of the theorem.

We now focus on Property 3. Note that the spins τ^\dagger defined by the interfaces of odd current in \mathbf{n} satisfy

$$\tau_u^\dagger = (-1)^{H(u)} \quad (3.4)$$

for $u \in U$, where H is the height function on C_G . By Corollary 3.5 we already know that H restricted to U has the law of the height function on $(G^*)^d$ restricted to U . From the relationship between the double random current \mathbf{n}^\dagger on G^* and the alternating flow model on \vec{G}^* , one can see that the parity of this height function at a face u changes with the change of the orientation of the outer boundary of the cluster of \mathbf{n}^\dagger containing u (see Fig. 3.2 for a

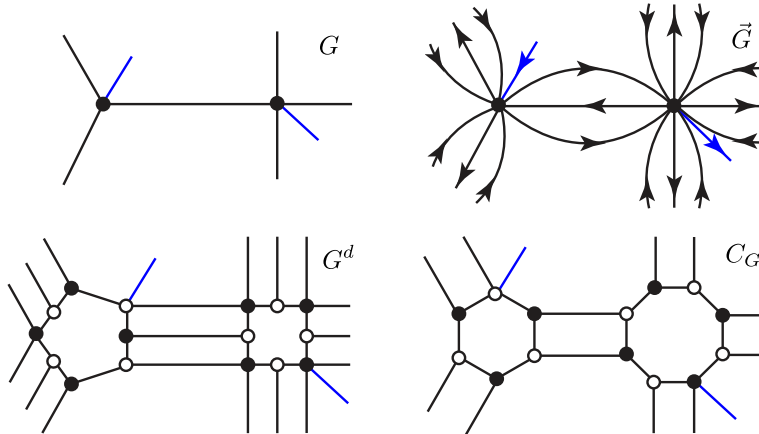


Figure 3.7: Corner insertions in the relevant models can be realized by considering additional edges connecting a vertex and a neighbouring face.

dual example). Therefore $(-1)^{H(u)}$ is distributed as an independent assignment of a sign to each cluster of \mathbf{n}^\dagger . This yields Property 3. A dual argument for

$$\tau_v = i(-1)^{H(v)} \quad (3.5)$$

with $v \in V$, and i the imaginary unit, yields the dual correspondence. Here, the factor i appears due to the fact that the height function takes half-integer values on V .

Finally, (3.4) and (3.5) together imply Property 5. \square

We leave it to the interested reader to check that the resulting coupling of the primal and dual double random current model is the same as the one described in [52] (where no connection with the dimer model is used).

3.2 Disorder and source insertions

It will be important for our analysis to introduce the so-called sources in dimers, alternating flows, and double random currents, and to see how they relate to order-disorder variables in the Ising model.

A *corner* $c = (u, v)$ of a planar graph G is a pair composed of a face $u = u(c)$ (also seen as a vertex of the dual graph) and a vertex $v = v(c)$ bordering u . One can visualize corners as segments from the center of the face u to the vertex v (see Fig. 3.7). In this section we discuss correlations of disorder insertions, by which we mean modifications of the state space of the appropriate model that are localized at the corners of G , and describe their mutual relationships. In what follows, consider two corners c_i and c_j , and a simple dual path γ connecting $u(c_i)$ to $u(c_j)$. For a collection of edges H of G , \vec{G} , G^d or C_G , we define $\text{sgn}_\gamma(H) = -1$ if the number of edges in H crossed by γ is odd and $\text{sgn}_\gamma(H) = 1$ otherwise.

In the following subsections we introduce correlation functions of corner insertions in the relevant models and relate them to each other.

3.2.1 Kadanoff–Ceva fermions via double random currents

The two-point correlation function of *Kadanoff–Ceva fermions* is defined by

$$\langle \chi_{c_i} \chi_{c_j} \rangle := \frac{1}{Z_{\text{hT}}^\emptyset} \sum_{\eta \in \mathcal{E}^{\{v(c_i), v(c_j)\}}} \text{sgn}_\gamma(\eta) \prod_{e \in \eta} x_e, \quad (3.6)$$

where $Z_{\text{hT}}^\emptyset := \sum_{\eta \in \mathcal{E}^\emptyset} \prod_{e \in \eta} x_e$. Here, \mathcal{E}^\emptyset is the collection of sets of edges $\eta \subseteq E$ such that each vertex in the graph (V, η) has even degree, and $\mathcal{E}^{\{v(c_i), v(c_j)\}}$ is the collection of sets of edges such that each vertex has even degree except for $v(c_i)$ and $v(c_j)$ that have odd degree. Note that the sign of this correlator depends (in this notation, implicitly) on the choice of γ . However, its amplitude depends only on the corners c_i and c_j .

The next lemma was proved in [6, Lemma 6.3]. It expresses Kadanoff–Ceva correlators in terms of double currents for which $u(c_i)$ is connected to $u(c_j)$ in the dual configuration. Below, for $(\mathbf{n}_{\text{odd}}, \mathbf{n}_{\text{even}}) \in \Omega^B$, let

$$w_{\text{dcur}}(\mathbf{n}_{\text{odd}}, \mathbf{n}_{\text{even}}) := \sum_{\mathbf{n} \in \Omega^B: \vartheta(\mathbf{n}) = (\mathbf{n}_{\text{odd}}, \mathbf{n}_{\text{even}})} w(\mathbf{n}).$$

For a current \mathbf{n} , recall the definition of \mathbf{n}^* from Section 2.6 and for two faces u and u' , let $u \xleftrightarrow{\mathbf{n}^*} u'$ mean that u is connected to u' in \mathbf{n}^* , i.e., that u and u' belong to the same connected component of the graph (U, \mathbf{n}^*) . We stress the fact that the identity below involves the weight w_{dcur} and not the single current weight w .

Lemma 3.6 (fermions via double currents [6]). *We have*

$$\langle \chi_{c_i} \chi_{c_j} \rangle = \frac{1}{Z_{\text{dcur}}^\emptyset} \sum_{(\mathbf{n}_{\text{odd}}, \mathbf{n}_{\text{even}}) \in \Omega^{\{v(c_i), v(c_j)\}}} \text{sgn}_\gamma(\mathbf{n}_{\text{odd}}) w_{\text{dcur}}(\mathbf{n}_{\text{odd}}, \mathbf{n}_{\text{even}}) \mathbf{1}\{u(c_i) \xleftrightarrow{\mathbf{n}^*} u(c_j)\}.$$

3.2.2 Sink and source insertions in alternating flows

Consider the graph \vec{G} with two additional directed edges $c_i = (u(c_i), v(c_i))$ and $-c_j = (v(c_j), u(c_j))$, and let $\mathcal{F}^{c_i, -c_j}$ be the set of alternating flows on this graph that contain both c_i and $-c_j$. By an alternating flow here we mean a subset of edges of the extended graph that satisfies the alternating condition at every vertex of \vec{G} . The weights of c_i and $-c_j$ are set to 1. With γ defined as above, introduce

$$Z_{\text{flow}}^\gamma(c_i, -c_j) := \sum_{F \in \mathcal{F}^{c_i, -c_j}} \text{sgn}_\gamma(F) w_{\text{flow}}(F).$$

Here, c_i plays the role of the *source* and $-c_j$ is the *sink* of the flow F .

Recall that $\theta : \mathcal{F}^\emptyset \rightarrow \Omega^\emptyset$ is the measure preserving map sending sourceless alternating flows on \vec{G} to images by ϑ of sourceless double current configurations on G . With a slight abuse of notation, we also write θ for the analogous map from $\mathcal{F}^{c_i, -c_j}$ to the image by ϑ of the set $\Omega^{\{v(c_i), v(c_j)\}}$ of currents on G with sources at $v(c_i)$ and $v(c_j)$ (for currents there is no distinction between sources and sinks).

The next lemma is closely related to [53, Theorem 4.1].

Lemma 3.7 (Symmetry between sinks and sources). *We have*

$$Z_{\text{flow}}^\gamma(c_i, -c_j) = Z_{\text{flow}}^\gamma(c_j, -c_i).$$

Proof. Note that the flow's weights on \vec{G} are invariant under the reversal of direction of the flow, i.e., the weights of the three directed edges e_{s1}, e_m, e_{s2} of \vec{G} corresponding to a single edge e of G satisfy $x_{e_{s1}} + x_{e_{s2}} + x_{e_{s1}}x_{e_{s2}}x_{e_m} = x_{e_m}$ by construction. Hence, for a fixed $(\mathbf{n}_{\text{odd}}, \mathbf{n}_{\text{even}}) \in \Omega^{\{v(c_i), v(c_j)\}}$, we have

$$\sum_{F \in \mathcal{F}^{c_i, -c_j}: \theta(F) = (\mathbf{n}_{\text{odd}}, \mathbf{n}_{\text{even}})} w_{\text{flow}}(F) = \sum_{F \in \mathcal{F}^{c_j, -c_i}: \theta(F) = (\mathbf{n}_{\text{odd}}, \mathbf{n}_{\text{even}})} w_{\text{flow}}(F).$$

We finish the proof by summing both sides of this identity over $(\mathbf{n}_{\text{odd}}, \mathbf{n}_{\text{even}}) \in \Omega^{\{v(c_i), v(c_j)\}}$, and using the fact that $\text{sgn}_\gamma(F)$ depends only on $\theta(F)$. \square

The next result is a direct analog of Lemma 3.6 with an additional factor of $1/2$ that corresponds to the fact that the connected component of the flow that connects c_i to $-c_j$ has a fixed orientation.

Lemma 3.8 (Dual connection in alternating flows). *We have*

$$\theta(\mathcal{F}^{c_i, -c_j}) = \{(\mathbf{n}_{\text{odd}}, \mathbf{n}_{\text{even}}) \in \Omega^{\{v(c_i), v(c_j)\}} : u(c_i) \xleftrightarrow{\mathbf{n}^*} u(c_j)\},$$

and moreover

$$Z_{\text{flow}}^\gamma(c_i, -c_j) = \frac{1}{2} \sum_{(\mathbf{n}_{\text{odd}}, \mathbf{n}_{\text{even}}) \in \Omega^{\{v(c_i), v(c_j)\}}} \text{sgn}_\gamma(\mathbf{n}_{\text{odd}}) w_{\text{dcurr}}(\mathbf{n}_{\text{odd}}, \mathbf{n}_{\text{even}}) \mathbf{1}\{u(c_i) \xleftrightarrow{\mathbf{n}^*} u(c_j)\}.$$

Proof. We first argue that for each $(\mathbf{n}_{\text{odd}}, \mathbf{n}_{\text{even}}) = \theta(F)$ with $F \in \mathcal{F}^{c_i, -c_j}$, we have that $u(c_i) \xleftrightarrow{\mathbf{n}^*} u(c_j)$. This follows from topological arguments and the alternating condition for flows. Indeed, assume by contradiction that there is a cycle of edges in F separating $u(c_i)$ from $u(c_j)$, and choose the innermost such cycle surrounding $u(c_i)$. Consider the vertex v of this cycle that is first visited on a path from c_i to $-c_j$. The alternating condition implies that the edges of the cycle on both sides of v should be oriented away from v . Following that orientation around the cycle, we must arrive at another vertex v' of the cycle where both incident edges are oriented towards v' . That is in contradiction with the alternating condition and the fact that the cycle is minimal. The fact that the image of the map is $\{u(c_i) \xleftrightarrow{\mathbf{n}^*} u(c_j)\}$ follows from the same arguments as in [53, Lemma 5.4].

The second part of the statement follows from the proof of [53, Theorem 4.1] or [27, Theorem 1.7] (the weights of flows in [53] are the same as ours up to a global factor). The multiplicative constant $1/2$ is a consequence of the fact that the orientation of the cluster containing the corners is fixed to one of the two possibilities, and in the double random current measure there is an additional factor of 2 for each cluster (see [53, Theorem 3.2]). \square

Corollary 3.9. *We have*

$$\langle \chi_{c_i} \chi_{c_j} \rangle = 2 \frac{Z_{\text{flow}}^\gamma(c_i, -c_j)}{Z_{\text{flow}}^\gamma} = 2 \frac{Z_{\text{flow}}^\gamma(c_j, -c_i)}{Z_{\text{flow}}^\gamma}.$$

Proof. This follows directly from Lemmata 3.6 and 3.8. \square

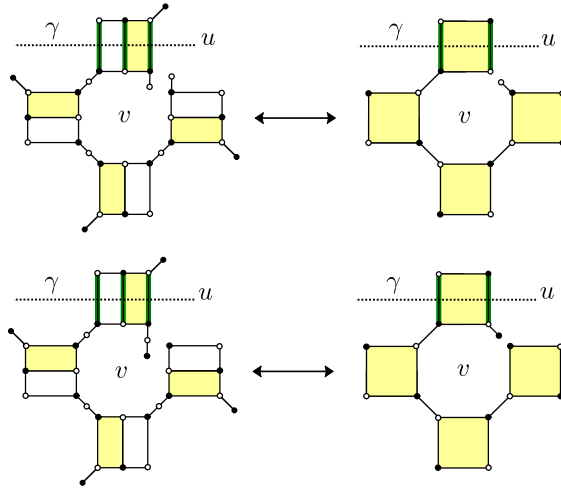


Figure 3.8: Behaviour of corner monomer insertions under urban renewal. Insertion of a monomer is modelled by the addition of edges with weight one into the dimer model: above (resp. below), the insertion of a black (resp. white) monomer at the corner $c = uv$ with a disorder operator at u . The green edges crossing γ are assigned negative weights. Urban renewal is applied to the yellow quadrilaterals on the left-hand side yielding the yellow quadrilaterals on the right-hand side. Note that the colour of the monomer insertions on the left-hand and right-hand sides agree.

3.2.3 Monomer insertions on G^d and C_G

We identify the faces and vertices of the graphs G and \vec{G} with the corresponding subsets of the faces of the dimer graphs G^d and C_G . We say that a vertex of G^d or C_G is a *corner (vertex)* corresponding to $c = vu$ if it is incident both on the vertex v and the face u of G in this identification.

Lemma 3.10 (Symmetry between white and black corners). *Let b_i and w_i (resp. b_j and w_j) be a black and white corner vertex of G^d corresponding to the corner c_i (resp. c_j). If there is no such vertex of the chosen colour, we modify G^d by splitting the corner vertex of the opposite colour (using the vertex splitting operation from Figure 3.3). Then*

$$Z_{G^d}^\gamma(b_i, w_j) = Z_{G^d}^\gamma(w_i, b_j) = Z_{\text{flow}}^\gamma(c_i, c_j).$$

Proof. By the definition of the measure preserving map F_* between dimers and alternating flows, a corner monomer insertion in dimers is a source or sink insertion in alternating flows, which yields

$$Z_{\text{flow}}^\gamma(c_i, c_j) = Z_{G^d}^\gamma(b_i, w_j).$$

The statement then follows immediately from Lemma 3.7. \square

Lemma 3.11 (Monomer insertions in G^d and C_G). *Let b and w be respectively black and white corner vertices of G^d , and let \tilde{b} and \tilde{w} be the corresponding black and white vertices of C_G . Then*

$$Z_{G^d}^\gamma(b, w) = Z_{C_G}^\gamma(\tilde{b}, \tilde{w}).$$

Proof. We use urban renewal as in Fig. 3.8 to transform G^d with monomer insertions to C_G with monomer insertions. Note that here we use urban renewal with some of the long edges having negative weight. However, this is not a problem since the opposite edges in a quadrilateral being transformed by urban renewal always have the same sign, which results in a non-zero multiplicative constant for the partition functions. The resulting weights of C_G are negative if and only if the edge crosses γ . This implies the claim readily. \square

We finally combine the previous results to obtain the following identity. We note that it can also be derived using the approach of [22] after taking into account the symmetry of the underlying six-vertex model (that we do not discuss here and that is also not discussed in [22]).

Corollary 3.12. *In the setting of Lemma 3.10, we have*

$$\langle \chi_{c_i} \chi_{c_j} \rangle = 2 \frac{Z_{C_G}^\gamma(w_i, b_j)}{Z_{C_G}} = 2 \frac{Z_{C_G}^\gamma(w_j, b_i)}{Z_{C_G}}.$$

Proof. This follows from Lemmata 3.11 and 3.10, as well as Corollary 3.9. \square

The final item of this section is the proof of Lemma 3.3 which explicitly computes the canonical reference 1-form (3.4) on C_G in terms of the underlying Ising measures.

Proof of Lemma 3.3. By the corollary above, for a street $\{w, b\}$ of C_G corresponding to an edge $e = \{v, v'\}$ of G , we have

$$\mathbf{P}_{C_G}^\theta(\{w, b\} \in M) = \frac{2x}{1+x^2} \frac{Z_{C_G}^\gamma(w, b)}{Z_{C_G}} = \frac{x}{1+x^2} \langle \chi_c \chi_{c'} \rangle, \quad (3.7)$$

where $x = x_e = \tanh \beta J_e$ is the high-temperature Ising weight, $\frac{2x}{1+x^2}$ is the weight of the edge $\{w, b\}$ in the dimer model on C_G as in Fig. 3.1, and where c and c' are the two corners of G corresponding to the two roads of C_G that are incident on w and b respectively. Indeed, the first identity is a consequence of the fact that in this case the path γ can be chosen empty and therefore the numerator $Z_{C_G}^\gamma(w, b)$ is actually the *unsigned* partition function of dimer covers of the graph where w and b are removed.

We now compute $\langle \chi_c \chi_{c'} \rangle$ in terms of the Ising two-point function $\mu_G[\sigma_v \sigma_{v'}]$. To this end, recall that \mathcal{E}^\emptyset is the collection of sets of edges $\eta \subseteq E$ such that each vertex in the graph (V, η) has even degree, and $\mathcal{E}^{\{v, v'\}}$ is the collection of sets of edges such that each vertex has even degree except for v and v' that have odd degree. Let

$$Z_+ := \sum_{\substack{\eta \in \mathcal{E}^\emptyset \\ e \in \eta}} \prod_{e' \in \eta} x_{e'}, \quad \text{and} \quad Z_- := \sum_{\substack{\eta \in \mathcal{E}^\emptyset \\ e \notin \eta}} \prod_{e' \in \eta} x_{e'},$$

and $Z = Z_{\text{hT}}^\emptyset$. By definition (3.6) of Kadanoff–Ceva fermions with γ empty, the high-temperature expansion of spin correlations, and the fact that $\eta \mapsto \eta \Delta \{e\}$ is a bijection between \mathcal{E}^\emptyset and $\mathcal{E}^{\{v, v'\}}$, (3.7) gives

$$\mathbf{P}_{C_G}^\theta(\{w, b\} \in M) = \frac{x}{1+x^2} \frac{1}{Z} (x^{-1} Z_+ + x Z_-) = \frac{x}{1+x^2} \mu_G[\sigma_v \sigma_{v'}]. \quad (3.8)$$

The same argument applied to the other street $\{w', b'\}$ corresponding to the same edge e yields $\mathbf{P}_{C_G}^\emptyset(\{w, b\} \in M) = \mathbf{P}_{C_G}^\emptyset(\{w', b'\} \in M)$ as the last displayed expression depends only on e . Moreover by the Kramers–Wannier duality and the same computation for the dual Ising model on the dual graph G^* , we have

$$\mathbf{P}_{C_G}^\emptyset(\{w, b\} \in M) = \mathbf{P}_{C_G}^\emptyset(\{w', b'\} \in M) = \frac{x^*}{1 + (x^*)^2} \mu_{G^*}[\sigma_u \sigma_{u'}] = \frac{1 - x^2}{2(1 + x^2)} \mu_{G^*}[\sigma_u \sigma_{u'}], \quad (3.9)$$

where $x^* := (1 - x)/(1 + x)$ is the dual weight, and where $\{u, u'\}$ is the dual edge of $\{v, v'\}$. This yields the second bullet of the lemma.

To prove the first bullet of the lemma, we need to relate the dual energy correlators $\mu_G[\sigma_v \sigma_{v'}]$ and $\mu_{G^*}[\sigma_u \sigma_{u'}]$ with each other. Interpreting the graphs in \mathcal{E}^\emptyset as interfaces between spins of different value on the vertices of G^* , and using the low-temperature expansion we get

$$\mu_{G^*}[\sigma_u \sigma_{u'}] = \frac{Z_- - Z_+}{Z}.$$

This together with the second equality of (3.8), and the fact that $Z_+ + Z_- = Z$, yields

$$2x\mu_G[\sigma_v \sigma_{v'}] + (1 - x^2)\mu_{G^*}[\sigma_u \sigma_{u'}] = 1 + x^2.$$

Therefore adding (3.8) and (3.9) gives

$$\mathbf{P}_{C_G}^\emptyset(\{w, b\} \in M) + \mathbf{P}_{C_G}^\emptyset(\{w, b'\} \in M) = 1/2.$$

This means that the probability of seeing the road containing w in the dimer configuration is 1/2. By symmetry this is true for all roads of C_G . This finishes the proof. \square

3.3 Kasteleyn theory and complex-valued fermionic observables

In this section, we introduce a Kasteleyn orientation which will be directly related to complex-valued observables introduced by Chelkak and Smirnov [19].

3.3.1 A choice of Kasteleyn's orientation

A *Kasteleyn weighting* of a planar bipartite graph is an assignment of complex phases $\varsigma_e \in \mathbb{C}$ with $|\varsigma_e| = 1$ to the edges of the graph satisfying the *alternating product condition* meaning that for each cycle e_1, e_2, \dots, e_{2k} in the graph, we have

$$\prod_{i=1}^k \varsigma_{e_{2i-1}} \varsigma_{e_{2i}}^{-1} = (-1)^{k+1}. \quad (3.10)$$

Note that it is enough to check the condition around every bounded face of the graph.

To define an explicit Kasteleyn weighting for C_G , consider the *diamond graph* of G , i.e., the graph whose vertices are the vertices and faces of G , and whose edges are the corners of G (see Fig. 3.9). Recall that the edges of C_G that correspond to the corners of G are called roads and the remaining edges (forming the quadrangles) are called streets. To each street there is assigned an angle θ_e between the two neighbouring corners in the diamond graph. We now define

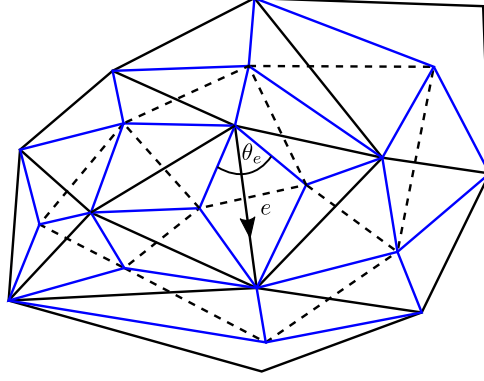


Figure 3.9: A piece of the primal graph G and its dual G^* (black solid and dashed edges respectively) and the corresponding diamond graph (blue edges) used to define the Kasteleyn weighting. Each street e of C_G can be identified with a directed edge of G or G^* . Then, the angle θ_e is the angle in the diamond graph at the origin of this directed edge as depicted in the figure. By definition, these angles sum up to 2π around every vertex and face of G , and around every face of the diamond graph. This guarantees that the associated weighting satisfies the Kasteleyn condition.

- $\varsigma_e = -1$ if e is a road,
- $\varsigma_e = \exp(\frac{i}{2}\theta_e)$ if e is a street that crosses a primal edge of G ,
- $\varsigma_e = \exp(-\frac{i}{2}\theta_e)$ if e is a street that crosses a dual edge of G^* .

That ς is a Kasteleyn orientation of C_G follows from the fact that the angles sum up to 2π around every vertex and face of G , and around every face of the diamond graph. Note that if G is a finite subgraph of an embedded infinite graph Γ , then one can as well use the angles from the diamond graph of Γ since, as already mentioned, one needs to check condition (3.10) only on the bounded faces of C_G . In particular, for subgraphs of the square lattice with the standard embedding, we will take $\theta_e = \pi/2$ for all edges e .

Fix a bipartite coloring of C_G , and let $K = K_{C_G}$ be a Kasteleyn matrix for a dimer model on the bipartite graph C_G with the weighting as above, i.e., the matrix whose rows are indexed by the black vertices and the columns by the white vertices, and whose entries are

$$K(b, w) := \varsigma_{bw} x_{bw}$$

if bw is an edge of C_G and $K(b, w) = 0$ otherwise, where b and w are respectively black and white vertices, and x is the edge weight for C_G as in Fig. 3.1.

We assume that the set of corners of G comes with a prescribed order c_1, \dots, c_m , and we order the rows and columns of K according to this order (for each white and black vertex of C_G , there is exactly one corner of G that the vertex corresponds to). We denote by b_i and w_i the black and white vertex of C_G corresponding to c_i .

The following lemma is a known observation.

Lemma 3.13. *We have that*

$$K^{-1}(w_i, b_j) = i\kappa_\gamma \frac{Z_{C_G}^\gamma(w_i, b_j)}{Z_{C_G}}, \quad (3.11)$$

where γ is a dual path connecting a face u_i adjacent to b_i with a face u_j adjacent to w_j , κ_γ is a global complex phase depending only on γ given by

$$\kappa_\gamma = (-1)^{i+j+1+N} \text{sgn}(\pi) i \prod_{k=1}^{m-1} \tilde{\zeta}_{\tilde{b}_k \tilde{w}_{\pi(k)}}, \quad (3.12)$$

and $Z_{C_G}^\gamma(b_i, w_j)$ is the partition function of dimers on C_G with b_i and w_j removed, and with negative weights assigned to the edges crossing γ .

The factor i is due to an arbitrary choice of κ_γ which is made for later convenience. We will now justify (3.11) and explicitly identify the complex phase κ_γ in this expression.

Proof. To compute the inverse matrix, we use the cofactor representation as a ratio of determinants:

$$K^{-1}(w_i, b_j) = (-1)^{i+j} \frac{\det K^{b_j, w_i}}{\det K},$$

where $K^{w_i, b_j} =: \tilde{K}$ is the matrix K with the j -th row and i -th column removed.

By definition of the determinant, we have

$$\det K = \sum_{\pi \in S_m} \text{sgn}(\pi) \prod_{k=1}^m \varsigma_{b_k w_{\pi(k)}} x_{b_k w_{\pi(k)}}.$$

In this sum, only terms where π corresponds to a perfect matching on C_G are nonzero. Moreover, by a classical theorem of Kasteleyn [40], the complex phase $\text{sgn}(\pi) \prod_{i=1}^m \varsigma_{b_i w_{\pi(i)}}$ is constant for such π . In particular, we can take π to be the identity. Since $\varsigma_{b_i w_i} = -1$, we get that

$$\det K = (-1)^N Z_{C_G},$$

where N is the number of corner edges in C_G .

We now want to interpret \tilde{K} as a Kasteleyn matrix for the graph \tilde{C}_G obtained from C_G by removing the vertices w_i and b_j . To this end, if w_i and b_j are not incident on the same face $u_i = u_j$, we need to introduce a sign change to the Kasteleyn weighting along a dual path γ which connects u_i to u_j . We do it as follows. Define modified weights $\tilde{\zeta}$ and \tilde{x} by $\tilde{\zeta}_e = -\varsigma_e$ (resp. $\tilde{x}_e = -x_e$), if e is crossed by γ , and $\tilde{\zeta}_e = \varsigma_e$ (resp. $\tilde{x}_e = x_e$) otherwise. Then $\varsigma_e x_e = \tilde{\zeta}_e \tilde{x}_e$, and hence $\tilde{K}(b, w) = \tilde{\zeta}_{bw} \tilde{x}_{bw}$ if bw is an edge of \tilde{C}_G , and $\tilde{K}(b, w) = 0$ otherwise. We leave it to the reader to verify that $\tilde{\zeta}$ is indeed a Kasteleyn weighting for \tilde{C}_G .

We can therefore again apply Kasteleyn's theorem to obtain

$$\det \tilde{K} = \sum_{\pi \in S_{m-1}} \text{sgn}(\pi) \prod_{k=1}^{m-1} \tilde{\zeta}_{\tilde{b}_k \tilde{w}_{\pi(k)}} \tilde{x}_{\tilde{b}_k \tilde{w}_{\pi(k)}} = \tilde{\kappa}_\gamma Z_{C_G}^\gamma(w_i, b_j),$$

where $\tilde{b}_1, \dots, \tilde{b}_{m-1}$ (resp. $\tilde{w}_1, \dots, \tilde{w}_{m-1}$) is an order preserving renumbering of the black (resp. white) vertices where b_j (resp. w_i) is removed. Again,

$$\tilde{\kappa}_\gamma = \text{sgn}(\pi) \prod_{k=1}^{m-1} \tilde{\zeta}_{\tilde{b}_k \tilde{w}_{\pi(k)}}$$

is a constant complex factor independent of the permutation π defining a perfect matching of \tilde{C}_G . This justifies (3.11). \square

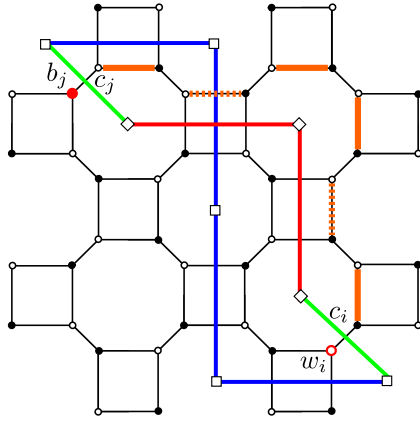


Figure 3.10: An illustration of the proof of Lemma 3.14 in the case where G is a piece of the square lattice. The green lines represent corners c_i and c_j , the red lines represent the primal path ρ from $v(c_i)$ to $v(c_j)$, and the blue lines show the dual path γ from $u(c_j)$ to $u(c_i)$. The red vertices w_i and b_j are removed in the graph $C_{\tilde{G}}$. The matching M_ρ corresponding to ρ contains the orange streets and all remaining roads. The dashed (resp. solid) orange edges carry a phase $\exp(\frac{i\pi}{4})$ (resp. $\exp(-\frac{i\pi}{4})$) in the original Kasteleyn weighting ζ of C_G . The orange edge crossed by γ gets an additional -1 sign in the Kasteleyn weighting $\tilde{\zeta}$ of \tilde{C}_G .

We now proceed to giving κ_γ a concrete representation in terms of the winding angle of γ . To this end, we first need to introduce some complex factors. We follow [17] and for each directed edge or corner e , we fix a square root of the corresponding direction in the complex plane and denote by η_e its *complex conjugate*. Recall that we always assume that a corner c is oriented towards its vertex $v(c)$, and we write $-c$ whenever we consider the opposite orientation. For two directed edges or corners e, g that do not point in opposite directions, we define $\angle(e, g)$ to be the *turning angle* from e to g , i.e., the number in $(-\pi, \pi)$ satisfying

$$e^{-i\angle(e,g)} = (\overline{\eta_e}\eta_g)^2.$$

Lemma 3.14. *Let c_i, c_j , and γ be as above. Define $\tilde{\gamma}$ to be the extended path starting at $-c_j$, following γ , and ending at c_i . Then,*

$$\kappa_\gamma = \exp(\frac{i}{2}\text{wind}(\tilde{\gamma})),$$

where $\text{wind}(\tilde{\gamma})$ is the total winding angle of the path $\tilde{\gamma}$, i.e., the sum of all turning angles along the path.

Proof. Let ρ be a simple primal path starting at $v(c_i)$ and ending at $v(c_j)$, and let $\tilde{\rho}$ be the extended path that starts at c_i , then follows ρ , and ends at $-c_j$. We will define a perfect matching M_ρ of \tilde{C}_G that corresponds to ρ in a natural way (see Fig. 3.10). Note that there is a unique sequence of streets S_ρ such that the first edge contains b_i and the last edge contains w_j , and where all the edges are directly to the right of the oriented path $\tilde{\rho}$ (the orange edges in Fig. 3.10). We define M_ρ to contain S_ρ and all the remaining roads denoted by R_ρ .

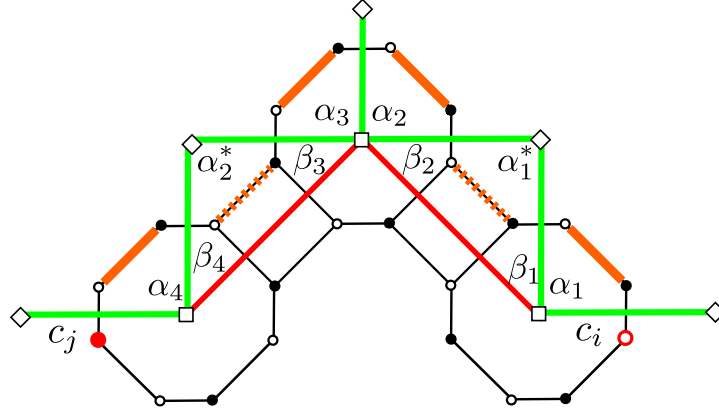


Figure 3.11: An illustration of the proof of (3.13). The path ρ goes from c_i to $-c_j$, and is composed of the two red edges. The orange edges represent S_ρ .

Moreover, let ℓ be the loop (closed path) which is the concatenation of $\tilde{\rho}$ and $\tilde{\gamma}$. We claim that

$$\prod_{bw \in S_\rho} \tilde{s}_{bw} = (-1)^{t(\ell)} \prod_{bw \in S_\rho} s_{bw} = (-1)^{t(\ell)+1} i \exp(-\frac{i}{2} \text{wind}(\tilde{\rho})), \quad (3.13)$$

where $t(\ell)$ is the number of self-crossings of ℓ . Indeed, the first identity follows since the self-crossings of ℓ only come from a crossing between γ and ρ , and each such edge gets an additional -1 factor in the Kasteleyn weighting $\tilde{\sigma}$. We now argue for the second inequality by inspecting the contribution of the phases ζ at each turn of $\tilde{\rho}$. To this end we consider all the corners adjacent to ρ . We denote by α_k (resp. α_k^*), $k = 1, 2, \dots$, the unsigned angles between two consecutive corners that share a vertex (resp. a face) of G , and by β_k we denote the angles between the edges of ρ and the corners (see Fig. 3.11). Note that there is exactly $|\rho|$ angles of type α^* , and $2|\rho|$ angles of type β (there can be more angles of type α). Moreover, $\alpha_k^* = \pi - \beta_{2k-1} - \beta_{2k}$ for each $k \in \{1, \dots, |\rho|\}$. Finally, the sum of all angles of type α and β around a vertex of G is by definition equal to π plus the turning angle of ρ at that vertex. Writing A (resp. B) for the sum of all angles of type α (resp. β), and using the definition of ζ , we find

$$\prod_{bw \in S_\rho} s_{bw} = \prod_k e^{-\frac{i\alpha_k}{2}} \prod_k e^{\frac{i\alpha_k^*}{2}} = e^{-\frac{i}{2}(A+B-|\rho|\pi)} = e^{-\frac{i}{2}(\text{wind}(\tilde{\rho})+\pi)} = -i \exp(-\frac{i}{2} \text{wind}(\tilde{\rho})),$$

which justifies (3.13).

On the other hand, a classical fact due to Whitney [80] (see also [17, Lemma 2.2]) says that

$$\exp(\frac{i}{2} \text{wind}(\ell)) = (-1)^{t(\ell)+1}. \quad (3.14)$$

Factorizing the left-hand side into the contributions coming from $\tilde{\rho}$ and $\tilde{\gamma}$, we get

$$\exp(\frac{i}{2} \text{wind}(\ell)) = \kappa_\gamma \exp(\frac{i}{2} \text{wind}(\tilde{\rho})).$$

Combining with (3.13) we arrive at

$$\prod_{bw \in M_\rho} \tilde{\zeta}_{bw} = \prod_{bw \in S_\rho} \tilde{\zeta}_{bw} \prod_{bw \in R_\rho} \tilde{\zeta}_{bw} = (-1)^{|R_\rho|} \mathbf{i}^{\kappa_\gamma},$$

where the second equality holds true since roads have complex phase $\varsigma = -1$. On the other hand, by (3.12) we have

$$\kappa_\gamma = (-1)^{i+j+1+N} \operatorname{sgn}(\pi) \mathbf{i} \prod_{k=1}^{m-1} \tilde{\zeta}_{b_k w_{\pi(k)}} = (-1)^{i+j+1+N} \operatorname{sgn}(\pi) \mathbf{i} \prod_{bw \in M_\rho} \tilde{\zeta}_{bw},$$

where $\pi \in S_{k-1}$ is the permutation defining the matching M_ρ , and N is the number of all corner edges in C_G . Therefore to finish the proof, it is enough to show that

$$\operatorname{sgn}(\pi) = (-1)^{i+j+N+|R_\rho|}. \quad (3.15)$$

To this end, first note that M_ρ naturally defines a bijection $\tilde{\pi}$ of the set of corners of G with the two corners c_i and c_j identified as one corner, called from now on \tilde{c} , where $\tilde{\pi}(c) = c'$ if the black vertex corresponding to c is connected by an edge in M_ρ to the white vertex corresponding to c' . This bijection can be thought of as a permutation of $\{1, \dots, k-1\}$ where the index corresponding to \tilde{c} is $m-1$, and where the first $m-2$ indices respect the original order on the remaining corners of C_G . Clearly $\tilde{\pi}$ has only one nontrivial cycle whose length is $|S_\rho| + 1$, and hence $\operatorname{sgn}(\tilde{\pi}) = (-1)^{|S_\rho|}$. Without loss of generality, let $j > i$ and for an index $l \in \{1, \dots, k-1\}$, let $p_l \in S_{k-1}$ be the permutation such that $p_l(l) = k-1$ and that does not change the order of the remaining indices. Note that $\operatorname{sgn}(p_l) = (-1)^{k-1-l}$ as p_l is a composition of $k-1-l$ transpositions. One can check that $\pi = p_i^{-1} \tilde{\pi} p_{j-1}$, and as a result $\operatorname{sgn}(\pi) = (-1)^{i+j-1+|S_\rho|}$. To show (3.15) and finish the proof, we count the roads whose both endpoints are covered by a street in S_ρ , to get that $N = |S_\rho| + 1 + |R_\rho|$. \square

All in all, from (3.11) together with Corollary 3.12 we obtain the following statement.

Corollary 3.15. *We have*

$$K^{-1}(w_i, b_j) = \frac{1}{2} \mathbf{i}^{\kappa_\gamma} \langle \chi_{c_i} \chi_{c_j} \rangle, \quad (3.16)$$

where the complex phase κ_γ is as in Lemma 3.14.

3.3.2 Complex-valued fermionic observables

In this section we rewrite $\langle \chi_{c_i} \chi_{c_j} \rangle$, and hence the right-hand side of (3.16), in terms of complex-valued fermionic observables of Chelkak–Smirnov [19], and Hongler–Smirnov [38]. This correspondence is well-known (and can be e.g. found in [17]) but we choose to present the details for completeness of exposition. In the next section, we will use it together with the available scaling limit results to derive the scaling limit of K^{-1} for the critical model on C_{D^δ} .

We first define the complex version of the Kadanoff–Ceva observable for two corners c_i and c_j by

$$f(c_i, c_j) := \frac{1}{Z_{\text{hT}}^\emptyset} \sum_{\eta \in \mathcal{E}^{v(c_i), v(c_j)}} \exp(-\frac{1}{2} \operatorname{wind}(\rho_\eta)) \prod_{e \in \eta} x_e, \quad (3.17)$$

where $\text{wind}(\rho_\eta)$ is again the total winding angle of the path ρ_η , i.e. the sum of all turning angles along the path, and where ρ_η is a simple path contained in $\eta \cup \{c_i, c_j\}$ that starts at c_i and ends at $-c_j$, and is defined as follows: for each vertex v of degree larger than two in η , one connects the edges around v into pairs in a non-crossing way, thus giving rise to a collection of non-crossing cycles \mathcal{C}_η and a path from c_i to $-c_j$ that we call ρ_η .

It is a standard fact that the definition of $f(c_i, c_j)$ does not depend on the way the connections at each vertex of η are chosen (as long as they are noncrossing). Moreover, for all $\eta \in \mathcal{E}^{v(c_i), v(c_j)}$, we have

$$-\bar{\kappa}_\gamma \exp(-\frac{i}{2} \text{wind}(\rho_\eta)) = \text{sgn}_\gamma(\eta), \quad (3.18)$$

where as before, γ is a fixed dual path connecting $u(c_i)$ and $u(c_j)$, and $\kappa_\gamma = \exp(\frac{i}{2} \text{wind}(\tilde{\gamma}))$, with $\tilde{\gamma}$ being the path starting at $-c_j$, then following γ , and ending at c_i . To justify this identity, we consider the loop ℓ which is the concatenation of ρ_η and the path $\tilde{\gamma}$, and write

$$\exp(-\frac{i}{2} \text{wind}(\ell)) = \bar{\kappa}_\gamma \exp(-\frac{i}{2} \text{wind}(\rho_\eta)).$$

We then again use Whitney's identity (3.14) and the fact that the collection of cycles \mathcal{C}_η must, by construction, cross γ an even number of times (since \mathcal{C}_η does not cross ρ_η , and \mathcal{C}_η crosses ℓ an even number of times for topological reasons). This justifies (3.18) and implies that

$$\langle \chi_{c_i} \chi_{c_j} \rangle = -\bar{\kappa}_\gamma f(c_i, c_j),$$

which together with Corollary 3.15 gives the following proposition.

Proposition 3.16. *We have*

$$K^{-1}(w_i, b_j) = -\frac{i}{2} f(c_i, c_j). \quad (3.19)$$

To make the connection with the scaling limit results of [38], we still need to introduce an observable that is indexed by two directed edges of G instead of two corners. To this end, for each edge e of G , let z_e be its midpoint. Also, for a directed edge $e = (v_1, v_2)$, let $h(e)$ be the *half-edge* $\{z_e, v_2\}$, let $-e = (v_2, v_1)$ be its reversal, and let $\bar{e} = \{v_1, v_2\}$ be its undirected version. Moreover, for two directed edges $e = (v_1, v_2)$ and $g = (\tilde{v}_1, \tilde{v}_2)$, let $\mathcal{E}^{e,g}$ be the collections of edges $\tilde{\eta} \in \mathcal{E}^{v_2, \tilde{v}_1}$ that *do not contain* \bar{e} and \bar{g} . We define

$$f(e, g) := \frac{1}{Z_{\text{hT}}^\emptyset} \sum_{\tilde{\eta} \in \mathcal{E}^{e,g}} \exp(-\frac{i}{2} \text{wind}(\rho_{\tilde{\eta}})) \prod_{e \in \tilde{\eta}} x_e,$$

where $\rho_{\tilde{\eta}}$ is a simple path in $\tilde{\eta} \cup \{h(e), h(-g)\}$ that starts at z_e and ends at z_g , and is analogous to ρ_η from (3.17). Note that the winding of $\rho_{\tilde{\eta}}$ is constant (independent of $\tilde{\eta}$) modulo 2π and equal to $\angle(e, g)$, and therefore

$$f(e, g) \in \bar{\eta}_e \eta_g \mathbb{R}. \quad (3.20)$$

4 Proof of Theorem 2.1

Let D be a bounded simply connected domain, and let D^δ be an approximation of D by $\delta\mathbb{Z}^2$. We consider the critical double random current model with free boundary conditions on D^δ , and the corresponding dimer model on Dubédat's square-octagon graph C_{D^δ} . We call U^δ and V^δ the set of faces of C_{D^δ} that correspond to the faces and vertices of D^δ respectively. In this section we show that the moments of the associated height function h^δ converge to the moments of $\frac{1}{\sqrt{\pi}}$ times the Dirichlet GFF.

4.1 Scaling limit of inverse Kasteleyn matrix

We start by establishing the scaling limit of the inverse Kasteleyn matrix on C_{D^δ} . This is crucial for the computation of the moments of the height function that is done in the next section.

Our method is to use Proposition 3.16 obtained in the previous section, as well as the existing scaling limit results for discrete s -holomorphic observables in the Ising model [18, 38]. It is important to note that for the purpose of proving the main conjecture of Wilson, we need to work with continuum domains D with an arbitrary (possibly fractal) boundary. Therefore, we state a generalized version of the scaling limit results of Hongler and Smirnov [38] for the critical fermionic observable with two points in the bulk of the domain. Their result, as stated, is valid only for domains whose boundary is a rectifiable curve (see also [37]). Even though the stronger result that we need is most likely known to the experts, for the sake of completeness, we will outline its proof, which is a direct consequence of the robust framework of Chelkak, Hongler and Izyurov [18] that was used to establish scaling limits for critical spin correlations.

From now on, we assume that the observables are critical, i.e., the weight x_e is constant and equal to $x_c = \sqrt{2} - 1$ so that $\prod_{e \in \eta} x_e = x_c^{|\eta|}$. Also, we define

$$f(e, z_g) := x_c(f(e, g) + f(e, -g)), \quad (4.1)$$

which is the observable of Hongler and Smirnov [38] (when e is a horizontal edge pointing to the right) that is indexed by a directed edge e and a midpoint of an edge z_g . The next lemma relates this observable to the corner observable in a linear fashion. This type of identities is well-known (see e.g. [17]) and is closely related to the notion of s -holomorphicity introduced by Smirnov [77] for the square lattice, and generalized by Chelkak and Smirnov [19], and Chelkak [13, 16]. We omit the proof.

Lemma 4.1. *Let c_i and c_j be two corners that do not share a vertex, and let e and g be directed edges incident to $v(c_i)$ and $v(c_j)$ respectively. Then*

$$f(c_i, c_j) = \frac{1}{\sqrt{2}} \sum_{e' \in \{e, -e\}} (1 + (\overline{\eta_{c_i}} \eta_{e'})^2) (f(e', z_g) - (\overline{\eta_{e'}} \eta_{c_j})^2 \overline{f(e', z_g)}).$$

We also need to introduce the continuum counterparts of the discrete holomorphic observables. To this end, let $D \subsetneq \mathbb{C}$ be a simply connected domain different from \mathbb{C} , and let $\psi_w = \psi_w^D$ be the unique conformal map from D to the unit disk with $\psi_w(w) = 0$ and $\psi'_w(w) > 0$. For $w, z \in D$, we define

$$f_-^D(w, z) := \frac{1}{2\pi} \sqrt{\psi'_w(w) \psi'_w(z)} \quad \text{and} \quad f_+^D(w, z) := \frac{1}{2\pi} \sqrt{\psi'_w(w) \psi'_w(z)} \frac{1}{\psi_w(z)}.$$

Lemma 4.2 (Conformal covariance of f_{\pm}^D). *Let $\varphi : D \rightarrow D'$ be a conformal map. Then*

$$\begin{aligned} f_-^D(w, z) &= \overline{\varphi'(w)}^{\frac{1}{2}} \varphi'(z)^{\frac{1}{2}} f_-^{D'}(\varphi(w), \varphi(z)), \\ f_+^D(w, z) &= \varphi'(w)^{\frac{1}{2}} \overline{\varphi'(z)}^{\frac{1}{2}} f_+^{D'}(\varphi(w), \varphi(z)). \end{aligned}$$

Moreover, for the upper half-plane \mathbb{H} , we have

$$f_-^{\mathbb{H}}(w, z) = \frac{i}{2\pi(z - \bar{w})} \quad \text{and} \quad f_+^{\mathbb{H}}(w, z) = \frac{1}{2\pi(z - w)}.$$

The proof is an easy computation and is omitted.

We now proceed to the generalization of [38, Theorem 8] mentioned at the beginning of the section. In the proof we will very closely follow the proof of [18, Theorem 2.16] dealing with the convergence of discrete s-holomorphic spinors.

Theorem 4.3. *Let $D \subsetneq \mathbb{C}$ be a bounded simply connected domain, and let D^δ approximate D as $\delta \rightarrow 0$. Fix $w, z \in D$, and let $e = e^\delta$ and $g = g^\delta$ be edges of D^δ whose midpoints converge to w and z respectively as $\delta \rightarrow 0$. Then*

$$f^\delta(e, z_g) = \delta(f_-^D(w, z) + \bar{\eta}_e^2 f_+^D(w, z) + o(1)) \quad \text{as } \delta \rightarrow 0,$$

where f^δ is the observable from (4.1) defined on D^δ . Moreover the convergence is uniform on compact subsets of $\{(w, z) \in D^2 : w \neq z\}$.

Before giving a sketch of the proof of this theorem, we state a corollary that will be convenient for us when computing moments of the height function in the next section.

Corollary 4.4. *Consider the setting from the lemma above and let $c_i = c_i^\delta$ and $c_j = c_j^\delta$ be two corners of D^δ whose vertices converge to w and z respectively. Then*

$$K^{-1}(w_i, b_j) = -\frac{1}{\sqrt{2}} \delta i (f_-^D(w, z) - \bar{\eta}_{c_i}^2 \eta_{c_j}^2 \overline{f_-^D(w, z)} + \bar{\eta}_{c_i}^2 f_+^D(w, z) - \eta_{c_j}^2 \overline{f_+^D(w, z)} + o(1)),$$

where K^{-1} is the inverse Kasteleyn matrix on C_{D^δ} .

Again, it is a simple computation and we omit the proof here.

Sketch of proof of Theorem 4.3. Based on the scaling limit results of Hongler–Smirnov [38], we first argue that the statement holds true for a domain D with a smooth boundary. Indeed, in [38] it is assumed that $\eta_e^2 = 1$ and hence, in that case, the result follows directly from [38, Theorem 8]. Applying this to a rotated domain together with the conformal covariance properties from Lemma 4.2 yields the statement for a general direction of e .

We now briefly describe how to use the robust framework of Chelkak, Hongler and Izyurov to extend this to general simply connected domains. In [18, Theorem 2.16], a scaling limit result was established for a discrete holomorphic spinor F^δ defined on an approximation D^δ of an arbitrary bounded simply connected domain D . The two observables F^δ and f^δ satisfy the same boundary conditions (of [38, Proposition 18] and [18, (2.7)]). Moreover, both observables are s-holomorphic away from the diagonal. The difference however is their singular behaviour near the diagonal. In [18], the full plane version $F_{\mathbb{C}}^\delta$ (the discrete analog

of $1/\sqrt{z-w}$ of the observable is subtracted from F^δ in order to cancel out the discrete-holomorphic singularity on the diagonal. The details of the proof of [18, Theorem 2.16] can be carried out verbatim for f^δ instead of F^δ and its full plane version $f_{\mathbb{C}}^\delta$ (the discrete analog of $1/(z-w)$) introduced in [38] instead of $F_{\mathbb{C}}^\delta$. Indeed, the arguments in [18] depend only on the fact that the observables in question are s-holomorphic and satisfy the correct boundary value problem.

Since the scaling limit is conformally invariant and was uniquely identified for domains with a smooth boundary by the argument above. This finishes the proof. \square

4.2 Moments of h^δ

For simplicity of exposition, we only consider the height function on C_{D^δ} restricted to U^δ which has the same distribution as the nesting field of the critical double random current on D with free boundary conditions. The case of mixed moments (for the joint height function on both the faces and vertices of D^δ) follows in the same manner as the faces and vertices of D^δ play a symmetric role in the graph C_{D^δ} . To this end, let a_1, a_2, \dots, a_n be distinct points in D , and let $h^\delta(a_i)$ ($i = 1, \dots, n$) be the height function evaluated at the face $u_i^\delta = u_i^\delta(a_i) \in U^\delta$ of D^δ , in which the point a_i lies (we choose a face arbitrarily if a_i lies on an edge of D^δ).

Let $G_D(z, w)$ be the Dirichlet Green's function in D , i.e., the Green's function of standard Brownian motion in D killed upon hitting ∂D . In particular for the upper-half plane \mathbb{H} , we have

$$G_{\mathbb{H}}(z, w) = \frac{1}{2\pi} \ln \left| \frac{z - \bar{w}}{z - w} \right|.$$

This section is devoted to the proof of the following theorem. Below, $\mathbf{P}_{D^\delta, D^\delta}^{\emptyset, \emptyset}$ denotes the probability measure of the double random current model with free boundary conditions together with the independent labels used to define the nesting field.

Theorem 4.5. *For every even integer n and any distinct points $a_1, a_2, \dots, a_n \in D$, we have*

$$\lim_{\delta \rightarrow 0} \mathbf{E}_{D^\delta, D^\delta}^{\emptyset, \emptyset} \left[\prod_{i=1}^n h^\delta(a_i) \right] = \sum_{\pi \text{ pairing of } \{a_1, \dots, a_n\}} \prod_{\{z, w\} \in \pi} \frac{1}{\pi} G_D(z, w),$$

where a pairing is a partition into sets of size two.

Note that the field h^δ is symmetric, and therefore the corresponding moments for n odd vanish.

In the proof of the theorem, we follow the line of computation due to Kenyon [43] but with several adjustments to our setting. In particular, we start with an algebraic manipulation to take care of the behaviour of K^{-1} near the boundary of D^δ : for $a_1^0, \dots, a_n^0 \in D$, write

$$\mathbf{E}_{D^\delta, D^\delta}^{\emptyset, \emptyset} \left[\prod_{i=1}^n h^\delta(a_i) \right] = \mathbf{E}_{D^\delta, D^\delta}^{\emptyset, \emptyset} \left[\prod_{i=1}^n (h^\delta(a_i) - h^\delta(a_i^0)) \right] - \sum_{\substack{t \in \{0,1\}^n \\ t \neq (1, \dots, 1)}} (-1)^{\sum_i (1-t_i)} \mathbf{E}_{D^\delta, D^\delta}^{\emptyset, \emptyset} \left[\prod_{i=1}^n h^\delta(a_i^{t_i}) \right], \quad (4.2)$$

where $a_i^1 = a_i$ for $i = 1, \dots, n$.

The advantage of this formulation is that the first term on the right-hand side can be computed using Kasteleyn theory, and that the others are small when a_1^0, \dots, a_n^0 are close to the boundary. This latter fact is not obvious and is relying on discrete properties of the double random current obtained in [28] (note that it is basically saying that the field is uniformly small – in terms of moments – near the boundary).

We start by proving that the remaining terms are small.

Proposition 4.6. *For any $\varepsilon > 0$ and $a_1, \dots, a_n \in D$, one may choose $a_1^0, \dots, a_n^0 \in D$ so that*

$$\left| \mathbf{E}_{D^\delta, D^\delta}^{\emptyset, \emptyset} \left[\prod_{i=1}^n h^\delta(a_i) \right] - \mathbf{E}_{D^\delta, D^\delta}^{\emptyset, \emptyset} \left[\prod_{i=1}^n (h^\delta(a_i) - h^\delta(a_i^0)) \right] \right| < \varepsilon \quad (4.3)$$

uniformly in $\delta > 0$.

Remark 4.7. This proposition, which basically claims that the second term on the right-hand side of (4.2) is approximately zero provided the a_i^0 are close enough to the boundary, is a restatement of the fact that boundary conditions for the limiting height function are zero. It is therefore the main place where we identify boundary conditions. Note that this proposition relies heavily on the main result in [28] and is as such non-trivial.

To prove this proposition, we need to introduce some auxiliary notions. We say that a cluster of the double random current is *relevant* for $A = \{a_1, \dots, a_n\} \subsetneq D$ if it is odd around u_i^δ for at least two different $i \in \{1, \dots, n\}$ (it is possible that $u_i^\delta = u_j^\delta$ even though $a_i \neq a_j$). We denote by $R^\delta(A)$ the number of relevant clusters for A in D^δ , and by $I^\delta(A)$ the event that all faces $u_1^\delta, \dots, u_n^\delta$ are surrounded by at least one relevant cluster for A . We start with three lemmata.

Lemma 4.8. *For every $n \geq 2$ even, there exists $P_n \in (0, \infty)$ such that for all sets of points $A = \{a_1, \dots, a_n\} \subsetneq D$, we have*

$$\mathbf{E}_{D^\delta, D^\delta}^{\emptyset, \emptyset} \left[\prod_{i=1}^n h^\delta(a_i) \right] \leq P_n \sqrt{\mathbf{E}_{D^\delta, D^\delta}^{\emptyset, \emptyset} [R^\delta(A)^n] \mathbf{P}_{D^\delta, D^\delta}^{\emptyset, \emptyset} [I^\delta(A)]}.$$

Proof. For a cluster \mathcal{C} of the double random current, let

$$\text{Odd}(\mathcal{C}) := \{a_i \in A : \mathcal{C} \text{ is odd around } u_i^\delta\}.$$

We denote a partition of A by $\{A_1, \dots, A_k\}$. We call such a partition even if all its elements have even cardinality. Using the correspondence with the nesting field of the critical double

random current on D^δ with free boundary conditions defined in (2.1), we have

$$\begin{aligned}
\mathbf{E}_{D^\delta, D^\delta}^{\theta, \theta} \left[\prod_{i=1}^n h^\delta(a_i) \right] &= \mathbf{E}_{D^\delta, D^\delta}^{\theta, \theta} \left[\prod_{i=1}^n \left(\sum_{\mathcal{C}_i} \epsilon_{\mathcal{C}_i} \mathbf{1}_{\{\mathcal{C}_i \text{ odd around } u_i^\delta\}} \right) \right] \\
&= \mathbf{E}_{D^\delta, D^\delta}^{\theta, \theta} \left[\sum_{(\mathcal{C}_1, \dots, \mathcal{C}_n)} \prod_{i=1}^n \epsilon_{\mathcal{C}_i} \mathbf{1}_{\{\mathcal{C}_i \text{ odd around } u_i^\delta\}} \right] \\
&= \sum_{\{A_1, \dots, A_k\} \text{ even}} \mathbf{E}_{D^\delta, D^\delta}^{\theta, \theta} \left[\sum_{(\mathcal{C}_1, \dots, \mathcal{C}_k)} \mathbf{1}_{\{A_i \subseteq \text{Odd}(\mathcal{C}_i), \mathcal{C}_i \text{ distinct } \forall i \in \{1, \dots, k\}\}} \right] \\
&\leq \sum_{\{A_1, \dots, A_k\} \text{ even}} \mathbf{E}_{D^\delta, D^\delta}^{\theta, \theta} \left[\sum_{(\mathcal{C}_1, \dots, \mathcal{C}_k)} \mathbf{1}_{\{\mathcal{C}_i \text{ relevant for } A\}} \mathbf{1}_{l^\delta(A)} \right] \\
&\leq P_n \mathbf{E}_{D^\delta, D^\delta}^{\theta, \theta} [\mathbf{R}^\delta(A)^{n/2} \mathbf{1}_{l^\delta(A)}] \\
&\leq P_n \sqrt{\mathbf{E}_{D^\delta, D^\delta}^{\theta, \theta} [\mathbf{R}^\delta(A)^n] \mathbf{P}_{D^\delta, D^\delta}^{\theta, \theta} [l^\delta(A)]},
\end{aligned}$$

where P_n is the number of even partitions of a set of size n (we used that $k \leq n/2$), and where in the last inequality we used the Cauchy–Schwarz inequality. \square

Lemma 4.9 (Log bound on the number of clusters). *There exists $C \in (0, \infty)$ such that for every bounded domain D and every $A = \{a_1, \dots, a_n\} \subsetneq D$,*

$$\mathbf{E}_{D^\delta, D^\delta}^{\theta, \theta} [\mathbf{R}(A)^N] \leq \frac{1}{N!} \left[Cn \log \left(\frac{\text{diam}(D)}{\min_{i \neq j} |a_i - a_j|} \right) \right]^N,$$

uniformly in $\delta > 0$.

Proof. Consider the constant C given by Theorem 2.11. Set $\kappa := \frac{1}{2} \min_{i \neq j} |a_i - a_j|$ and $d := \text{diam}(D)$.

Consider the family $\mathcal{B} = (\Lambda_{r_k}(x_k) : k \in \mathcal{K})$ containing the boxes $\Lambda_{\frac{r}{4C}}(x)$ with $r := 2^j \kappa$, $x \in \frac{r}{4C} \mathbb{Z}^2 \cap \text{Ann}(a_i, r, 2r)$ for every $1 \leq i \leq n$ and $0 \leq j \leq \lfloor \log_2(d/\kappa) \rfloor$. One may easily check that every cluster that surrounds at least two vertices in A must contain, for some $k \in \mathcal{K}$, a crossing from $\Lambda_{r_k}(x_k)$ to $\Lambda_{2Cr_k}(x_k)$. We deduce that if X_k is the number of disjoint $\Lambda_{Cr_k}(x_k)$ -clusters crossing $\text{Ann}(x_k, r_k, 2Cr_k)$ from inside to outside, then

$$\mathbf{R}(A) \leq \sum_{k \in \mathcal{K}} X_k.$$

Now, for each $k \in \mathcal{K}$, $\Lambda_{3Cr_k}(x_k)$ intersects at most $O(C^2)$ boxes $\Lambda_{3Cr_l}(x_l)$ for $l \in \mathcal{K}$. We may therefore partition \mathcal{K} in $I = O(C^2)$ disjoint sets $\mathcal{K}_1, \dots, \mathcal{K}_I$ for which the $\Lambda_{3Cr_k}(x_k)$ with $k \in \mathcal{K}_i$ are all disjoint. Set $S_i := \sum_{k \in \mathcal{K}_i} X_k$. Hölder's inequality implies that

$$\mathbf{E}_{D^\delta, D^\delta}^{\theta, \theta} [\mathbf{R}(A)^N] \leq \mathbf{E}_{D^\delta, D^\delta}^{\theta, \theta} [(S_1 + \dots + S_{|I|})^N] \leq |I|^{N-1} \sum_{i=1}^{|I|} \mathbf{E}_{D^\delta, D^\delta}^{\theta, \theta} [S_i^N].$$

The mixing property of the double random current proved in [28] and Theorem 2.11 imply the existence of $C_{\text{mix}} \in (0, \infty)$ (independent of everything) such that S_i is stochastically

dominated by $C_{\text{mix}}\tilde{S}_i$, where \tilde{S}_i is the sum of $|\mathcal{K}_i|$ independent Geometric random variables ($\tilde{X}_k : k \in \mathcal{K}_i$) of parameter $1/2$. We deduce that

$$\mathbf{E}_{D^\delta, D^\delta}^{\theta, \theta}[S_i^N] \leq C_{\text{mix}}^N \times \frac{(C_0|\mathcal{K}_i|)^N}{N!}.$$

Since $|\mathcal{K}_i| \leq |\mathcal{K}| \leq C_1 n \log(d/\kappa)$, we deduce that

$$\mathbf{E}_{D^\delta, D^\delta}^{\theta, \theta}[\mathbf{R}(A)^N] \leq \frac{(C_2 n \log(d/\kappa))^N}{N!}.$$

This concludes the proof. \square

We now turn to the third lemma that we will need. Let $\partial_\alpha \Omega$ be the set of points in Ω that are exactly at a Euclidean distance equal to α away from $\partial\Omega$.

Lemma 4.10 (Large double random current clusters do not come close to the boundary). *For every $C, \alpha, \varepsilon > 0$, there exists $\beta = \beta(C, \alpha, \varepsilon) > 0$ such that for every $D \subseteq \Lambda_C$,*

$$\mathbf{P}_{D^\delta, D^\delta}^{\theta, \theta}[\partial_\alpha D \xleftrightarrow{\mathbf{n}_1 + \mathbf{n}_2} \partial_\beta D] \leq \varepsilon. \quad (4.4)$$

Proof. Assume that $\partial_\alpha D$ is not empty otherwise there is nothing to prove. Since $D \subseteq \Lambda_C$, one may find a collection of $k = O((C/\alpha)^2)$ vertices $x_1, \dots, x_k \in \frac{1}{3}\alpha\mathbb{Z}^2$ such that

- $\Lambda_{2\alpha/3}(x_i) \subseteq D$ for $1 \leq i \leq k$;
- $\Lambda_\alpha(x_i) \not\subseteq D$ for $1 \leq i \leq k$;
- $\partial_\alpha D \subseteq \Lambda_{\alpha/3}(x_1) \cup \dots \cup \Lambda_{\alpha/3}(x_k)$.

Then, Theorem 2.14 implies that

$$\mathbf{P}_{D^\delta, D^\delta}^{\theta, \theta}[\partial_\alpha D \xleftrightarrow{\mathbf{n}_1 + \mathbf{n}_2} \partial_\beta D] \leq \sum_{i=1}^k \mathbf{P}_{D^\delta, D^\delta}^{\theta, \theta}[\Lambda_{\alpha/3}(x_i) \xleftrightarrow{\mathbf{n}_1 + \mathbf{n}_2} \partial_\beta D] \leq k\varepsilon(\beta/\alpha). \quad (4.5)$$

We then choose β so that the right-hand side is smaller than ε . \square

These ingredients are enough for the proof of Proposition 4.6.

Proof of Proposition 4.6. First, Lemma 4.9 shows that for every $n \geq 2$, there exist $C_n, M_n < \infty$ such that for all sets of points $A = \{a_1, \dots, a_n\} \subsetneq D$, we have

$$\mathbf{E}_{D^\delta, D^\delta}^{\theta, \theta}[\mathbf{R}^\delta(A)^n] \leq C_n \left| \log(\min_{i \neq j} |a_i - a_j|) \wedge \log \frac{1}{\delta} \right|^{M_n}. \quad (4.6)$$

Lemma 4.10 implies that for every $n \geq 2$ and every $\eta > 0$, there exists a function $\rho : [0, \infty) \rightarrow [0, \infty)$ satisfying $\rho(0) = 0$ and continuous at 0, and such that for all δ and all sets of points $A = \{a_1, \dots, a_n\} \subsetneq D$ that are pairwise at least η away from each other, we have

$$\mathbf{P}_{D^\delta, D^\delta}^{\theta, \theta}[\mathbf{l}^\delta(A)] \leq \rho(\min_i \text{dist}(u_i, \partial D)).$$

The proof is then a direct combination of these two inequalities with Lemma 4.8 and (4.2). \square

We now turn to the computation of the first term on the right-hand side of (4.2) using the approach of Kenyon [43]. The next result is an analog of [43, Proposition 20].

Proposition 4.11. *Let $a_1, a_1^0, \dots, a_n, a_n^0$ be distinct points in D , and let $\gamma_1, \dots, \gamma_n$ be pairwise disjoint curves in D connecting a_i^0 to a_i for $i = 1, \dots, n$. Then,*

$$\lim_{\delta \rightarrow 0} \mathbf{E}_{D^\delta, D^\delta}^{\theta, \theta} \left[\prod_{i=1}^n (h^\delta(a_i) - h^\delta(a_i^0)) \right] = i^n \sum_{\epsilon \in \{\pm 1\}^n} \prod_{i=1}^n \epsilon_i \int_{\gamma_1} \cdots \int_{\gamma_n} \det [f_{\epsilon_i, \epsilon_j}(z_i, z_j)]_{1 \leq i, j \leq n} dz_1^{(\epsilon_1)} \cdots dz_n^{(\epsilon_n)},$$

where $dz_i^{(1)} = dz_i$, $dz_i^{(-1)} = d\bar{z}_i$, and

$$f_{\epsilon_i, \epsilon_j}(z_i, z_j) = \begin{cases} 0 & \text{if } i = j, \\ f_-(z_i, z_j) & \text{if } (\epsilon_i, \epsilon_j) = (-1, 1), \\ f_+(z_i, z_j) & \text{if } (\epsilon_i, \epsilon_j) = (1, 1), \\ \overline{f_-(z_i, z_j)} & \text{if } (\epsilon_i, \epsilon_j) = (1, -1), \\ \overline{f_+(z_i, z_j)} & \text{if } (\epsilon_i, \epsilon_j) = (-1, -1). \end{cases}$$

Moreover the limit is conformally invariant.

Proof. We start by proving a stronger version of the conformal invariance statement. Namely, if one expands the determinant under the integrals as a sum of terms over permutations ι , then each multiple integral of the term $T_{\epsilon, \iota}$ corresponding to a fixed ϵ and ι is conformally invariant. This follows from the conformal covariance of the functions $f_\pm(z_i, z_j)$ stated in Lemma 4.2 and an integration by substitution. Indeed, it is enough to notice that $T_{\epsilon, \iota}$ is a product of n functions $f_\pm(z_i, z_j)$ or their conjugates with the property that each variable z_i appears in it exactly twice and in a way that, under a conformal map φ , it contributes a factor $\varphi'(z_i)$ if $\epsilon_i = 1$ and $\overline{\varphi'(z_i)}$ if $\epsilon_i = -1$.

We now turn to the convergence part. To this end, we fix dual paths $\gamma_1^\delta, \dots, \gamma_n^\delta$ connecting $(u_i^0)^\delta$ with u_i^δ for every $i = 1, \dots, n$. It will be convenient to choose the paths γ in such a way that:

- the faces of C_{D^δ} visited by each γ alternate with each step between U^δ and V^δ (by definition, the paths start and end in U^δ),
- the restriction of each γ to U^δ is a path in the dual of D^δ , meaning that consecutive faces share an edge in D^δ ,
- the restriction of each γ to V^δ is a path in D^δ given by the left endpoints of the edges of D^δ crossed by the path.

Note that paths satisfying these conditions only cross corner edges of C_{D^δ} .

We enumerate the edges crossed by γ_i^δ (there is always an even number of them) using the symbols $c_{i,1}^+, c_{i,1}^-, \dots, c_{i,l_i}^+, c_{i,l_i}^-$. With a slight abuse of notation we will also write $c_{i,t}^\pm$ for the indicator functions that the edge belongs to the dimer cover, and $\hat{c}_{i,t}^\pm := c_{i,t}^\pm - \mathbf{E}[c_{i,t}^\pm]$ for the centred version. Since the height increments are centered by the choice of the reference

1-form f_0 (3.3) and since $|f_0| = 1/2$ on all roads, we find

$$\begin{aligned}
\mathbf{E}_{D^\delta, D^\delta}^{\emptyset, \emptyset} \left[\prod_{i=1}^n (h^\delta(a_i) - h^\delta(a_i^0)) \right] &= \mathbf{E}_{D^\delta, D^\delta}^{\emptyset, \emptyset} \left[\prod_{i=1}^n \sum_{t=1}^{l_i} (c_{i,t}^+ - c_{i,t}^-) \right] \\
&= \mathbf{E}_{D^\delta, D^\delta}^{\emptyset, \emptyset} \left[\prod_{i=1}^n \sum_{t=1}^{l_i} (\hat{c}_{i,t}^+ - \hat{c}_{i,t}^-) \right] \\
&= \sum_{t_1=1}^{l_1} \cdots \sum_{t_n=1}^{l_n} \sum_{s \in \{\pm\}^n} (-1)^{\#_-(s)} \mathbf{E} \left[\prod_{i=1}^n \hat{c}_{i,t_i}^{s_i} \right], \quad (4.7)
\end{aligned}$$

where $\#_-(s)$ is the number of minuses in s .

Fix t_1, \dots, t_n and $s \in \{\pm\}^n$, and let $\hat{c}_i := \hat{c}_{i,t_i}^{s_i}$. By [43, Lemma 21], the determinant of the inverse Kasteleyn matrix gives correlations of height increments, hence

$$\mathbf{E}_{D^\delta, D^\delta}^{\emptyset, \emptyset} \left[\prod_{i=1}^n \hat{c}_i \right] = \left(\prod_{i=1}^n K(b_i, w_i) \right) \det \hat{C} = (-1)^n \det \hat{C} = \det \hat{C}, \quad (4.8)$$

where \hat{C} is the $n \times n$ matrix given by

$$\hat{C}_{i,j} = \begin{cases} K^{-1}(w_i, b_j) & \text{if } i \neq j, \\ 0 & \text{otherwise.} \end{cases}$$

Here we used that the edges of C^δ (roads) corresponding to the corners in D^δ are assigned weight -1 in the Kasteleyn weighting as defined in Section 3.3.1.

Let e_i be the edge satisfying $c^\pm(e_i) = c_{i,t_i}^\pm$, and let z_i be its midpoint. We write $f_\pm := f_\pm^D$ and $f^\delta := f^{D^\delta}$. Proposition 4.4 gives

$$K^{-1}(w_i, b_j) = -\frac{\delta i}{\sqrt{2}} (f_-(z_i, z_j) - \bar{\eta}_{c_i}^2 \eta_{c_j}^2 \overline{f_-(z_i, z_j)} + \bar{\eta}_{c_i}^2 f_+(z_i, z_j) - \eta_{c_j}^2 \overline{f_+(z_i, z_j)} + o(1)).$$

We now expand the determinant from (4.8) as a sum over permutations. Let us investigate the term in this expansion coming from a fixed permutation ι , and for simplicity of notation, let us assume that ι is the cycle $\iota(i) = i + 1 \pmod{n}$. The case of a general permutation will follow in a similar manner. The term under consideration reads

$$\begin{aligned}
&\text{sgn}(\iota) \frac{\delta^n}{\sqrt{2}^n} i^n \prod_{i=1}^n \left(f_-(z_i, z_{i+1}) + \bar{\eta}_{c_i}^2 f_+(z_i, z_{i+1}) - \right. \\
&\quad \left. \bar{\eta}_{c_i}^2 \eta_{c_{i+1}}^2 \overline{f_-(z_i, z_{i+1})} - \eta_{c_{i+1}}^2 \overline{f_+(z_i, z_{i+1})} \right) + o(\delta^n) \\
&= \text{sgn}(\iota) \frac{\delta^n}{\sqrt{2}^n} i^n \prod_{i=1}^n \left(f_{-1,1}(z_i, z_{i+1}) + \eta_{c_i}^{-2} f_{1,1}(z_i, z_{i+1}) - \right. \\
&\quad \left. \eta_{c_i}^{-2} \eta_{c_{i+1}}^2 f_{1,-1}(z_i, z_{i+1}) - \eta_{c_{i+1}}^2 f_{-1,-1}(z_i, z_{i+1}) \right) + o(\delta^n). \quad (4.9)
\end{aligned}$$

We can now expand the product into a sum of 4^n terms. Note that for each corner c_i , the factors $\eta_{c_i}^2$ and $\eta_{c_i}^{-2}$ appear in exactly one out of n brackets, meaning that each final term contains a multiplicative factor of $\eta_{c_i}^{r_{c_i}}$, where $r_{c_i} \in \{-2, 0, 2\}$.

The first important observation is that the terms for which there exists i such that $r_{c_i} = 0$ cancel out to $o(\delta^n)$ after summing over all sign choices $s \in \{-1, 1\}^n$ in (4.7). Indeed, for each such term, take the smallest i for which $r_{c_i} = 0$ and consider the corresponding term assigned in (4.7) to a different sign choice s' which differs from s only at the coordinate i . By (4.9) the two terms differ by $o(\delta^n)$, and the cancellation in (4.7) is caused by the fact that $\#_-(s) = -\#_-(s')$.

There are exactly 2^n remaining terms indexed by $\epsilon \in \{-1, 1\}^n$ that satisfy $r_{c_i} = -2\epsilon_i$ for all i . Note that in the embedding of the square lattice $\delta\mathbb{Z}^2$, all corners have length $\delta\sqrt{2}/2$, and therefore

$$\eta_{c_i}^{\pm 2} = \sqrt{2}\delta^{-1}dc_i^{(\mp 1)},$$

where $dc_i^{(1)} := dc_i$ and $dc_i^{(-1)} := \overline{dc_i}$. Hence, the $\sqrt{2}$ -terms cancel out, and each such term is of the form

$$\text{sgn}(\iota)i^n \left(\prod_{i=1}^n \epsilon_i \right) \left(\prod_{i=1}^n f_{\epsilon_i, \epsilon_{i+1}}(z_i, z_{i+1}) \right) dc_i^{(\epsilon_1)} \cdots dc_n^{(\epsilon_n)} + o(\delta^n). \quad (4.10)$$

The term $\prod_{i=1}^n \epsilon_i$ arises as the product of the signs from the expansion of (4.9).

Since

$$d(c_{i,t_i}^+)^{(\epsilon_i)} - d(c_{i,t_i}^-)^{(\epsilon_i)} = d(z_i^\delta)^{(\epsilon_i)},$$

keeping the permutation ι and the signs ϵ fixed, and summing (4.10) over all $s \in \{-1, 1\}^n$, we obtain

$$\text{sgn}(\iota)i^n \left(\prod_{i=1}^n \epsilon_i \right) \left(\prod_{i=1}^n f_{\epsilon_i, \epsilon_{i+1}}(z_i, z_{i+1}) \right) d(z_1^\delta)^{(\epsilon_1)} \cdots d(z_n^\delta)^{(\epsilon_n)} + o(\delta^n).$$

Finally, summing back over all permutations, we obtain that (4.7) is equal to

$$\begin{aligned} & i^n \sum_{t_1=1}^{l_1} \cdots \sum_{t_n=1}^{l_n} \left(\sum_{\epsilon \in \{\pm\}^n} \left(\prod_{i=1}^n \epsilon_i \right) \det [f_{\epsilon_i, \epsilon_j}(z_i, z_j)]_{1 \leq i, j \leq n} d(z_1^\delta)^{(\epsilon_1)} \cdots d(z_n^\delta)^{(\epsilon_n)} + o(\delta^n) \right) \\ &= i^n \sum_{\epsilon \in \{\pm\}^n} \left(\prod_{i=1}^n \epsilon_i \right) \int_{\gamma_1} \cdots \int_{\gamma_n} \det [f_{\epsilon_i, \epsilon_j}(z_i, z_j)]_{1 \leq i, j \leq n} dz_1^{(\epsilon_1)} \cdots dz_n^{(\epsilon_n)} + o(1). \end{aligned} \quad (4.11)$$

This concludes the proof of Proposition 4.11. \square

Proof of Theorem 4.5. We already proved in Proposition 4.11 that the desired limit exists and is conformally invariant. Hence, it is enough to identify it for the upper half-plane \mathbb{H} . In this case, by Lemma 4.2 we have an explicit formula

$$f_{\epsilon_i, \epsilon_j}(z_i, z_j) = \frac{i^{\frac{\epsilon_j - \epsilon_i}{2}}}{2\pi(z_j^{(\epsilon_j)} - z_i^{(\epsilon_i)})},$$

where $z_i^{(1)} = z_i$ and $z_i^{(-1)} = \overline{z_i}$. Up to conjugation by a diagonal matrix with entries $i^{\frac{\epsilon_i}{2}}$, this is the same matrix as in [44, Lemma 3.1], and hence

$$\det [f_{\epsilon_i, \epsilon_j}(z_i, z_j)]_{1 \leq i, j \leq n} = \frac{1}{(2\pi)^n} \sum_{\pi \text{ pairing of } \{1, \dots, n\}} \prod_{\{i, j\} \in \pi} \frac{1}{(z_j^{(\epsilon_j)} - z_i^{(\epsilon_i)})^2}.$$

This means that, after exchanging the order of summations, integrals and products, (4.11) is equal to

$$\begin{aligned} & \frac{i^n}{(2\pi)^n} \sum_{\pi \text{ pairing of } \{1, \dots, n\}} \prod_{\{i, j\} \in \pi} 2\Re \left[\int_{\gamma_j} \int_{\gamma_i} \frac{dz_i dz_j}{(z_j - z_i)^2} - \frac{d\bar{z}_i dz_j}{(z_j - \bar{z}_i)^2} \right] \\ &= \pi^{-\frac{n}{2}} \sum_{\pi \text{ pairing of } \{1, \dots, n\}} \prod_{\{i, j\} \in \pi} \frac{1}{2\pi} \ln \left| \frac{(u_j - u_i)(u_j^0 - u_i^0)(u_j^0 - \bar{u}_i)(u_j - \bar{u}_i^0)}{(u_j^0 - u_i)(u_j - u_i^0)(u_j - \bar{u}_i)(u_j^0 - \bar{u}_i^0)} \right|. \end{aligned}$$

Note that the terms in the product above converge to $G_{\mathbb{H}}(u_i, u_j)$ as u_i^0 and u_j^0 get close to $\partial\mathbb{H}$. This together with (4.3) implies that, up to the explicit multiplicative constant, the moments have the same scaling limit as in [44], which ends the proof. \square

4.3 Convergence of h^δ as a random distribution

Recall that for $a \in D$ we write $h^\delta(a)$ for the evaluation of the nesting field at a face $u^\delta = u^\delta(a)$ of D^δ containing a . For a test function $g : D \rightarrow \mathbb{R}$, define

$$h^\delta(g) := \int_D g(a) h^\delta(a) da. \quad (4.12)$$

Theorem 4.12. *Let h_D be the GFF in D with zero boundary conditions, and let g_1, \dots, g_k be continuous test functions with compact support. Then, for $l_1, \dots, l_k \in \mathbb{N}$,*

$$\lim_{\delta \rightarrow 0} \mathbf{E}_{D^\delta, D^\delta}^{\theta, \theta} \left[\prod_{i=1}^k h^\delta(g_i)^{l_i} \right] = \mathbf{E} \left[\prod_{i=1}^k \left(\frac{1}{\sqrt{\pi}} h_D(g_i) \right)^{l_i} \right],$$

Proof. To simplify notation, we only consider moments $\mathbf{E}[h^\delta(g)^l]$ of one test function g for l even. The general case follows in a similar way. To this end, we fix $l \geq 2$, and define

$$D_\delta^l := \{(a_1, \dots, a_l) \in D^l : |a_i - a_j| < \delta \text{ for some } i \neq j\}.$$

Then by Lemma 4.8 and (4.6) we have

$$\begin{aligned} \int_D \cdots \int_D \mathbf{E}_{D^\delta, D^\delta}^{\theta, \theta} \left[\prod_{i=1}^l g(a_i) h^\delta(a_i) \right] \mathbf{1}_{(a_1, \dots, a_l) \in D_\delta^l} da_1 \cdots da_l &\leq C \|g\|_\infty^l (\log \frac{1}{\delta})^{lM} \lambda^{2l}(D_\delta^l) \\ &\leq C' \|g\|_\infty^l \lambda^2(D)^{l-1} (\log \frac{1}{\delta})^M \delta^2 \end{aligned}$$

for some constants C, C' and M that depend on l , where λ^{2l} is the $2l$ -dimensional Lebesgue measure. Note that the right-hand side tends to zero as $\delta \rightarrow 0$. The function

$$(a_1, \dots, a_l) \mapsto |\log(\min_{i \neq j} |a_i - a_j|)|^{lM}$$

is integrable over D^l , and hence by dominated convergence, Lemma 4.8 and (4.6) again, we

have

$$\begin{aligned}
\lim_{\delta \rightarrow 0} \mathbf{E}_{D^\delta, D^\delta}^{\theta, \theta} [h^\delta(g)^l] &= \lim_{\delta \rightarrow 0} \int_D \cdots \int_D \mathbf{E}_{D^\delta, D^\delta}^{\theta, \theta} \left[\prod_{i=1}^l g(a_i) h^\delta(a_i) \right] da_1 \cdots da_l \\
&= \lim_{\delta \rightarrow 0} \int_D \cdots \int_D \mathbf{E}_{D^\delta, D^\delta}^{\theta, \theta} \left[\prod_{i=1}^l g(a_i) h^\delta(a_i) \right] \mathbf{1}_{(a_1, \dots, a_l) \in D^l \setminus D_\delta^l} da_1 \cdots da_l \\
&= \int_D \cdots \int_D \left(\prod_{i=1}^l g(a_i) \right) \lim_{\delta \rightarrow 0} \mathbf{E}_{D^\delta, D^\delta}^{\theta, \theta} \left[\prod_{i=1}^n h^\delta(a_i) \right] \mathbf{1}_{(a_1, \dots, a_l) \in D^l \setminus D_\delta^l} da_1 \cdots da_l \\
&= \int_D \cdots \int_D \left(\prod_{i=1}^l g(a_i) \right) \sum_{\pi \text{ pairing}} \prod_{\{i, j\} \in \pi} \frac{1}{\pi} G_D(a_i, a_j) da_1 \cdots da_l \\
&= \mathbf{E}[(\frac{1}{\sqrt{\pi}} h_D(g))^l],
\end{aligned}$$

where the second last equality follows from Theorem 4.5. \square

Remark 4.13. We note that the same convergence as in Theorem 4.12 holds if the height function is considered as a function on all faces of C_{G^δ} and not only on the faces of G^δ .

We are now ready to conclude the proof the main theorem of this section.

Proof of Theorem 2.1. By Theorem 4.12, all moments of h^δ converge to the corresponding moments of $\frac{1}{\sqrt{\pi}} h_D$, and since h_D is a Gaussian process, we conclude that h^δ tends to $\frac{1}{\sqrt{\pi}} h_D$ in distribution as δ tends to 0 in the space of generalized functions acting on continuous test functions with compact support. \square

5 Proof of Propositions 2.3, 2.5, and 2.9

We now present the proofs of Propositions 2.3, 2.5, and 2.9. These proofs rely heavily on the results from [28].

5.1 Proof of Proposition 2.3

Proof of tightness and Property 1. We already know that h^δ converges as $\delta \rightarrow 0$ to the GFF in D with zero boundary conditions. Furthermore, the tightness of ϵ^δ is trivial once the one of (B^δ, A^δ) has been justified. We therefore focus on the latter. Recall the tightness criterion [3, **H1**]: a family of random variables \mathcal{F}^δ (with law \mathbb{P}_δ) taking values in $\mathfrak{C}(\Omega)$ satisfies **H1** if for every $k < \infty$ and every annulus $\text{Ann}(x, r, R)$ with $\delta \leq r \leq R \leq 1$, the following bound holds uniformly in $\delta > 0$:

$$\mathbb{P}_\delta[\text{Ann}(x, r, R) \text{ is crossed by } k \text{ separate pieces of interfaces in } \mathcal{F}^\delta] \leq C(k) \left(\frac{r}{R}\right)^{\lambda(k)}, \quad (5.1)$$

with $C(k) > 0$ and $\lambda(k)$ tending to infinity as $k \rightarrow \infty$.

We apply this criterion to the family $(B^\delta \cup A^\delta)$ (we can also apply it to B^δ or A^δ). The event that $\text{Ann}(x, r, R)$ is crossed by k separate pieces of interfaces in $A^\delta \cup B^\delta$ is included in the (rescaled version of the) event $A_{2k}(r/\delta, R/\delta)$, so that we may apply Theorem 2.11. \square

Until the end of this section, consider (B, A, ϵ, h) to be the limit of a converging subsequence $(B^{\delta_n}, A^{\delta_n}, \epsilon^{\delta_n}, h^{\delta_n})$.

Proof of Property 2. Every loop in A is surrounded by a loop in B by construction.

The fact that the loops in A and B do not intersect is a direct consequence of Theorem 2.12. Indeed, fix $\alpha, \beta, \epsilon > 0$. For two loops of A^{δ_n} of diameter at least α to come within distance β of each other, there must be $x \in \Omega^{\delta_n}$ such that the translate by x of the rescaled version of the event $A_4^{\square}(\beta/\delta_n, \alpha/\delta_n)$ occurs. Yet, Theorem 2.12 implies that provided that $\beta \leq \beta_0(\alpha, \epsilon)$, this occurs with probability smaller than ϵ . The same is true for two loops of B^{δ_n} .

The fact that the loops in A and B are simple is also direct consequence of Theorem 2.12. Indeed, the event that a single loop comes within distance β of itself after going away to distance α also implies the same event. Letting β tend to zero, then α , and finally ϵ , we obtain the result.

The fact that A is not equal to $\{\partial D\}$ is an easy consequence of Theorem 2.14. \square

Proof of Property 3. Let $\mathcal{C}(\ell)$ be the cluster whose exterior boundary is ℓ . Notice that the definition of the nesting field implies that

$$h^{\delta_n} = \sum_{\ell \in B^{\delta_n}} \sum_{\gamma \in A^{\delta_n}(\ell)} (h_{\gamma}^{\delta_n} + \epsilon_{\mathcal{C}(\ell)} \mathbf{1}_{O(\gamma) \text{ odd hole of } \mathcal{C}(\ell)}),$$

where $h_{\gamma}^{\delta_n}$ is the nesting field in $O(\gamma)$ (we use that $\mathcal{C}(\ell)$ is either odd around *every* face in $O(\gamma)$, or it is odd around none of them). Let us start by showing that for every test function g ,

$$\lim_{\alpha \rightarrow 0} \lim_{n \rightarrow \infty} \int_{D^{\delta_n}} g(x) h^{\delta_n}(x) \mathbf{1}_{x \in E_{\alpha}^{\delta_n}} dx = 0, \quad (5.2)$$

where, if $\Lambda_{\alpha}(y) := y + [-\alpha, \alpha]^2$,

$$E_{\alpha}^{\delta_n} := \text{union of the } \Lambda_{\alpha}(y) \text{ for } y \in \alpha \mathbb{Z}^2 \text{ such that } \Lambda_{2\alpha}(y) \text{ intersects some } \gamma \in A^{\delta_n}$$

(note that in particular every x that is within a distance α of some γ in A^{δ_n} must be in $E_{\alpha}^{\delta_n}$).

In order to prove this statement, we fix $\epsilon > 0$ and see that

$$\begin{aligned} \epsilon \mathbb{P}_{\delta} \left[\int_{D^{\delta_n}} g(x) h^{\delta_n}(x) \mathbf{1}_{x \in E_{\alpha}^{\delta_n}} dx \geq \epsilon \right] &\leq \mathbb{E}_{\delta} \left[\left| \int_{D^{\delta_n}} g(x) h^{\delta_n}(x) \mathbf{1}_{x \in E_{\alpha}^{\delta_n}} dx \right| \right] \\ &\leq \sum_{y \in \alpha \mathbb{Z}^2} \mathbb{E}_{\delta} \left[\left| \int_{\Lambda_{\alpha}(y)} g(x) h^{\delta_n}(x) \mathbf{1}_{x \in E_{\alpha}^{\delta_n}} dx \right| \right] \\ &= \sum_{y \in \alpha \mathbb{Z}^2} \mathbb{E}_{\delta} \left[\mathbf{1}_{y \in E_{\alpha}^{\delta_n}} \left| \int_{\Lambda_{\alpha}(y)} g(x) h^{\delta_n}(x) dx \right| \right] \\ &\leq \sum_{y \in \alpha \mathbb{Z}^2} \mathbb{P}_{\delta} [y \in E_{\alpha}^{\delta_n}]^{1/2} \mathbb{E}_{\delta} \left[\left(\int_{\Lambda_{\alpha}(y)} g(x) h^{\delta_n}(x) dx \right)^2 \right]^{1/2} \\ &\leq \sum_{y \in \alpha \mathbb{Z}^2} \alpha^c \times C(g) \alpha^2 \log(1/\alpha) \leq C(g, D) \log(1/\alpha) \alpha^c. \end{aligned}$$

Above, we used Markov's inequality in the first inequality, the triangle inequality in the second, the fact that $x \in E_\alpha^{\delta_n}$ is equivalent to $y \in E_\alpha^{\delta_n}$ in the third, and Cauchy–Schwarz in the fourth. In the fifth, we combine an easy estimate on the second moment of $\int_{\Lambda_\alpha(y)} g(x) h^{\delta_n}(x) dx$ based on the definition of the nesting field and RSW type estimates from [28], together with the fact that for $\Lambda_\alpha(y)$ to intersect a loop γ in A^{δ_n} , there must be a primal path in $\mathbf{n}_1 + \mathbf{n}_2$ from $\Lambda_\alpha(x)$ to $\Lambda_\beta(x)$ or a path in $(\mathbf{n}_1 + \mathbf{n}_2)^*$ from $\partial\Lambda_\beta(x)$ to $\partial\Lambda_{d(x, \partial D)}(x)$, where $\beta := \sqrt{\alpha d(x, \partial D)}$.

Then, (5.2) follows by sending n to infinity, then α to 0, and finally ε to 0.

Now for every fixed $\alpha > 0$, the convergence of A^{δ_n} , the spatial Markov property (in each $O(\gamma)$, the double random current has free boundary conditions) and Theorem 2.1 imply that the functions $h_\gamma^{\delta_n}$ converge to independent GFF in $O(\gamma)$ with zero boundary conditions for every γ with radius at least α (here the convergence is the convergence of the random variables obtained by averaging against a test function with compact support in $O(\gamma)$). Also, the convergence of h^{δ_n} implies that $\mathbb{P}_{\delta_n}[\mathcal{C}(\ell) \text{ odd around } \gamma | A^{\delta_n}, B^{\delta_n}]$ also converges⁷ to a quantity that we denote $c(\gamma) \in [0, 1]$. Overall, we deduce by integrating against test functions and first conditioning on $A^{\delta_n}, B^{\delta_n}$, that the limit h has the same law as

$$\sum_{\ell \in B} \sum_{\gamma \in A(\ell)} (h_\gamma + \epsilon_{\mathcal{C}(\ell)} c(\gamma))$$

where the h_γ are independent GFF in each $O(\gamma)$.

It remains to check that $c(\gamma) \in \{0, 1\}$ when γ can be reached by a finite sequence of loops and that $c(\gamma)$ is equal to 0 or 1 depending only on the parity of the length of the sequence. Recall that we say that a hole of a double random current cluster is *odd* if \mathcal{C} is odd around the hole. Otherwise we say that it is *even*. By Theorem 2.12, we know that γ is the scaling limit of the boundary of a hole of the cluster of $\mathbf{n}_1 + \mathbf{n}_2$ whose external boundary converges to ℓ . Note that this is really a consequence of the theorem and that it is not direct as one may be worried that several loops of $A^{\delta_n} \cup B^{\delta_n}$ collapse into a single loop (that would be counted with multiplicity) in the limit.

Now, we know from Theorem 2.13 that two adjacent big holes in the discrete must have, with probability very close to 1, an odd $(\mathbf{n}_1 + \mathbf{n}_2)$ -flux between them, and therefore must correspond to a height function that is changing by 1, or in other words if one of the holes is odd, then the second one is even, etc. The result follows readily. \square

Proof of Property 4. Fix $\alpha, \beta, \varepsilon > 0$. For a loop of A^{δ_n} of diameter at least α and with inner boundary value 0 to come within a distance β of a loop in B^{δ_n} of diameter at least α , there must be $x \in \Omega^{\delta_n}$ such that the translate by x of the rescaled version of the event $A_4^\blacksquare(\beta/\delta_n, \alpha/\delta_n)$ occurs. Yet, Theorem 2.13 implies that provided that $\beta \leq \beta_0(\alpha, \varepsilon)$, this occurs with probability smaller than ε . Letting β tend to zero, then α , and finally ε , we obtain the result. \square

Proof of Property 5. For this item, we invoke [10]. Indeed, the Kramers-Wannier duality implies that the odd part $\eta_i^{\delta_n} = \eta(\mathbf{n}_i^{\delta_n})$ of $\mathbf{n}_i^{\delta_n}$ can be seen as the low temperature expansion of a critical Ising model with plus boundary conditions on the dual graph $(\Omega^{\delta_n})^\dagger$. We can therefore use [10] to prove that the large interfaces converge to CLE_3 . More precisely, we

⁷In fact, we may also further extract subsequential limits to guarantee the convergence.

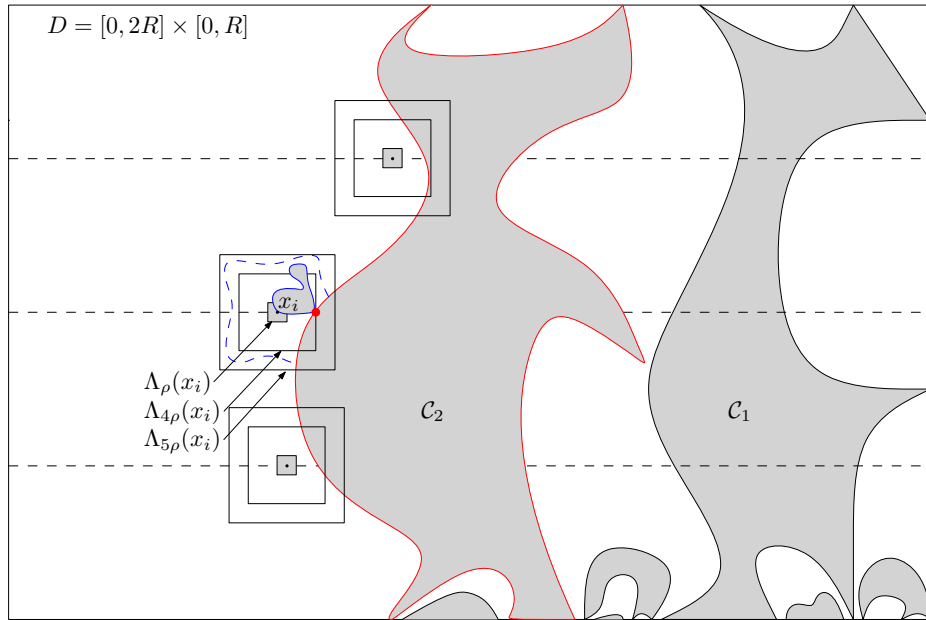


Figure 5.1: The two right-most clusters crossing D from top to bottom. We also depicted three examples of $\Lambda_\rho(x_i)$. In blue, we explained one example of an event $E_2(i)$ occurring, with one XOR cluster of pluses going from $\Lambda_\rho(x_i)$ to $\partial\mathcal{C}_2$, and the absence of a crossing from inside to outside in $\Lambda_{5\rho}(x_i) \setminus \Lambda_{4\rho}(x_i)$.

know that the collection $\mathcal{F}_\alpha(\eta_1^{\delta_n})$ of loops in $\eta_1^{\delta_n}$ that are larger than α converges weakly to the set of loops in CLE_3 that are larger than α (here we do not insist on the decomposition into loops of the even graph $\mathcal{F}_\alpha(\eta_1^{\delta_n})$ as it was proved in [10] that it is irrelevant for the scaling limit). We deduce that the loops in B , which are more exterior than the limit of the outer boundaries of the outermost clusters in the union of $\mathcal{F}_\alpha(\eta_1^{\delta_n})$ and $\mathcal{F}_\alpha(\eta_2^{\delta_n})$, must be more exterior than the outer boundaries of the outermost clusters in the union of the loops that are larger than α in two independent CLE_3 . Since CLE_4 can be obtained as the outer boundaries of the outermost clusters in the union of two CLE_3 (see [75]), we obtain the result. \square

Remark 5.1. At this stage, it is unclear whether B is strictly bigger than CLE_4 or not, as the even parts of $\mathbf{n}_1^{\delta_n}$ and $\mathbf{n}_2^{\delta_n}$ could increase the size of the double random current clusters substantially, thus making B strictly larger than CLE_4 . In fact, even the fact that the outer boundaries of the outermost clusters of the union of $\eta(\mathbf{n}_1^{\delta_n})$ and $\eta(\mathbf{n}_2^{\delta_n})$ is CLE_4 is not obvious, since we obtained this result by first considering loops that are larger than α and then by taking the limit as α tends to 0. It could in fact be that the “dust” made of tiny loops in both configurations play a role that is similar to the even part of each current in the last sentence, and that loops are strictly larger than CLE_4 .

5.2 Proof of Proposition 2.5

Proof of tightness. The tightness is a consequence of Remark 7.3 of [28]. \square

Proof of Property 1. This is a consequence of Theorem 2.4. □

Proof of Property 2. This follows from the same argument as the one leading to Property 3 of Proposition 2.3. The reason for the difference in gaps in the two propositions comes from the construction of the nesting field in the discrete. The proof of the last property regarding odd and even holes is the same as in the previous proposition. □

5.3 Proof of Proposition 2.9

Proof of tightness. This follows directly from Theorem 2.11. The fact that C is not equal to $\{\partial D\}$ is a direct consequence of Corollary 2.16. □

Proof of Property 1. This is the object of Proposition 2.3. □

Proof of Property 2. The fact that $S \subseteq B$ and that every loop in $S \cup \tilde{S}$ is encircled by a loop in C is a straightforward consequence of tightness. The two other points in Item 3 follow from the construction in the discrete and the following statement: for every $\varepsilon > 0$, there exists $\eta > 0$ such that for every δ small enough,

$$\mathbb{P}_{\Omega^\delta}[E(\varepsilon, \eta, \delta)] \leq \varepsilon, \tag{5.3}$$

where $E(\varepsilon, \eta, \delta)$ is the event that there exists $\gamma \in B^\delta$ that has diameter ε and comes within a distance η of a loop $\ell \in C^\delta$ without intersecting it.

To see this, condition on the outer boundaries of the exterior-most XOR clusters, as well as the clusters in $\mathbf{n}_1 + \mathbf{n}_2$ that are adjacent to those clusters (note that they have the opposite spin). We need to prove that in the unexplored region \mathbf{D} , the probability that there exists a cluster of $\mathbf{n}_1 + \mathbf{n}_2$ of diameter at least ε coming within a distance η of $\partial \mathbf{D}$ is bounded by ε , uniformly in any possible realization of \mathbf{D} .

Introduce the events

$$A := \{\exists \text{ a cluster in } \mathbf{n}_1 + \mathbf{n}_2 \text{ from } \partial_\alpha \mathbf{D} \text{ to } \partial_\eta \mathbf{D}\},$$

$$B := \{\exists \text{ a cluster in } \mathbf{n}_1 + \mathbf{n}_2 \text{ in } \mathbf{D} \text{ of radius at least } \varepsilon \text{ remaining within distance } \alpha \text{ of } \partial \mathbf{D}\}.$$

To bound the probability of \mathbf{D} , further condition on the clusters of $\mathbf{n}_1 + \mathbf{n}_2$ that contain a vertex that is at a distance at least α from $\partial \mathbf{D}$ and call \mathbf{D}' the remaining domain. Then, one considers a box of size $\varepsilon/3$, and use the merging-vertices trick from [28] (we refer to the paper for details) to prove that the probability that there exists a cluster intersecting the box and the complement of it is bounded by $\exp[-c_0\varepsilon/\alpha]$. We omit the details here since similar reasoning have been implemented repeatedly in [28]. Since one may pave Ω by of order $O(1/\varepsilon^2)$ boxes of size $\varepsilon/3$, we deduce that

$$\mathbb{P}_{\Omega^\delta}[B|\mathbf{D}, \mathbf{D}'] \leq \mathbf{P}_{\mathbf{D}', \mathbf{D}'}^{\emptyset, \emptyset}[B] \leq \frac{C_0}{\varepsilon^2} \exp[-c_0\varepsilon/\alpha] \leq \varepsilon/2,$$

where the second inequality follows by choosing $\alpha = \alpha(\varepsilon)$ small enough. Averaging over \mathbf{D} gives

$$\mathbb{P}_{\Omega^\delta}[B] \leq \varepsilon/2. \tag{5.4}$$

Then, one uses Corollary 4.10 to show that the probability of the event A satisfies

$$\mathbb{P}_{\Omega^\delta}[A] \leq \varepsilon/2 \quad (5.5)$$

provided $\eta = \eta(\varepsilon, \alpha)$ is chosen small enough (note that \mathbf{D} can be made of a number of connected components, but that only $N = N(\alpha)$ are such that they contain a point at a distance at least α of $\partial\mathbf{D}$).

The two previous displayed equations imply the claim. \square

Proof of Property 3. In the discrete, conditioning on C^{δ_n} and then on S^{δ_n} implies that in each hole $O(\ell)$ with $\ell \in \tilde{S}^{\delta_n}$, we have a double random current model with free boundary conditions and height function h^{δ_n} equal to 0 on the boundary. We deduce that

$$h^{\delta_n} = \sum_{\ell \in S^{\delta_n} \cup \tilde{S}^{\delta_n}} h_\ell^{\delta_n},$$

where $h_\ell^{\delta_n}$ for $\ell \in \tilde{S}^{\delta_n}$ has the law of the associated nesting field in $O(\gamma)$, and \tilde{h}^{δ_n} is a height function on the complement of the vertices enclosed by the loops in \tilde{S}^{δ_n} .

Proving Item 3 from this equality is following the same lines as the end of the proof of Item 2 of Proposition 2.3, namely one first condition on holes larger than α and then prove that the error made by forgetting the other holes is not contributing anything when taking the limit as n tends to infinity and then α to 0. The fact that each $h_\ell^{\delta_n}$ for ℓ of diameter at least α converges can be deduced from the convergence of h^{δ_n} tested against well-chosen test-functions (those with support in $O(\ell)$). \square

Proof of Property 5. Let us first briefly sketch the proof in the first paragraph. We first make trivial manipulations to focus on bounding the probability of having an XOR interface staying close on the left to the j -th right-most cluster \mathcal{C}_j crossing a $R \times 2R$ rectangle. Then, one picks points at a distance between $2r$ and $3r$ (with $r := \lfloor \eta R \rfloor$ with $\eta \ll 1$) to the left of \mathcal{C}_j and use Theorem 2.14 to show that with a probability that remains bounded away from zero uniformly, the box of size r around these points is connected by pluses to $\partial\mathcal{C}_j$.

We now turn to a formal proof. We rescale everything by $R := \lfloor 1/\delta \rfloor$. Fix $\eta > 0$ and set $r := \lfloor \eta R \rfloor$. By paving the domain, it suffices to show that for every $\varepsilon > 0$, there exists $\eta = \eta(\varepsilon) > 0$ such that for every R and every domain $\Omega \supset \Lambda_{3R}$,

$$\mathbb{P}_\Omega \left[\begin{array}{l} \text{there are interfaces in the XOR and double random current crossing} \\ \text{from } \partial\Lambda_R \text{ to } \partial\Lambda_{2R} \text{ and remaining at a distance } \eta R \text{ of each other} \end{array} \right] \leq \varepsilon. \quad (5.6)$$

For the event in (5.6) to occur, there must exist a rectangle D chosen out of the translates by a vector in $R\mathbb{Z}^2$ of the rectangles $[0, R] \times [0, 2R]$ and $[0, 2R] \times [0, R]$ that are included in Λ_{2R} such that there exist interfaces in the XOR and the double random current model crossing D between the two long sides and staying within a distance r of each other. We now assume that D is equal to $[0, 2R] \times [0, R]$ (we may translate and rotate everything to get into this situation) and bound the probability that this event happens.

Let \mathcal{C}_j be the j -th right-most D -cluster crossing D from bottom to top, when it exists and assume that it has spin $+$. For a fixed k , set $\rho := R/(12k)$ (we forget the rounding operation) and consider, for every $1 \leq i \leq k$, the left-most vertex x_i on the horizontal line at height $12\rho i$ such that $\Lambda_{3\rho}(x_i)$ intersects \mathcal{C}_j but $\Lambda_{2\rho}(x_i)$ does not. We refer to Fig. 5.1 for a picture.

Let $E_j(i)$ be the event that $\Lambda_\rho(x_i)$ is connected by pluses to $\partial\mathcal{C}_j$, and $\Lambda_{4\rho}(x_i)$ is *not* connected to $\Lambda_{5\rho}(x_i)$ on the left of \mathcal{C}_j . When $\Lambda_{4\rho}(x_i)$ is not connected to $\Lambda_{5\rho}(x_i)$ on the left of \mathcal{C}_j in $\mathbf{n}_1 + \mathbf{n}_2$, let $D_j(i)$ be the connected component of x_i in the set of points in $\Lambda_{5\rho}(x_i)$ that are not connected to $\partial\Lambda_{5\rho}(x_i)$ in $\mathbf{n}_1 + \mathbf{n}_2$. Using [28, Corollary 3.5] in the first inequality and then Theorem 2.14 for $D_j(i)$, we get that

$$\mathbb{P}_\Omega[E_j(i)|\mathcal{C}_j] \geq c_0 \mathbb{P}_\Omega[\Lambda_\rho(x_i) \xrightarrow{+} \partial\mathcal{C}_j | \mathcal{C}_j, \Lambda_{5\rho}(x_i) \not\xrightarrow{-} \Lambda_{4\rho}(x_i) \text{ in } \mathbf{n}_1 + \mathbf{n}_2] \geq c_1.$$

Therefore, the mixing property from [28, Section 3.2] implies that the number of integers i between $k/3$ and $2k/3$ such that $E_j(i)$ occurs dominates a Binomial random variable of parameter $k/3$ and $c_2 := c_{\text{mix}}c_1$.

We now fix j and set $k = k(\eta) := \log(1/\eta)$. Consider the event E_j that $E_j(i)$ occurs for some i . We deduce that

$$\mathbb{P}_\Omega[E_j^c] \leq \eta^{c_3} \mathbb{P}_\Omega[\mathcal{C}_j \text{ exists and has spin } +].$$

Since the expected number of clusters crossings D is bounded by [28, Corollary 7.2], the union bound gives that

$$\mathbb{P}_\Omega[\cup_j E_j^c] \leq C_3 \eta^{c_3}. \quad (5.7)$$

Noticing that if $\cap_j E_j$ occurs, there is no XOR interface crossing D and remaining on the left and at a distance r of an interface of the double random current crossing D , we conclude the proof by using (5.7), and by doing the same with spin $-$ and with the left-most crossings of D instead of the right-most ones. \square

5.4 Nested interfaces

In this section, we extend these results to nested interfaces. First, we deal with the free boundary conditions. We work directly with the results for both the double random current and the XOR-Ising model.

Let $(C_0^\delta, s_0^\delta, S_0^\delta, \tilde{S}_0^\delta, \epsilon_0^\delta, B_0^\delta, A_0^\delta)$ be defined as $(C^\delta, s^\delta, S^\delta, \tilde{S}^\delta, \epsilon^\delta, B^\delta, A^\delta)$. For $i \geq 0$, given $(C_i^\delta, s_i^\delta, S_i^\delta, \tilde{S}_i^\delta, \epsilon_i^\delta, B_i^\delta, A_i^\delta)_\delta$, define by recursion for every $\ell \in A_i^\delta$, by replacing D by $O(\ell)$, the tuple $(C_\ell^\delta, s_\ell^\delta, S_\ell^\delta, \tilde{S}_\ell^\delta, \epsilon_\ell^\delta, B_\ell^\delta, A_\ell^\delta)$, and let

$$(C_{i+1}^\delta, s_{i+1}^\delta, S_{i+1}^\delta, \tilde{S}_{i+1}^\delta, \epsilon_{i+1}^\delta, B_{i+1}^\delta, A_{i+1}^\delta)$$

defined by $\#_{i+1}^\delta$ (for $\#$ equal to $C, s, S, \tilde{S}, \epsilon, B, A$) to be the union of the $\#_\ell^\delta$ for $\ell \in A_i^\delta$. Finally, set

$$(C_{\text{nested}}^\delta, s_{\text{nested}}^\delta, S_{\text{nested}}^\delta, \tilde{S}_{\text{nested}}^\delta, \epsilon_{\text{nested}}^\delta, B_{\text{nested}}^\delta, A_{\text{nested}}^\delta, h^\delta),$$

where $\#_{\text{nested}}^\delta$ is the union of the $\#_i^\delta$.

Proposition 5.2 (Nested version for free boundary conditions). *Fix a simply connected domain D and consider the coupling measure \mathbb{P}_{D^δ} between the double random current and the XOR-Ising model. The family*

$$(C_{\text{nested}}^\delta, s_{\text{nested}}^\delta, S_{\text{nested}}^\delta, \tilde{S}_{\text{nested}}^\delta, \epsilon_{\text{nested}}^\delta, B_{\text{nested}}^\delta, A_{\text{nested}}^\delta, h^\delta)_{\delta > 0}$$

is tight for the topology of weak convergence, and for every subsequential limit

$$(C_{\text{nested}}, s_{\text{nested}}, S_{\text{nested}}, \tilde{S}_{\text{nested}}, \epsilon_{\text{nested}}, B_{\text{nested}}, A_{\text{nested}}, h),$$

the following holds: For every ℓ in $A_{\text{nested}} \cup \tilde{S}_{\text{nested}}$, conditioned on ℓ , $h|_{D \setminus O(\ell)}$ and all the loops that are not surrounded by ℓ as well as their spins and labels, the next layer of interfaces in $O(\ell)$ satisfy the same properties of Propositions 2.3 and 2.9, except that (2.6) needs to be replaced by

$$\epsilon(\gamma) = (-1)^k s(\ell), \quad (5.8)$$

where k is the number of odd holes surrounding ℓ .

Proof. The proof can be adapted from the previous proof very easily using the spatial Markov property implying that in each hole of the outermost double random current clusters, \mathbf{n}_1 and \mathbf{n}_2 are independent random current configurations with free boundary conditions. \square

For the wired boundary conditions, consider the tuple of nested objects

$$(\hat{A}^\delta, C_{\text{nested}}^\delta, s_{\text{nested}}^\delta, S_{\text{nested}}^\delta, \tilde{S}_{\text{nested}}^\delta, \epsilon_{\text{nested}}^\delta, B_{\text{nested}}^\delta, A_{\text{nested}}^\delta, h^\delta),$$

where \hat{A}^δ was introduced above Proposition 2.5 and then the nested elements are defined recursively as in the case of free boundary conditions.

Proposition 5.3 (Nested version for wired and plus/plus boundary conditions). *Fix a simply connected domain D with C^1 boundary and consider the coupling measure $\hat{\mathbb{P}}_{D^\delta}$ between the double random current with wired boundary conditions and the XOR-Ising model with plus/plus boundary conditions. The family*

$$(\hat{A}^\delta, C_{\text{nested}}^\delta, s_{\text{nested}}^\delta, S_{\text{nested}}^\delta, \tilde{S}_{\text{nested}}^\delta, \epsilon_{\text{nested}}^\delta, B_{\text{nested}}^\delta, A_{\text{nested}}^\delta, h^\delta)_{\delta > 0}$$

is tight for the topology of weak convergence, and for every subsequential limit

$$(\hat{A}, C_{\text{nested}}, s_{\text{nested}}, S_{\text{nested}}, \tilde{S}_{\text{nested}}, \epsilon_{\text{nested}}, B_{\text{nested}}, A_{\text{nested}}, h),$$

the following holds: For every ℓ in $\hat{A} \cup A_{\text{nested}} \cup \tilde{S}_{\text{nested}}$, conditioned on ℓ , $h|_{D \setminus O(\ell)}$ and all the loops that are not surrounded by ℓ as well as their spins and labels, the next layer of interfaces in $O(\ell)$ satisfy the same properties of Propositions 2.3 and 2.9, except that (2.6) needs to be replaced by

$$\epsilon(\gamma) = (-1)^k s(\ell), \quad (5.9)$$

where k is the number of odd holes surrounding ℓ .

Proof. The only observation is that conditioned on the loops in \hat{A}^δ , the double random current in the holes is a double random current with free boundary conditions. Then, the proof follows readily from arguments that are similar to the previous ones. \square

6 Preliminaries in the continuum

In this section, we recall some background on the continuum side, notably on the Gaussian free field and its local sets, which will be the main tools of our proofs. Throughout, let $D \subsetneq \mathbb{C}$ be a simply connected domain whose boundary is a Jordan curve. We also continue to use the notations fixed in Section 2.2.1.

6.1 Schramm-Loewner evolution

The Schramm-Loewner evolution (SLE) was introduced by Schramm in [68] as a candidate for the scaling limit of interfaces in a class of statistical physics models. For each $\kappa \geq 0$, an SLE_κ is a random non self-crossing curve parametrized by the Loewner evolution with a random driving function which is equal to $\sqrt{\kappa}$ times a standard Brownian motion. The most common forms of SLE are the chordal (connecting two boundary points) and radial (connecting one boundary point and one interior point) SLEs.

It was shown in [78] that SLE_κ is a.s. a simple curve for $\kappa \in (0, 4]$, is a.s. self-intersecting for $\kappa \in (4, 8)$, and is a.s. space-filling for $\kappa \geq 8$. In this work, we will only consider the case $\kappa = 4$. As we will explain in Section 6.2, SLE_4 -type curves are level lines of the Gaussian free field.

One common variant of the chordal (resp. radial) SLE_κ is the chordal (resp. radial) $\text{SLE}_\kappa(\rho_1, \dots, \rho_n)$ process, introduced in [50]. It is a chordal (resp. radial) SLE with n additional marked points x_1, \dots, x_n on the boundary (in addition to the starting and ending points of the curve).

It was shown in [73] that the chordal and radial parametrizations of SLE can be interchanged, namely an SLE targeting a boundary point can be equivalently viewed as targeting an interior point (with a changed driving function), and vice versa. The precise coordinate change formula was computed in [73]. In particular, if an $\text{SLE}_\kappa(\rho_1, \dots, \rho_n)$ satisfies $\rho_1 + \dots + \rho_n = \kappa - 6$, then this process is *target-invariant*, namely it has the same law when viewed as targeting different points. For example, the target-invariant branching $\text{SLE}_\kappa(\kappa - 6)$ process plays an important role in the construction of Conformal loop ensembles (CLE) in [74], as we will explain in Section 6.3.

6.2 Gaussian free field and local sets

Recall that the Gaussian free field (GFF) h with zero boundary condition in D is defined by (2.3). The notion of *local set* for GFF was introduced by Schramm and Sheffield in [70]. Here, we write down its definition for a GFF in the unit disk \mathbb{U} . For any other simply connected domain D , one can simply map D conformally onto \mathbb{U} . Let Γ be the space of all closed nonempty subsets of $\overline{\mathbb{U}}$. We view Γ as a metric space, endowed by the Hausdorff metric induced by the Euclidean distance. Note that Γ is naturally equipped with the Borel σ -algebra on Γ induced by this metric. Given $A \in \Gamma$, let A_δ denote the closure of the δ -neighborhood of A in \mathbb{U} . Let \mathcal{A}_δ be the smallest σ -algebra in which A and the restriction of h to the interior of A_δ are measurable. Let

$$\mathcal{A} := \bigcap_{\delta \in \mathbb{Q}, \delta > 0} \mathcal{A}_\delta.$$

Intuitively, this is the smallest σ -field in which A and the values of h in an infinitesimal neighborhood of A are measurable.

Definition 6.1 (Local set [70]). *Let h be a GFF in \mathbb{U} . We say that A is a local set of h if A is a closed subset of $\overline{\mathbb{U}}$ and one can write $h = h_A + h^A$, where*

- h_A is an \mathcal{A} -measurable random distribution which on $\mathbb{U} \setminus A$ a.s. has finite pointwise values and is harmonic.
- h^A is a random distribution which is independent of \mathcal{A} . It is a.s. zero on A and equal to an independent zero boundary GFF in each connected component of $\mathbb{U} \setminus A$.

Local sets behave nicely when one takes their conditionally independent union. More precisely, if A_1 and A_2 are local sets of h , then we can construct a triple (A_1, A_2, h) so that A_1 and A_2 are independent conditionally on h . The *conditionally independent union* $A = A_1 \check{\cup} A_2$ is defined to be $A_1 \cup A_2$ for the previous triple (A_1, A_2, h) .

Lemma 6.2 (Lemmata 3.10 and 3.11, [70]). *If A_1 and A_2 are local sets coupled with the GFF h on D , then their conditionally independent union $A = A_1 \check{\cup} A_2$ is also local. Moreover, when A_1 and A_2 are connected local sets, $h_A - h_{A_2}$ is a.s. an harmonic function in $D \setminus A$ that tends to zero on all sequences of points in $D \setminus A$ that tend to a limit in $A_2 \setminus A_1$ (unless A_2 is a single point).*

An important family of local sets for GFF consists of the *level lines*. In [69, 70], Schramm and Sheffield studied level lines of the discrete GFF, and showed that they converge in the scaling limit to SLE₄ type curves which are coupled with the GFF as its local sets. This is in fact a particular case of the coupling between SLE _{κ} and GFF for $\kappa \in (0, 8)$, see [24, 57–60, 70] and the references therein. Let us record in the following the properties of this coupling for $\kappa = 4$. Throughout, let

$$\lambda := \sqrt{\pi/8}.$$

Proposition 6.3 (Coupling SLE₄ and GFF, [24, 57, 70]). *Let D be a simply connected domain. Let h be a GFF in D with piecewise constant boundary conditions with finitely many pieces. Fix $x \in \partial D$ and $y_1, y_2 \in \partial D \setminus \{x\}$ such that the clockwise boundary arc from x to y_1 has boundary condition strictly smaller than λ and the clockwise boundary arc from y_2 to x has boundary condition strictly larger than $-\lambda$. Fix $y \in \partial D$, then there a.s. exists a unique curve η from x targeting y (however this curve may end before reaching y) which satisfies the following property.*

- *Let us parametrize η by the time interval $[0, 1]$ in a continuous injective way. For any $t \in [0, 1]$, $\eta([0, t])$ is a local set of h such that h_A (as given by Definition 6.1 for $A = \eta([0, t])$) is equal to $-\lambda$ on the right side of η and equal to λ on the left side of η .*
- *We call η a 0-height level line of h . Moreover, η is distributed as an SLE₄(ρ_1, \dots, ρ_n) curve in D from x to y where ρ_1, \dots, ρ_n are related to the boundary conditions of h as in Fig. 6.1.*
- *If for $y_3, y_4 \in \partial D$ the clockwise boundary arc from y_3 to y_4 has boundary condition larger than or equal to λ or smaller than or equal to $-\lambda$, then η a.s. does not intersect any point on this arc except possibly the endpoints y_3, y_4 .*

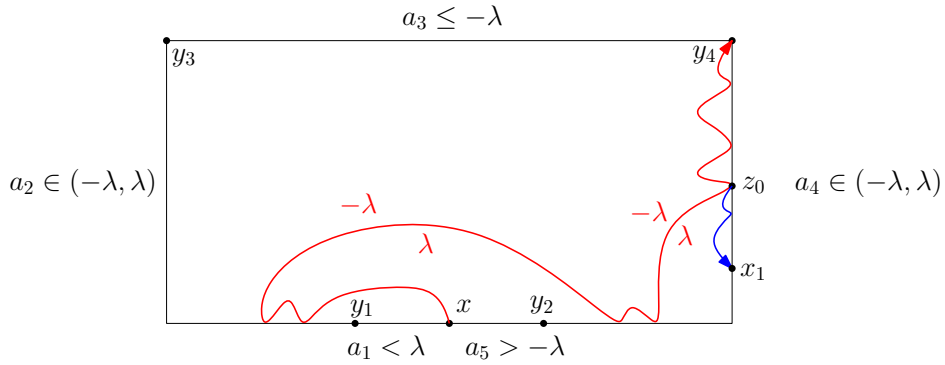


Figure 6.1: We depict a 0-height level line of a GFF with piecewise constant boundary conditions. The boundary conditions of h on the clockwise arcs (x, y_1) , (y_1, y_3) , (y_3, y_4) , (y_4, y_2) , (y_2, x) are given by a_1, \dots, a_5 . The red curve is the 0-height level line from x targeting y_4 . The level line from x targeting x_1 is given by the concatenation of the red curve from x to z_0 and the blue curve from z_0 to x_1 . These two level lines from x (targeting y_4 and x_1 respectively) coincide with each other until the first time that the curve separates the two target points, after which they evolve in the different connected components towards their targets. Take the level line from x targeting x_1 for example, it is distributed as an $\text{SLE}_4(\rho_1, \dots, \rho_6)$ from x to x_1 with marked points x^-, y_1, y_3, y_4 on its left and x^+, y_2 on its right. Let ρ_1, \dots, ρ_6 be respectively the parameters for the points $x^-, y_1, y_3, y_4, x^+, y_2$. The rule is that for the marked points on the left we have $-\lambda(1 + \rho_1 + \dots + \rho_i) = a_i$ for $i = 1, 2, 3, 4$, and for the marked points on the right we have $\lambda(1 + \rho_5) = a_5$ and $\lambda(1 + \rho_5 + \rho_6) = a_4$. A level line cannot always reach its target point (this depends on the continuation threshold of the corresponding SLE curve). For example, in this picture, the level line from x targeting a point y on the arc (y_3, y_4) ends at y_4 , because a 0-height level line can never intersect (y_3, y_4) due to the boundary condition $a_3 \leq -\lambda$.

We have combined several results in Proposition 6.3. A fundamental point of it is the uniqueness of level lines (given their starting and target points) [70]. This is at the very basis of many other results about local sets, including the uniqueness of two-valued sets (Lemma 6.16) and the results in the present work. Lemma 6.2 will allow us to consider the union of multiple level lines which is still a local set of h . We will almost always use Lemma 6.2 in this context, so the conditionally independent union $\check{\cup}$ is in fact the usual union \cup , since level lines are deterministic functions of h .

Remark 6.4. By taking limits, the statements of Proposition 6.3 can be extended to the case of piecewise constant boundary conditions with infinitely many pieces (see [63]).

Remark 6.5. Proposition 6.3 is stated only for level lines targeting boundary points, but the target point only serves to determine for each t in which connected component of $D \setminus \eta([0, t])$ η continues to evolve after time t (the level lines are target-invariant), so we can also define level lines targeting interior points.

Remark 6.6. The curve η in Proposition 6.3 is called a *level line* of the GFF h with *height* 0, and it is a deterministic function of h . For each $a \in \mathbb{R}$, one can also consider level lines of a GFF h at height a , which consists of curves that are local sets of h with boundary conditions $a - \lambda$ and $a + \lambda$ at the two sides of the curve. The existence and boundary-intersecting

behavior of such level lines can be deduced from Proposition 6.3 applied to $h - a$.

For a given GFF in D , its level lines at different heights interact with each other according to the following rules.

Lemma 6.7 (Theorem 1.5 in [57]). *Let h be a GFF in D with piecewise constant boundary values. Fix $u_1, u_2 \in \mathbb{R}$ and x_1, x_2, y on ∂D in a counterclockwise order. Let η_1 (resp. η_2) be the level line of h at height u_1 (resp. u_2) starting from x_1 (resp. x_2) (whenever it is possible) and targeting y .*

- *If $u_2 > u_1$, then η_2 a.s. stays to the right of η_1 .*
- *If $u_2 < u_1$, then η_1 may intersect η_2 and, upon intersecting, η_2 crosses to the left of η_1 and never crosses back.*
- *If $u_2 = u_1$, then η_1 may intersect η_2 and, upon intersecting, the two curves merge and never separate.*

Remark 6.8. Proposition 6.3 and Lemma 6.7 are stated for given points x, x_1, x_2 and y on ∂D , so that the description of the level line η from x (resp. x_1, x_2) targeting y holds a.s. The same statements hold if x, x_1, x_2 and y are chosen independently of h . These results, as stated, do not rule out the existence of x, x_1, x_2, y on ∂D (which are chosen in a way depending on h) for which the a.s. description does not hold (even though we can deduce results that apply to all points, we prefer to avoid this discussion here). If ∂D is a continuous curve and I_1, I_2 are two positive portions of ∂D , then for a.e. $x \in I_1$ and a.e. $y \in I_2$ (see Definition 6.9), the a.s. properties of the level line from x targeting y (such as the boundary-intersecting behavior) described in Proposition 6.3 hold.

Let us now introduce the following notion which is applied to boundaries of simply connected domains (in particular loops). It will be used throughout this work.

Definition 6.9 (Positive portion of a boundary). *For a simply connected domain $D \subsetneq \mathbb{C}$, we say that a set $I \subseteq \partial D$ is a positive portion of the boundary if the following holds: for a conformal map f from D onto the unit disk, the set $f(I)$ is connected and has positive Lebesgue measure on the unit circle. When we say “almost everywhere (a.e.)” on I , we mean that it is a.e. with respect to the preimage of the Lebesgue measure under f . This definition does not depend on the choice of f .*

6.3 Conformal loop ensemble and other level loops

Let us recall a few basic facts about the conformal loop ensembles (CLE) (introduced and studied in [74, 75]) and other level loops of the GFF. The family of CLE depends on a parameter $\kappa \in (8/3, 8)$, and each element is denoted by CLE_κ . In this work, we will consider the case $\kappa = 4$ only. In this regime (in fact for $\kappa \in (8/3, 4]$), a CLE in D is a random countable collection of simple loops in D which are disjoint from each other. The gasket of CLE_κ a.s. has Lebesgue measure zero. The law of a CLE is invariant under all conformal automorphisms from D onto itself.

In [74], Sheffield constructed CLE_κ for all $\kappa \in (8/3, 8)$ using a *branching SLE* $_\kappa(\kappa - 6)$ *exploration tree*. In particular, each loop in CLE_κ locally looks like an SLE_κ curve. Since SLE_4 -type curves are coupled with the GFF as its level lines, CLE_4 is also coupled with

the GFF (see Section 2.2.1 and Fig. 2.1 for a detailed description of the coupling). The $SLE_\kappa(\kappa - 6)$ process has the particularly nice property of target-invariance. More generally, the family of branching $SLE_\kappa(\rho, \kappa - 6 - \rho)$ exploration trees has the target-invariance property, and can be used to construct CLE and its variant BCLE (introduced in [61]).

For $\kappa = 4$, the branching $SLE_4(\rho, -2 - \rho)$ exploration tree is used to construct $BCLE_4(\rho)$ in [61]. By varying ρ , this allows one to construct level loops of the GFF at all heights. Below, we will describe the symmetric case of $\rho = -1$ which turns out to be particularly useful (the gasket of $BCLE_4(-1)$ is the same as $\mathbb{A}_{-\lambda, \lambda}$ in [8], see the next subsection).

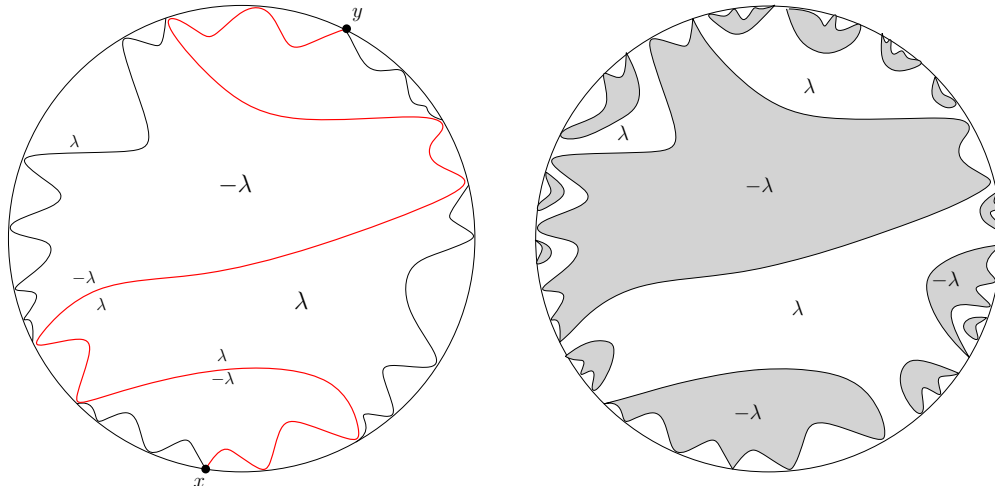


Figure 6.2: **Left:** We illustrate the branching $SLE_4(-1, -1)$ process which is used to construct $BCLE_4(-1)$. One branch from x to y is depicted in red. **Right:** We color the domains encircled by the counterclockwise loops in the $BCLE_4(-1)$ in grey. The white area corresponds to the domains encircled by the clockwise loops in the $BCLE_4(-1)$. The GFF restricted to each of the grey (resp. white) domains has boundary condition $-\lambda$ (resp. λ).

Let us now define the $SLE_4(-1, -1)$ exploration tree coupled to h as its level lines. Fix two distinct points $x, y \in \partial D$ (see Fig. 6.2). By Proposition 6.3, the 0-height level line of h from x to y is a.s. distributed as an $SLE_4(-1, -1)$ from x to y . Fix $x, y_1, y_2 \in \partial D$ distinct. Let η_1 (resp. η_2) be a 0-height level line of h , which has the law of $SLE_4(-1, -1)$ from x to y_1 (resp. y_2). Due to the uniqueness of level lines (Proposition 6.3), η_1 and η_2 a.s. agree with each other until the first time T such that y_1 and y_2 are in two different connected components of $D \setminus \eta([0, T])$ (this is also consistent with the target-invariance of $SLE_4(-1, -1)$). After time T , η_1 and η_2 evolve independently in the two connected components that contain y_1 and y_2 (splitting into two branches in the exploration tree). The branching $SLE_4(-1, -1)$ exploration tree coupled with h is defined to be the closure of the union of 0-height level lines from x to y over a countable dense collection of points $y \in \partial D$. Let $BCLE_4(-1)$ be the collection of (clockwise and counterclockwise) loops traced by this branching exploration tree. For each counterclockwise (resp. clockwise) loop γ in $BCLE_4(-1)$, $h|_{O(\gamma)}$ is equal to a GFF with boundary value $-\lambda$ (resp. λ). The gasket of $BCLE_4(-1)$ is exactly equal to the branching $SLE_4(-1, -1)$ exploration tree, and is a local set of h with boundary values in $\{-\lambda, \lambda\}$.

One can further define the nested version of $BCLE_4(-1)$ by iterating (just like how we

define a nested CLE). The nested $\text{BCLE}_4(-1)$ can be constructed using the radial version of branching $\text{SLE}_4(-1, -1)$ targeting a dense countable collection of points in D . Fix the countable collection $\{z_i, i \geq 1\}$ of points with rational coordinates in D . Fix $x \in \partial D$. The branching radial $\text{SLE}_4(-1, -1)$ exploration tree is the union of all radial $\text{SLE}_4(-1, -1)$ from x targeting z_i . In order to describe the relation between this radial branching tree and the nested $\text{BCLE}_4(-1)$, let us first define the following collections of loops (see Fig. 6.3 right).

Definition 6.10 (Collections L_k). *Given a GFF h in D , let us define the collections of loops L_k for $k \in \mathbb{N}_0$, which are the loops in the k -th layer of the nested $\text{BCLE}_4(-1)$. The loops in L_k have the property that for each $\gamma_k \in L_k$, the restricted field $h|_{O(\gamma_k)}$ is equal to a zero-boundary GFF $h^0|_{O(\gamma_k)}$ plus a boundary value in $\bigcup_{j=0}^k \{(k-2j)\lambda\}$.*

More concretely, we proceed by induction. Let $L_0 := \{\partial D\}$. For $k \geq 0$, assume that we have defined the collections of loops L_k with the property that for each $\gamma_k \in L_k$, the restricted field $h|_{O(\gamma_k)}$ is equal to a zero-boundary GFF $h^0|_{O(\gamma_k)}$ plus a boundary value in $\bigcup_{j=0}^k \{(k-2j)\lambda\}$. Let L_{k+1} be the union of $\text{BCLE}_4(-1)(h^0|_{O(\gamma_k)})$ over all $\gamma_k \in L_k$. Then for each $\gamma_{k+1} \in L_{k+1}$, the restricted field $h|_{O(\gamma_{k+1})}$ is equal to a zero-boundary GFF $h^0|_{O(\gamma_{k+1})}$ plus a boundary value in $\bigcup_{j=0}^{k+1} \{(k+1-2j)\lambda\}$.

We now explain why the radial branching $\text{SLE}_4(-1, -1)$ exploration tree constructs the nested $\text{BCLE}_4(-1)$. See Fig. 6.3 (left). Fix $x \in \partial D$, $z \in D$, and run a 0-height level line η from x targeting z . Then η is distributed as a radial $\text{SLE}_4(-1, -1)$ from x to z . At the first time T_1 that η intersects itself, η completes a loop which is the loop $\gamma_1 \in L_1$ that encircles z . After that, η continues to evolve towards z in $O(\gamma_1)$ from $\eta(T_1)$. The first time $T_2 > T_1$ that the part of η after T_1 intersects itself (not counting intersecting γ_1), it completes a loop which is the loop $\gamma_2 \in L_2$ that encircles z . Iterating, η traces all the loops in L_k that encircle z for all $k \in \mathbb{N}$.

Remark 6.11. Due to the target-invariance of level lines (see Remark 6.5), the radial branching $\text{SLE}_4(-1, -1)$ exploration tree (which is coupled with h as its level lines) has the same boundary-intersecting behavior as described by Proposition 6.3. For both the chordal and radial exploration trees, the starting point x can be randomly chosen in a way which is independent of h (see Remark 6.8). For a.e. $x \in \partial D$, the above-described construction for level lines starting from x yields the same set (by Lemma 6.7, level lines from x will immediately merge into the exploration tree, because the tree visits a dense set of points on ∂D). For a given $z \in D$, at each time that the level line η targeting z completes a loop γ_k , instead of continuing to evolve from $\eta(T_k)$, one can also consider the level line of $h|_{O(\gamma_k)}$ emanating from another point $x_k \in \gamma_k$ to obtain further loops in L_j for $j > k$.

Remark 6.12. We have already mentioned that the gasket of $\text{BCLE}_4(-1)$ is equal to $\mathbb{A}_{-\lambda, \lambda}$ considered in [8], where the same construction using level lines targeting a dense set of boundary points is also employed. This set is also equal to the arc loop ensemble (ALE) in [64]. Among the equivalent names, we will most often use the notation of two-valued set ($\mathbb{A}_{-\lambda, \lambda}$ or $\mathcal{L}_{-\lambda, \lambda}$ depending on whether we consider the loops or the gasket, see the next subsection), which turns out to be the most convenient notation in this article.

The works [61] and [8] propose an alternative way to construct the Miller-Sheffield coupling of CLE_4 and the GFF (described in Section 2.2.1) using the nested version of $\text{BCLE}_4(-1)$ (or equivalently $\mathbb{A}_{-\lambda, \lambda}$). The construction is similar in spirit to that of $\mathbb{A}_{-2n\lambda, 2n\lambda}$ using nested

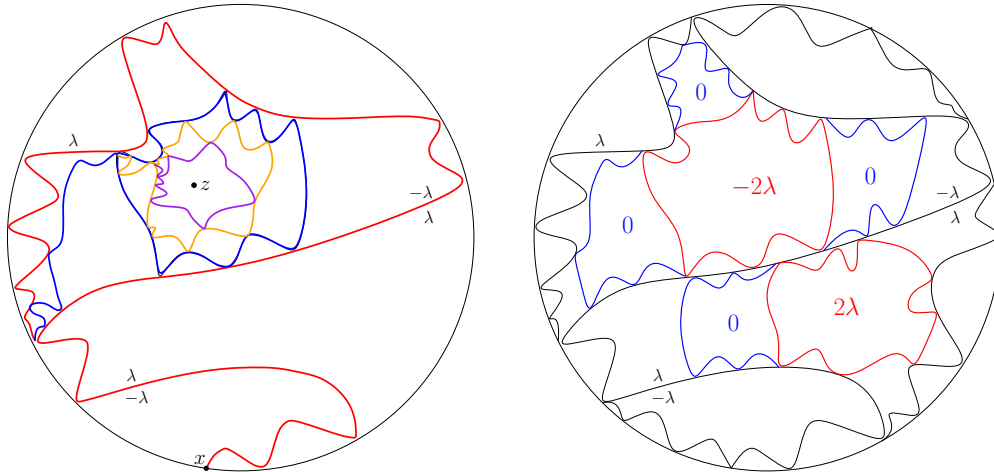


Figure 6.3: **Left:** We depict the branch of the radial $\text{SLE}_4(-1, -1)$ exploration tree targeting z . The part of SLE from x until the first time that it completes γ_1 is depicted in red. Then it continues to evolve as a radial $\text{SLE}_4(-1, -1)$ in $O(\gamma_1)$ until the first time that it completes γ_2 , depicted in blue. We depict two further layers of iteration in yellow and purple. **Right:** We depict the first and second layers of $\text{BCLE}_4(-1)$. In the second layer, the loops with boundary value -2λ or 2λ (in red) belong to the CLE_4 .

CLE_4 described in Section 2.2.1: we perform a random walk of steps $\pm\lambda$ until we reach the values $\pm 2\lambda$. More precisely, we start with $\Gamma = \emptyset$, and add loops into it successively. For each $\gamma \in L_2$ with boundary condition -2λ or 2λ , we add γ into Γ . For each $\gamma \in L_2$ with boundary condition 0, we iterate: for each loop $\gamma_1 \in L_2(h|_{O(\gamma)})$ with boundary condition -2λ or 2λ , we add γ_1 into Γ ; for each loop $\gamma_1 \in L_2(h|_\omega)$ with boundary condition 0, we continue the iteration by further splitting it into smaller loops. Whenever we encounter a loop with boundary condition -2λ or 2λ , we add it into Γ ; whenever we encounter a loop with boundary condition 0, we further split it. We end up with the collection of loops Γ being equal to $\text{CLE}_4(h)$.

Finally, let us record a lemma about the intersection between two loops in L_k and L_{k+1} that encircle the same point.

Lemma 6.13. *Fix $z \in D$ and $k \in \mathbb{N}$. Suppose $\gamma_1 \in L_k$ and $\gamma_2 \in L_{k+1}$ both encircle z . Then almost surely, $\gamma_1 \cap \gamma_2$ is non-empty and does not contain isolated points nor any positive portion of γ_1 or γ_2 .*

Proof. The curve γ_2 is part of an $\text{SLE}_4(-1, -1)$ curve η in $O(\gamma_1)$. If we parametrize η according to the usual chordal capacity for SLE, then the intersection between η and γ_1 is given by the set of $\eta(t)$ where t corresponds to the times at which a Bessel process (coming from the driving function of $\text{SLE}_4(-1, -1)$) hits zero (see e.g. [50]). The zeros of this Bessel process do not contain isolated points, nor any open interval. \square

6.4 Two-valued sets

The notion of two-valued sets is very useful in this work. It was introduced by Aru, Sepúlveda and Werner in [8], and denotes more precisely thin local sets with two prescribed boundary

values. We have given a heuristic account of two-valued sets in Section 2.2.1. We have also mentioned the examples of CLE_4 (whose gasket is a thin local set of a GFF with two boundary values in $\{-2\lambda, 2\lambda\}$) and $\text{BCLE}_4(-1)$ (whose gasket is a thin local set of a GFF with two boundary values in $\{-\lambda, \lambda\}$).

In [8], the authors first defined the more general family of *bounded type thin local sets* (denoted by BTLS), as follows.

Definition 6.14 (Bounded type thin local sets, [8]). *Let h be a GFF in D . Let A be a relatively closed subset of D . For $K > 0$, we say that A is a K -BTLS of h if*

1. (boundedness) A is a local set of h such that $|h_A(x)| \leq K$ for all $x \in D \setminus A$.
2. (thinness) for any smooth function f , we have $(h_A, f) = \int_{D \setminus A} h_A(x) f(x) dx$.

It was shown in [8] that a BTLS must be connected to the boundary of the domain.

Lemma 6.15 (Proposition 4, [8]). *If A is a BTLS, then $A \cup \partial D$ is a.s. connected.*

A two-valued set is defined to be a BTLS A such that $h_A \in \{-a, b\}$ for $a, b > 0$. The family of two-valued sets satisfies the properties of the following lemma.

Lemma 6.16 (Proposition 2 in [8]). *Let $-a < 0 < b$.*

- *When $a + b < 2\lambda$, it is not possible to construct a BTLS A such that $h_A \in \{-a, b\}$ a.s.*
- *When $a + b \geq 2\lambda$, there is a unique BTLS A coupled with h such that $h_A \in \{-a, b\}$ a.s. We denote this set A by $\mathbb{A}_{-a,b}$.*
- *If $[a, b] \subseteq [a', b']$, then $\mathbb{A}_{-a,b} \subseteq \mathbb{A}_{-a',b'}$ a.s.*

An important point of Lemma 6.16 is the uniqueness of $\mathbb{A}_{-a,b}$ when it exists. This is inherently due to the uniqueness of the level lines of the GFF (Proposition 6.3), which is also crucial for our proofs.

Let us quickly deduce a generalization of the third bullet point of Lemma 6.16 which will be used later on. Recall that we use $\mathcal{L}_{-a,b}$ to denote $\mathcal{L}(\mathbb{A}_{-a,b})$, so that $\mathbb{A}_{-a,b}$ is equal to the gasket of $\mathcal{L}_{-a,b}$.

Lemma 6.17. *Fix $a, b > 0$ with $a + b \geq 2\lambda$. Suppose that U is a collection of simple loops such that $\text{gask}(U)$ is a thin local set of h with the property that each loop $\gamma \in U$ has inner boundary value $c(\gamma) \in [-a, b]$. Then $\text{gask}(U) \subseteq \mathbb{A}_{-a,b}$.*

Proof. Define the following set of loops

$$\{\gamma \in U : c(\gamma) = -a \text{ or } b\} \cup \bigcup_{\gamma \in U : c(\gamma) \in (-a, b)} \mathcal{L}_{-a-c(\gamma), b-c(\gamma)}(h^0|_{O(\gamma)}).$$

The gasket of this collection of loops is clearly a thin local set of h with boundary values in $\{-a, b\}$, hence by uniqueness it is equal to $\mathbb{A}_{-a,b}$. This gasket clearly contains $\text{gask}(U)$. \square

The construction of $\mathbb{A}_{-a,b}$ also relies on the branching $\text{SLE}_4(\rho, -2 - \rho)$ processes. When $a + b = 2\lambda$, $\mathcal{L}_{-a,b}$ is equal to $\text{BCLE}_4(\rho)$. Properties of the $\text{SLE}_4(\rho, -2 - \rho)$ processes lead to the following intersecting behavior of the loops in $\mathcal{L}_{-a,b}$. Recall that we use $\mathcal{L}_{-a,b}^-$ (resp. $\mathcal{L}_{-a,b}^+$) to denote the collection of loops in $\mathcal{L}_{-a,b}$ with inner boundary value $-a$ (resp. b).

Lemma 6.18 (Intersecting behavior of the loops [7]). *1. There exists a loop in $\mathcal{L}_{-a,b}^+$ (resp. $\mathcal{L}_{-a,b}^-$) which intersects ∂D if and only if $b < 2\lambda$ (resp. $a < 2\lambda$).*

- 2. If $a + b < 4\lambda$, then one can connect any two loops η_1 and η_2 in $\mathcal{L}_{-a,b}$ by a finite sequence of loops $(\gamma_1, \dots, \gamma_n)$ so that $\gamma_1 = \eta_1$, $\gamma_n = \eta_2$ and γ_{k+1} intersects γ_k for each $1 \leq k \leq n-1$. Only loops with different inner boundary values can intersect each other.*
- 3. If $a + b = 2\lambda$, then two loops in $\mathcal{L}_{-a,b}$ intersect each other if and only if they share a positive portion of boundary.*
- 4. If $a + b \geq 4\lambda$, then all the loops in $\mathcal{L}_{-a,b}$ are disjoint from each other.*

7 Scaling limit of the double random current clusters

In this section, we identify the scaling limit of the double random current clusters with free boundary condition (Theorem 1.6) and wired boundary condition (Theorem 1.7). Concretely, we will focus on proving Theorem 2.2 which is the central piece of the identification. The strategy of the proof of Theorem 2.2 is explained in Section 7.1.

Then, Sections 7.2 and 7.3 are devoted to the proof of Theorem 7.8, which characterizes all thin local sets of the GFF with boundary values in $\{-\mu, 0, \mu\}$ for $\mu \geq 2\lambda$. In Section 7.2, we also characterize all simply connected open sets (and their contours) coupled with h with 0 boundary value. These two subsections can be read for their own interest, independently of everything else.

In Section 7.4, we complete the proof of Theorem 2.2. In Section 7.5, we prove Theorems 1.6, 2.4, and 1.7.

7.1 The strategy of the proof of Theorem 2.2

The proof of Theorem 2.2 takes Proposition 2.3 as an input. We use the same notations as in Proposition 2.3 and let (B, A, h, ϵ) be one subsequential limit of $(B^\delta, A^\delta, h^\delta, \epsilon^\delta)_\delta$. Our goal is to uniquely identify the law of (B, A, h, ϵ) .

Our strategy is to first define, using A , a new collection \tilde{A} of loops with the property that $\text{gask}(\tilde{A})$ is a thin local set of h with boundary values in $\{-2\sqrt{2}\lambda, 0, 2\sqrt{2}\lambda\}$. In the end, the set \tilde{A} will turn out to be equal to A , namely there in fact do not exist loops in A with boundary values other than $-2\sqrt{2}\lambda, 0$ and $2\sqrt{2}\lambda$. The main part of our proof is dedicated to the identification of the joint law of $(B, \tilde{A}, h, \epsilon)$.

Here is our definition of \tilde{A} . For each loop $\ell \in B$ and $\gamma \in A(\ell)$, let us define the collection U_γ of loops (where $c(\gamma)$ is the inner boundary value of γ)

- if $c(\gamma) \in (0, 2\sqrt{2}\lambda)$ and $\epsilon(\ell) = 1$, then let $U_\gamma := \mathcal{L}_{-c(\gamma), 2\sqrt{2}\lambda - c(\gamma)}(h^0|_{O(\gamma)})$;
- if $c(\gamma) \in (0, 2\sqrt{2}\lambda)$ and $\epsilon(\ell) = -1$, then let $U_\gamma := \mathcal{L}_{c(\gamma) - 2\sqrt{2}\lambda, c(\gamma)}(h^0|_{O(\gamma)})$;
- otherwise if $c(\gamma) \in \{0, 2\sqrt{2}\lambda\}$, then let $U_\gamma := \{\gamma\}$.

Let \tilde{A} be the union of U_γ over all $\gamma \in A$. It is easy to see that $\text{gask}(\tilde{A})$ is a thin local set of h with boundary values in $\{-2\sqrt{2}\lambda, 0, 2\sqrt{2}\lambda\}$. Note that there are infinitely many local sets

with this property. Our work consists in using additional information on B, h, ϵ to uniquely determine $(B, \tilde{A}, h, \epsilon)$. More precisely, we will prove the following proposition.

Proposition 7.1. *Almost surely, B is equal to $\text{CLE}_4(h)$, and each $\ell \in B$ has inner boundary value $\epsilon(\ell)2\lambda$. For each $\ell \in B$, let $\tilde{A}(\ell)$ denote the collection of loops in \tilde{A} encircled by ℓ . We have*

- if $\epsilon(\ell) = 1$, then $\tilde{A}(\ell) = \mathcal{L}_{-2\lambda, (2\sqrt{2}-2)\lambda}(h^0|_{O(\ell)})$;
- if $\epsilon(\ell) = -1$, then $\tilde{A}(\ell) = \mathcal{L}_{-(2\sqrt{2}-2)\lambda, 2\lambda}(h^0|_{O(\ell)})$.

The main point of Proposition 7.1 is to show that B is equal to the CLE_4 coupled with h so that the label of each loop in B corresponds to the sign of its inner boundary condition. Note that Property 5 of Proposition 2.3 provides one inequality between B and CLE_4 , but does not provide information on the coupling between B and h . More generally, due to the lack of Markov property in the discrete for the loops in B^δ , it is far from clear (relying on discrete properties only) that B is in fact coupled to h as its local set.

In order to prove Proposition 7.1, in Sections 7.2 and 7.3 we establish results characterizing thin local sets with boundary values in $\{-\mu, 0, \mu\}$ for $\mu \geq 2\lambda$. Sections 7.2 and 7.3 do not involve any discussion about double random currents or XOR-Ising models, and can be read independently. More precisely, we first show in Section 7.2 a key lemma (Lemma 7.3) which states that the contour of every simply connected open set coupled with h with boundary value 0 must be a loop in \mathbb{L}_0 , where \mathbb{L}_0 is defined as below.

Definition 7.2 (The collection \mathbb{L}_0). *Let \mathbb{L}_0 be the collection of loops in $\cup_{k \in \mathbb{N}} L_k$ (see Definition 6.10) which have inner boundary value 0.*

This then allows us to show in Section 7.3 that every thin local sets with boundary values in $\{-\mu, 0, \mu\}$ can be constructed by iteratively “splitting” the loops of H_μ (see Definitions 7.5 and 7.6).

In Section 7.4, we use the results of Sections 7.2 and 7.3 and information about (B, A, h, ϵ) to complete the proof of Theorem 2.2. Throughout, we let $\tilde{A}^0, \tilde{A}^+, \tilde{A}^-$ denote the collection of loops in \tilde{A} that respectively have inner boundary value 0, $2\sqrt{2}$ and $-2\sqrt{2}$. The result of Section 7.2 implies that $\tilde{A}^0 \subseteq \mathbb{L}_0$. Combined with additional properties of \tilde{A} and B , we can deduce that every loop in \tilde{A}^0 is encircled by a loop in $\text{CLE}_4(h)$, and further that each loop in B is encircled by a loop in $\text{CLE}_4(h)$. Together with Property 5 of Proposition 2.3, we can deduce that B is equal to $\text{CLE}_4(h)$, thus proving Proposition 7.1. Finally, we will use the adjacency properties of the loops in \tilde{A} to show that $\tilde{A} = A$, thus completing the proof of Theorem 2.2.

7.2 Characterization of simply connected open sets with 0 boundary value

The main purpose of this subsection is to prove Lemma 7.3 below. By definition, for every loop $\gamma \in \mathbb{L}_0$, $D \setminus O(\gamma)$ is a local set of h with boundary value 0. Lemma 7.3 states that \mathbb{L}_0 is exactly the collection of contours of all simply connected open sets with this property.

Lemma 7.3. *Let $U \subseteq D$ be a simply connected open set such that $\overline{D} \setminus U$ is a local set of h and $h|_U$ has 0 boundary value. Then ∂U is a.s. a loop in \mathbb{L}_0 .*

Proof. Our proof relies on the intersection behavior between level lines of the GFF and the boundary of the domain given in Proposition 6.3. We note that this was also the main tool used in [8] to prove the results about bounded type thin local sets.

Let U be as in the statement of the lemma. We will complete the proof in two steps. In Step 1, we will describe how ∂U interacts with the loops in L_k (see Definition 6.10) which are not part of 0-height level lines. (Recall that the *height* of a level line is defined in Remark 6.6. A level line with height a has boundary values $a - \lambda$ and $a + \lambda$ at its two sides.) In particular, Step 1 implies that ∂U cannot cross any loop in \mathbb{L}_0 . In Step 2, we will show that ∂U is in fact equal to a loop in \mathbb{L}_0 .

Here and in the remainder of this article, we say that two contours ∂U_1 and ∂U_2 cross each other if $U_1 \not\subseteq U_2$, $U_2 \not\subseteq U_1$ and $U_1 \cap U_2 \neq \emptyset$. We say that a contour ∂U_1 encircles another contour ∂U_2 if $U_2 \subseteq U_1$, and we say ∂U_1 strictly encircles ∂U_2 if $U_2 \subsetneq U_1$.

Step 1. Let us prove that, almost surely, for every $k \in \mathbb{N}$ and every $\gamma_k \in L_k$, if γ_k is not part of a 0-height level line coupled with h , then both points below are true.

- The loop γ_k cannot cross ∂U .
- If $O(\gamma_k) \subseteq U$, then either $\gamma_k = \partial U$ (this is only possible if γ_k has inner boundary value 0, i.e., $\gamma_k \in \mathbb{L}_0$) or γ_k can intersect ∂U at at most one point.

This will imply in particular that ∂U cannot cross any loop in \mathbb{L}_0 (note that the loops in \mathbb{L}_0 are at height either $-\lambda$ or λ).

For the sake of contradiction, suppose that with positive probability, the following event E_1 holds: there exists $k \in \mathbb{N}$ and $\gamma_k \in L_k$ such that the three points below are all true.

- The loop γ_k is part of an $a_0\lambda$ -height level line where a_0 is a non-zero integer.
- The loop γ_k is not equal to ∂U .
- Either γ_k crosses ∂U , or $O(\gamma_k) \subseteq U$ and γ_k intersects ∂U at more than one point.

On E_1 , let k be the smallest integer for which there exists such a loop $\gamma_k \in L_k$. It is clear that $U \cap O(\gamma_k) \neq \emptyset$ on E_1 . Fix $z \in D$, such that $E_1 \cap \{z \in U \cap O(\gamma_k)\}$ has positive probability. On the event $E_1 \cap \{z \in U \cap O(\gamma_k)\}$, let γ_{k-1} be the unique loop in L_{k-1} which encircles z . Due to the third condition satisfied by γ_k , one of the following two possibilities must be true.

- Either $\gamma_{k-1} \setminus U$ contains a positive portion of γ_{k-1} .
- Or $O(\gamma_k) \subseteq O(\gamma_{k-1}) \subseteq U$ and $\gamma_{k-1} \cap \partial U$ contains at least two points, say x_1, x_2 . Since $D \setminus O(\gamma_{k-1})$ and $D \setminus U$ are both local sets of h , the set $\gamma_{k-1} \cap \partial U$ is independent of $h^0|_{O(\gamma_{k-1})}$.

In both cases, by Remark 6.11, one can find $x_1 \in \gamma_{k-1} \setminus U$, such that the $\text{BCLE}_4(-1)$ coupled to $h|_{O(\gamma_{k-1})}$ can be constructed by running an exploration tree of level lines started from x_1 . Let η be the 0-height level line of $h^0|_{O(\gamma_{k-1})}$ from x_1 targeting z . Then γ_k is equal to the loop that η makes at the first time $t_0 > 0$ that $\eta(t_0)$ intersects its past $\eta([0, t_0))$. Since $\gamma_k \cap U \neq \emptyset$ and γ_k intersects ∂U at more than one point, there exists $t > 0$ such that with positive probability, $\eta(t) \in \gamma_k \cap U$ and the future part of η (after t) needs to hit ∂U in order

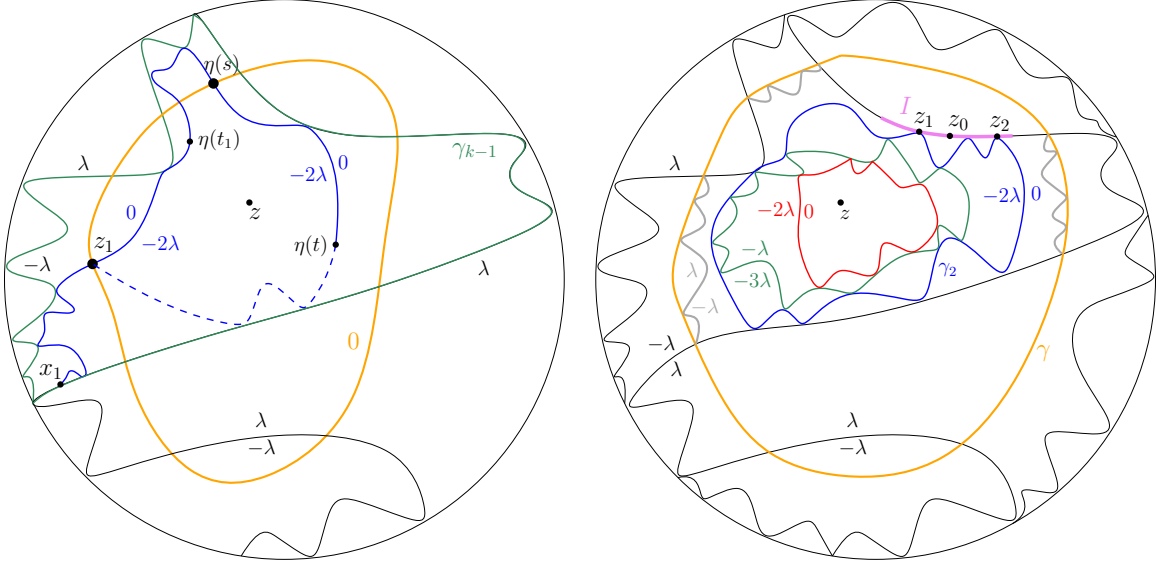


Figure 7.1: In both figures, the yellow loop represents ∂U . **Left:** Step 1 of the proof of Lemma 7.3. The blue curve is η which traces the loop γ_k . **Right:** Step 2 of the proof of Lemma 7.3. In this figure, $k_0 = 4$. The grey lines represent the 0-height level lines in the connected component of $U \setminus \mathbb{A}_{-\lambda, \lambda}(h)$ containing z .

to complete the loop γ_k . See Fig. 7.1 (left). Let $s \in (0, t)$ be the last time before t with $\eta(s) \in \partial U$. Let $O(z, t)$ be the connected component of $U \setminus \eta([0, t])$ containing z .

The curve η makes excursions into U . For any $s_1 < s_2$, we say that $\eta([s_1, s_2])$ is a *maximal excursion* of η into U if $\eta([s_1, s_2]) \subseteq U$ and $\eta(s_1), \eta(s_2) \in \partial U$. The boundary conditions of h in $O(z, t)$ are piecewise constant with possibly infinitely many pieces (i.e., if we map $O(z, t)$ conformally onto the unit disk, then we get piecewise constant boundary conditions): equal to $(a_0 - 1)\lambda$ and $(a_0 + 1)\lambda$ on the left and right sides of $\eta([s, t])$; equal to $(a_0 - 1)\lambda$ or $(a_0 + 1)\lambda$ on each maximal excursion of $\eta([0, s])$ into U (depending on whether this part of $\partial O(z, t)$ corresponds to the left or right side of η); and equal to 0 on the remaining part. By Proposition 6.3 and Remark 6.4, almost surely, the future part of η (after t) can only possibly hit $\partial O(z, t)$ at a point z_1 which is equal to $\eta(s)$, or an extremal point of a maximal excursion of $\eta([0, s])$ into U .

Since $z_1 \in \eta([0, s])$, η completes a loop upon hitting z_1 , and this loop should be equal to γ_k . If $z_1 = \eta(s)$, then γ_k does not cross ∂U and intersects ∂U at only one point z_1 . This contradicts the definition of γ_k . So $z_1 \neq \eta(s)$. This implies that $\eta([0, s])$ has made at least one maximal excursion into U . In particular, there exists $t_1 < s$ such that $\eta(t_1) \in U$. Then η must hit ∂U at some time in $(t_1, s]$. Let t_2 be the first time in $(t_1, s]$ that η hits ∂U . Again, Proposition 6.3, Remark 6.4 and the boundary conditions of $O(z, t_1)$ imply that $\eta(t_2)$ must belong to $\eta([0, t_1])$. This means that η completes tracing the loop γ_k at time t_2 . This contradicts the assumption that $\eta(t)$ is in the middle of tracing γ_k . Altogether, we have proved the statement of this step.

Step 2. Let $\hat{\gamma}$ be the smallest loop in \mathbb{L}_0 which encircles ∂U , i.e., $U \subseteq O(\hat{\gamma})$. To prove the lemma, it suffices to show that $\partial U = \hat{\gamma}$ almost surely. Since $h|_{O(\hat{\gamma})}$ is a zero-boundary GFF,

we can map $O(\hat{\gamma})$ onto D by a conformal map f and consider $(f(\partial U), f(h|_{O(\hat{\gamma})}))$ instead of $(\partial U, h)$. Therefore, without loss of generality, we can assume that $\hat{\gamma} = \partial D$. Under this assumption (conditionally on $\hat{\gamma} = \partial D$), ∂U is not encircled by any loop in $\mathbb{L}_0 \setminus \{\partial D\}$. Fix $z \in D$ such that $\{z \in U\}$ has positive probability. We aim to show that $\partial U = \partial D$ a.s. on the event $\{z \in U\}$. If this is true for any z , then we would have shown that $\partial U = \partial D$ almost surely, which completes the proof of the lemma.

From now on, we further condition on the event $\{z \in U\}$. By Step 1, ∂U should not cross any loop in \mathbb{L}_0 . By our assumption, ∂U is not encircled by any loop in $\mathbb{L}_0 \setminus \{\partial D\}$. Therefore, ∂U must strictly encircle all the loops in $\mathbb{L}_0 \setminus \{\partial D\}$ which encircle z .

For each $k \in \mathbb{N}$, let γ_k be the a.s. unique loop in L_k which encircles z . Let us show that $O(\gamma_2) \subsetneq U$ and γ_2 intersects ∂U at at most one point almost surely. Note that $h|_{O(\gamma_2)}$ has boundary value either -2λ , 0 or 2λ . If the boundary value of $h|_{O(\gamma_2)}$ is 0 , then $\gamma_2 \in \mathbb{L}_0$, hence $O(\gamma_2) \subsetneq U$ by our assumption. Then by Step 1, we also know that γ_2 intersects ∂U at at most one point. Suppose that the boundary value of $h|_{O(\gamma_2)}$ is -2λ (the case 2λ can be treated in the same way), then let k_0 be the smallest $k \geq 2$ such that $h|_{O(\gamma_k)}$ has boundary value 0 . For all $2 \leq j \leq k_0$, γ_j must not cross ∂U and $\gamma_j \neq \partial U$. Indeed, γ_j is a level line of h whose height is equal to the boundary value of $h|_{O(\gamma_{j-1})}$. For all $2 \leq j \leq k_0$, the boundary value of $h|_{O(\gamma_{j-1})}$ is non-zero, hence γ_j is not a 0-height level line. By Step 1, for all $2 \leq j \leq k_0$, γ_j cannot cross ∂U , and can intersect ∂U at at most one point. Moreover, since $\gamma_{k_0} \in \mathbb{L}_0$, we have $O(\gamma_{k_0}) \subsetneq U$ by our assumption. Since for all $j \in \mathbb{N}$, γ_j intersects γ_{j+1} at infinitely many points, it is not possible to have $O(\gamma_{j+1}) \subsetneq U \subsetneq O(\gamma_j)$ for any $2 \leq j \leq k_0 - 1$. Therefore, the only possibility is $O(\gamma_2) \subsetneq U$. Then the result of Step 1 further implies that γ_2 intersects ∂U at at most one point.

Now, let us show that γ_2 also belongs to $L_2(h|_U)$. First note that $\mathbb{A}_{-\lambda, \lambda}(h) \cap U$ is non-empty. Indeed, since $O(\gamma_2) \subseteq U$, if $\mathbb{A}_{-\lambda, \lambda}(h) \cap U$ is empty, then we must have $U \subseteq O(\gamma_1)$. However, since γ_1 intersects γ_2 at infinitely many points, ∂U would also intersect γ_2 at infinitely many points, which contradicts the previous section.

Then let us show that $\mathbb{A}_{-\lambda, \lambda}(h|_U)$ contains $\mathbb{A}_{-\lambda, \lambda}(h) \cap U$. By Lemma 6.2, $(D \setminus U) \cup \mathbb{A}_{-\lambda, \lambda}(h)$ is also a local set of h , and each connected component of $U \setminus \mathbb{A}_{-\lambda, \lambda}(h)$ has piecewise constant boundary conditions (with possibly infinitely many pieces), taking values in $\{-\lambda, 0, \lambda\}$. More precisely, it has boundary conditions $-\lambda$ or λ on $\mathbb{A}_{-\lambda, \lambda}(h)$ and 0 on ∂U . By Proposition 6.3 and Remark 6.4, in each connected component of $U \setminus \mathbb{A}_{-\lambda, \lambda}(h)$, we can run 0-height level lines of h between a dense countable set of points on the parts of the boundary with 0 boundary condition. If we take the closure of the union of these 0-height level lines with $\mathbb{A}_{-\lambda, \lambda}(h) \cap U$, then we obtain a thin local set of $h|_U$ with boundary values in $\{-\lambda, \lambda\}$, which is exactly $\mathbb{A}_{-\lambda, \lambda}(h|_U)$. See Fig. 7.1 (right).

Without loss of generality, assume that γ_1 has inner boundary value $-\lambda$. Let O denote the connected component of $U \setminus \mathbb{A}_{-\lambda, \lambda}(h)$ containing z . Since $O(\gamma_2) \subseteq U$ and $O(\gamma_2) \subseteq O(\gamma_1)$, we have $O(\gamma_2) \subseteq O$. Note that $\partial U \cap \gamma_2$ contains at most one point and $\gamma_1 \cap \gamma_2$ contains infinitely many points, hence there exists $z_1 \in \gamma_1 \cap \gamma_2$ which is not on ∂U . Then there should be a positive portion $I \subseteq \gamma_1$ containing z_1 which is disjoint from ∂U . Since ∂U must encircle z_1 , it also must encircle I . In particular, $I \subseteq \partial O$. Since $\gamma_1 \cap \gamma_2$ does not contain isolated points (see Lemma 6.13), there a.s. exists $z_2 \in \gamma_2 \cap I$ distinct from z_1 . We know that for a countable dense set of points on γ_1 , if we run the 0-height level line of $h^0|_{O(\gamma_1)}$ from a point in this set targeting z , then the first time that this level line encircles z , the loop that it

completes is equal to γ_2 (see Remark 6.11). Let $z_0 \in I$ be a point in this countable dense set and also on the portion of I between z_1 and z_2 . Let ξ be the 0-height level line of $h^0|_{O(\gamma_1)}$ (which is a $-\lambda$ -height level line of $h|_{O(\gamma_1)}$) from z_0 targeting z , stopped at the first time that ξ encircles z . Then ξ is a local set of $h|_{O(\gamma_1)}$ with boundary values 0 and -2λ at its two sides. By the choice of z_0 , ξ would first hit the portion of γ_2 between z_1 and z_2 , and then follow γ_2 . This ensures that $\xi \subseteq \bar{O}$. By Lemma 6.2, $(D \setminus O) \cup \xi$ is also a local set of h , which implies that ξ is also a $-\lambda$ -height level line of $h|_O$. Combined with the previous paragraph, ξ is part of the second layer of $\text{BCLE}_4(-1)$ coupled with $h|_U$, hence the loop γ_2 belongs to $L_2(h|_U)$.

We have now proved that γ_2 belongs to $L_2(h|_U)$. This implies that the ratio of the conformal radii of γ_2 and ∂U with respect to z should have the same law as the ratio of the conformal radii of γ_2 and ∂D with respect to z . This is possible only if $\partial U = \partial D$ a.s. This completes the proof of the lemma. \square

Remark 7.4. Following similar lines, one should also be able to characterize simply connected open sets in \bar{D} with boundary value $a \in \mathbb{R}$. Since this is not the main purpose of this work, we do not develop more on it.

7.3 Thin local sets with boundary values in $\{-\mu, 0, \mu\}$

The main goal of this subsection is to obtain Theorem 7.8 below, which characterises all thin local sets with boundary values in $\{-\mu, 0, \mu\}$ with $\mu \geq 2\lambda$. Throughout, we fix $\mu \geq 2\lambda$.

First, let us define a particular set of loops H_μ , such that $\text{gask}(H_\mu)$ is a thin local set of h with boundary values in $\{-\mu, 0, \mu\}$.

Definition 7.5 (Collection of loops H_μ). *Given a zero boundary GFF h , for every $\mu \geq 2\lambda$, let $H_\mu(h)$ be the union of the following two collections of loops:*

- *the union of $\mathcal{L}_{-\lambda, \mu-\lambda}(h^0|_{O(\gamma)})$ over all $\gamma \in \mathcal{L}_{-\lambda, \lambda}^+(h)$;*
- *the union of $\mathcal{L}_{-\mu+\lambda, \lambda}(h^0|_{O(\gamma)})$ over all $\gamma \in \mathcal{L}_{-\lambda, \lambda}^-(h)$.*

The collection H_μ will serve as the building block of any thin local set with boundary values in $\{-\mu, 0, \mu\}$ through the following operation.

Definition 7.6 (Iterations of H_μ). *Let $Z_0 := H_\mu(h)$ and $I_0 := \text{gask}(Z_0)$. For $n \in \mathbb{N}$, suppose that we have defined a collection of loops Z_n such that $I_n := \text{gask}(Z_n)$ is a thin local set with boundary values in $\{-\mu, 0, \mu\}$, let us define Z_{n+1} . For each loop $\gamma_n \in Z_n$ with 0 inner boundary value, we say that we split γ_n if we replace γ_n by the collection $H_\mu(h|_{O(\gamma_n)})$ of loops which are all encircled by γ_n . Let $U_n \subseteq Z_n$ be a set of loops with 0 inner boundary value. Let Z_{n+1} be the set of loops obtained from splitting the loops in U_n , namely*

$$Z_{n+1} := (Z_n \setminus U_n) \cup \bigcup_{\gamma_n \in U_n} H_\mu(h|_{O(\gamma_n)}).$$

The set $I_{n+1} := \text{gask}(Z_{n+1})$ is given by

$$I_{n+1} = I_n \cup \bigcup_{\gamma_n \in U_n} \text{gask}(H_\mu(h|_{O(\gamma_n)})).$$

Then I_{n+1} is again a thin local set of h with boundary values in $\{-\mu, 0, \mu\}$. For each n , we say that Z_n and I_n are obtained from n iterations of H_μ . Note that Z_n and I_n are determined by the choice of loops U_0, \dots, U_{n-1} .

One can also make infinite iterations of H_μ by carrying out the above splitting operation for an infinite sequence of collections of loops $(U_n)_{n \geq 0}$. This gives rise to the following set

$$I_\infty := \text{gask}(H_\mu(h)) \cup \bigcup_{n=0}^{\infty} \bigcup_{\gamma_n \in U_n} \text{gask}(H_\mu(h|_{O(\gamma_n)})).$$

A set I is said to be obtained from iterations of H_μ , if it can be obtained by iterating this operation a finite or countably infinite number of times.

In the following, for simplicity, we will call a loop an a -loop meaning that it is a loop with inner boundary value a .

Lemma 7.7. *If I is obtained from iterations of H_μ , then I is a thin local set with boundary values in $\{-\mu, 0, \mu\}$.*

Proof. The lemma is obvious when we perform only a finite number of iterations of H_μ . By Lemma 6.17, after a finite number of iterations of H_μ , the thin local set we obtain is always contained in $\mathbb{A}_{-\mu, \mu}(h)$. Taking limits, any (finite or infinite) number of iterations of H_μ gives rise to a subset of $\mathbb{A}_{-\mu, \mu}(h)$. In fact, $\mathbb{A}_{-\mu, \mu}(h)$ can be obtained from iterating H_μ infinitely until there are no more 0-loops. This is the ‘‘maximum’’ number of iterations we can do. Fix $z \in D$. Let $\gamma_{0,z}$ be the a.s. unique loop in $H_\mu(h)$ encircling z . For $k \geq 0$, if we have obtained $\gamma_{k,z}$ such that $h|_{O(\gamma_{0,z})}$ is a zero boundary GFF, then we will let $\gamma_{k+1,z}$ be the a.s. unique loop in $H_\mu(h|_{O(\gamma_{k,z})})$ encircling z . There a.s. exists a finite $k(z)$ such that $\gamma_{k(z),z}$ has inner boundary value $-\mu$ or μ , and $\gamma_{k(z),z}$ is equal to the loop in $\mathcal{L}_{-\mu, \mu}(h)$ encircling z . Suppose that I is obtained from iterations of H_μ , and let $\gamma(z, I)$ be the a.s. unique loop in $\mathcal{L}(I)$ which encircles z . Then there exists $0 \leq k \leq k(z)$ such that $\gamma(z, I) = \gamma_{k,z}$. Therefore $h|_{O(\gamma(z, I))}$ is a GFF with boundary conditions in $\{-\mu, 0, \mu\}$ which is conditionally independent of the value of h outside of $\gamma(z, I)$. Since this is true for Lebesgue a.e. $z \in D$, I is indeed a local set of h with boundary values in $\{-\mu, 0, \mu\}$. On the other hand, since I is a subset of $\mathbb{A}_{-\mu, \mu}(h)$, it must be thin as well. This completes the proof. \square

The following theorem states that the reverse of Lemma 7.7 is also true.

Theorem 7.8. *If I is a thin local set of h with boundary values in $\{-\mu, 0, \mu\}$, then either $I = \partial D$ or I is obtained from iterations of H_μ .*

In order to prove Theorem 7.8, we first collect Lemmata 7.9, 7.10 and 7.13.

Suppose that I is a thin local set with boundary values in $\{-\mu, 0, \mu\}$, then by Lemma 6.15, we know that $I \cup \partial D$ is a.s. connected. This implies that all the connected components of $D \setminus I$ are simply connected. We can therefore define $\mathcal{L}(I)$ to be the collection of outer boundaries of the connected components of $D \setminus I$. This is a collection of contours which will turn out later to be simple loops.

Lemma 7.9. *The contours in $\mathcal{L}(I)$ which are the boundaries of a simply connected set with boundary value μ (resp. $-\mu$) belong to $\mathcal{L}_{-\mu, \mu}^+$ (resp. $\mathcal{L}_{-\mu, \mu}^-$), and are therefore simple loops.*

Proof. Let K be the closure of the union of $\mathbb{A}_{-\mu,\mu}(h|_O)$ over all connected components O of $D \setminus I$ such that $h|_O$ has boundary value 0, together with I . Then K is a thin local set of h with boundary values in $\{-\mu, \mu\}$. By uniqueness of two-valued thin local sets (Lemma 6.16), we know that $K = \mathbb{A}_{-\mu,\mu}(h)$. Therefore, the contours in $\mathcal{L}(I)$ with inner boundary value μ or $-\mu$ belong to the set of loops in $\mathcal{L}(K) = \mathcal{L}_{-\mu,\mu}(h)$ with the same inner boundary value. This implies the claim. \square

We call a loop in $\mathbb{L}_0 \setminus \{\partial D\}$ *outermost* if the only loop in \mathbb{L}_0 which strictly encircles it is ∂D .

Lemma 7.10. *Every outermost loop in $\mathbb{L}_0 \setminus \{\partial D\}$ is encircled by a loop in H_μ .*

We remark that by Lemma 7.3, every 0-loop of H_μ belongs to \mathbb{L}_0 . Therefore, Lemma 7.10 implies that every 0-loop of H_μ is an outermost loop in $\mathbb{L}_0 \setminus \{\partial D\}$.

Proof. The outermost loops in $\mathbb{L}_0 \setminus \{\partial D\}$ are obtained from iteratively sampling $\mathcal{L}_{-\lambda,\lambda}$ until the first time that one gets a loop with inner boundary 0. More precisely, we first sample $\mathcal{L}_{-\lambda,\lambda}(h)$ (which is also equal to L_1). For each loop $\gamma \in L_1$, we again sample $\mathcal{L}_{-\lambda,\lambda}(h^0|_{O(\gamma)})$. For each loop $\xi \in \mathcal{L}_{-\lambda,\lambda}(h^0|_{O(\gamma)})$, if ξ has inner boundary value 0, then it is an outermost loop in $\mathbb{L}_0 \setminus \{\partial D\}$, otherwise we continue to sample $\mathcal{L}_{-\lambda,\lambda}(h^0|_{O(\xi)})$. For a fixed point $z \in D$, this iteration gives rise to a sequence of loops encircling z whose inner boundary values follow a simple random walk with steps in $-\lambda, \lambda$. We stop the process when the random walk value associated with the loop is 0.

The previous paragraph implies the following fact for every $n \in \mathbb{N}$. For each loop $\gamma \in L_1$ with inner boundary value λ , every outermost loop in $\mathbb{L}_0 \setminus \{\partial D\}$ which is encircled by γ is encircled by a loop in $\mathcal{L}_{-\lambda,n\lambda}(h^0|_{O(\gamma)})$. More precisely, every loop in $\mathcal{L}_{-\lambda,n\lambda}^-(h^0|_{O(\gamma)})$ is an outermost loop in $\mathbb{L}_0 \setminus \{\partial D\}$, and every loop in $\mathcal{L}_{-\lambda,n\lambda}^+(h^0|_{O(\gamma)})$ strictly encircles a collection of outermost loops in $\mathbb{L}_0 \setminus \{\partial D\}$. Indeed, one way to construct $\mathcal{L}_{-\lambda,n\lambda}(h^0|_{O(\gamma)})$ is to iteratively sample $\mathcal{L}_{-\lambda,\lambda}$. More precisely, we first sample $\mathcal{L}_{-\lambda,\lambda}(h^0|_{O(\gamma)})$. When we get a loop with inner boundary value 0 or $(n+1)\lambda$, it belongs to $\mathcal{L}_{-\lambda,n\lambda}(h^0|_{O(\gamma)})$ so we keep it. For any other loop ξ , we again sample $\mathcal{L}_{-\lambda,\lambda}(h^0|_{O(\xi)})$. For a fixed point $z \in O(\gamma)$, this iteration gives rise to a sequence of loops encircling z whose inner boundary values follow a simple random walk with steps in $-\lambda, \lambda$. We stop this random walk when it reaches 0 or $(n+1)\lambda$. Combined with the previous paragraph, it is clear that the loops of $\mathcal{L}_{-\lambda,n\lambda}(h^0|_{O(\gamma)})$ with inner boundary value 0 belong to the set of outermost loops in $\mathbb{L}_0 \setminus \{\partial D\}$, and the loops of $\mathcal{L}_{-\lambda,n\lambda}(h^0|_{O(\gamma)})$ with inner boundary value $(n+1)\lambda$ can be further split into outermost loops in $\mathbb{L}_0 \setminus \{\partial D\}$.

Now fix $n \in \mathbb{N}$ such that $n\lambda \geq \mu$. Note that for each λ -loop $\gamma \in L_1$, each loop in $\mathcal{L}_{-\lambda,n\lambda}(h^0|_{O(\gamma)})$ is encircled by a loop in $\mathcal{L}_{-\lambda,\mu-\lambda}(h^0|_{O(\gamma)})$. Indeed, starting with the collection of loops $\mathcal{L}_{-\lambda,\mu-\lambda}(h^0|_{O(\gamma)})$, if we further split each loop $\gamma_1 \in \mathcal{L}_{-\lambda,\mu-\lambda}^+(h^0|_{O(\gamma)})$ into the set of loops $\mathcal{L}_{-\mu,(n+1)\lambda-\mu}(h^0|_{O(\gamma_1)})$, then we obtain $\mathcal{L}_{-\lambda,n\lambda}(h^0|_{O(\gamma)})$. Combined with the previous paragraph, this implies that for each λ -loop $\gamma \in L_1$, every outermost loop in $\mathbb{L}_0 \setminus \{\partial D\}$ which is encircled by γ is encircled by a loop in $\mathcal{L}_{-\lambda,\mu-\lambda}(h^0|_{O(\gamma)})$. By symmetry, we can deduce that for every $-\lambda$ -loop in $\gamma \in L_1$, every outermost loop in $\mathbb{L}_0 \setminus \{\partial D\}$ which is encircled by γ is encircled by a loop in $\mathcal{L}_{\lambda-\mu,\lambda}(h^0|_{O(\gamma)})$. Altogether, we have proved the lemma. \square

We are now ready to prove Theorem 7.8.

Proof of Theorem 7.8. First of all, Lemma 7.9 implies that each contour in $\mathcal{L}(I)$ which is the outer boundary of a connected component with boundary conditions $\pm\mu$ is a simple loop. Then Lemma 7.3 implies that each contour in $\mathcal{L}(I)$ which is the outer boundary of a connected component with boundary condition 0 is also a simple loop. Therefore, every contour in $\mathcal{L}(I)$ is in fact a simple loop. Below, we will complete the proof in two steps. Assume that $I \neq \partial D$.

Step 1. Let us show that each loop in $\mathcal{L}(I)$ is either equal to a loop in H_μ , or is encircled by a 0-loop in H_μ . Since I and $\text{gask}(H_\mu)$ have Lebesgue measure 0 (because they are thin), upon showing this, we can deduce that each loop in H_μ with inner boundary value $-\mu$ or μ must belong to $\mathcal{L}(I)$.

Since we can obtain $\mathcal{L}_{-\mu,\mu}(h)$ by taking the union of the set of $\pm\mu$ -loops of H_μ together with the union of the sets $\mathcal{L}_{-\mu,\mu}(h|_{O(\xi)})$ for every 0-loops ξ of H_μ , we can deduce that each loop of $\mathcal{L}_{-\mu,\mu}(h)$ is either equal to a $\pm\mu$ -loop of H_μ , or encircled by a 0-loop of H_μ . On the other hand, Lemma 7.9 implies that the $\pm\mu$ -loops of $\mathcal{L}(I)$ are contained in $\mathcal{L}_{-\mu,\mu}(h)$. Therefore, each $\pm\mu$ -loop of $\mathcal{L}(I)$ is also either equal to a $\pm\mu$ -loop of H_μ , or is encircled by a 0-loop of H_μ .

Now, consider a 0-loop $\gamma \in \mathcal{L}(I)$. By Lemma 7.3, we know that γ belongs to \mathbb{L}_0 . Then by Lemma 7.10, γ is a.s. encircled by a loop in H_μ . It remains to prove that γ cannot be encircled by a $\pm\mu$ -loop of H_μ . Note that the union of the set of $\pm\mu$ -loops of $\mathcal{L}(I)$ together with the union of the sets $\mathcal{L}_{-\mu,\mu}(h|_{O(\xi)})$ for every 0-loops ξ of $\mathcal{L}(I)$ form $\mathcal{L}_{-\mu,\mu}(h)$. This implies that γ is not encircled by any loop in $\mathcal{L}_{-\mu,\mu}(h)$. Since the $\pm\mu$ -loops of H_μ all belong to $\mathcal{L}_{-\mu,\mu}(h)$, γ is not encircled by any $\pm\mu$ -loop of H_μ . Consequently, γ is encircled by a 0-loop of H_μ .

Altogether, we have proved the first sentence of this step.

Step 2. The previous step implies that for each 0-loop γ of H_μ , there exists $U \subseteq \mathcal{L}(I)$ such that

$$\bigcup_{\xi \in U} O(\xi) = \overline{O(\gamma)}. \quad (7.1)$$

If every 0-loop in H_μ belongs to $\mathcal{L}(I)$, then since every $\pm\mu$ -loop in H_μ also belongs to $\mathcal{L}(I)$, we have $H_\mu = \mathcal{L}(I)$ and we are done. Otherwise let γ be a 0-loop in H_μ which does not belong to $\mathcal{L}(I)$, and let U be given by (7.1). Conditionally on H_μ , $h|_{O(\gamma)}$ is a zero-boundary GFF in $O(\gamma)$. The set $O(\gamma) \setminus \bigcup_{\xi \in U} O(\xi)$ is a thin local set of $h|_{O(\gamma)}$ with boundary values in $\{-\mu, 0, \mu\}$ which is not equal to γ . This implies that we can apply the same reasoning as in Step 1 to $h|_{O(\gamma)}$ and U , just as we did for h and $\mathcal{L}(I)$. It follows that the $\pm\mu$ -loops of $H(h|_{O(\gamma)})$ must belong to U (hence to $\mathcal{L}(I)$), and the 0-loops of $H(h|_{O(\gamma)})$ either belong to U (hence to $\mathcal{L}(I)$), or are split into loops that belong to $\mathcal{L}(I)$. We can then iterate this procedure as many times as we want, until all the 0-loops of the iterated set belong to $\mathcal{L}(I)$. The number of iterations is at most countable, because $\mathcal{L}_{-\mu,\mu}$ can be obtained from iterating H_μ countably many times (since for each $z \in D$, the loop in $\mathcal{L}_{-\mu,\mu}$ which encircles z is obtained after a finite number of iterations of H_μ). This proves the theorem. \square

7.4 Proof of Theorem 2.2

We will now complete the proof of Theorem 2.2. Recall the notations of Section 7.1. First, we deduce from Proposition 2.3 the following properties for \tilde{A} in place of A . Recall that \tilde{A}^0

is the set of loops in \tilde{A} with 0 inner boundary value.

Lemma 7.11. *The quadruple $(B, \tilde{A}, \epsilon, h)$ satisfies the following properties a.s.*

1. h is a GFF with zero boundary conditions on ∂D .
2. The loops in \tilde{A} and B are simple, and do not cross each other. Every loop in \tilde{A} is encircled by some loop in B . The set \tilde{A} is not equal to $\{\partial D\}$.
3. The set $\text{gask}(\tilde{A})$ is a thin local set of h , with boundary values in $\{-2\sqrt{2}\lambda, 0, 2\sqrt{2}\lambda\}$. For each loop $\ell \in B$, every loop $\gamma \in \tilde{A}$ encircled by ℓ has inner boundary condition 0 or $\epsilon(\ell)2\sqrt{2}\lambda$.
4. The loops in \tilde{A}^0 do not touch the loops in B .
5. The loops in B are more exterior than CLE_4 loops.

Proof. Properties 1, 2, 3 and 5 directly follow from Proposition 2.3 and the definition of \tilde{A} . To get Property 4, note that the loops of A with inner boundary value 0 form a subset of \tilde{A}^0 and these loops do not touch the loops in B by Proposition 2.3. Any other loop of \tilde{A}^0 is encircled by a loop γ in A with inner boundary condition not in $\{-2\sqrt{2}\lambda, 0, 2\sqrt{2}\lambda\}$. By Property 3 of Proposition 2.3, such a loop γ cannot be reached from ℓ (where ℓ is the loop in B that encircles γ) via a finite sequence of loops in A , so in particular γ does not intersect ℓ . It follows that every loop of \tilde{A}^0 encircled by γ also cannot intersect ℓ . This implies Property 4 of the lemma. \square

Let us now prove the following lemma for \tilde{A}^0 .

Lemma 7.12. *Each loop in \tilde{A}^0 is encircled by a loop in $\text{CLE}_4(h)$.*

In order to prove Lemma 7.12, we need the following geometric property of $\mathcal{L}_{-a,b}$.

Lemma 7.13. *Let $D \neq \mathbb{C}$ be a simply connected domain. Let h be a zero boundary GFF in D . Fix $a, b > 0$ with $a + b \geq 2\lambda$. Almost surely, for each $z \in \partial D$ and $\epsilon > 0$, $B(z, \epsilon)$ intersects at least one loop $\gamma_1 \in \mathcal{L}_{-a,b}^+(h)$ and one loop $\gamma_2 \in \mathcal{L}_{-a,b}^-(h)$.*

Proof. Suppose that with positive probability, the following event E occurs: there exists $z \in \partial D$ and $\epsilon > 0$ such that $B(z, \epsilon)$ intersects only loops in $\mathcal{L}_{-a,b}^+(h)$. Note that $B(z, \epsilon)$ contains a positive portion ℓ_1 of ∂D . For $\delta > 0$, let $B(\ell_1, \delta)$ be the δ neighborhood of ℓ_1 in D . Then on the event E , we have $\mathbb{E} \left[\int_{B(\ell_1, \delta)} h(x) dx \right] = b$ for all δ sufficiently small. This is impossible because h has zero boundary condition in D . Therefore the event E should a.s. not occur. Similarly, we cannot have $B(z, \epsilon)$ which only intersects loops in $\mathcal{L}_{-a,b}^-(h)$. \square

Proof of Lemma 7.12. Consider the loops in $L_1(h)$ and $L_2(h)$ (see Definition 6.10). The loops in $L_1(h)$ have inner boundary values in $\{-\lambda, \lambda\}$ and the loops in $L_2(h)$ have inner boundary values in $\{-2\lambda, 0, 2\lambda\}$. Our first goal is to prove that

$$\tilde{A}^0 \cap L_2 = \emptyset \quad \text{a.s.} \quad (7.2)$$

Before proving (7.2), let us first explain how to deduce the lemma, assuming (7.2). Due to Lemma 7.3, we know that every loop $\gamma \in \tilde{A}^0$ belongs to \mathbb{L}_0 . Since $\gamma \in \tilde{A}_0$ is not equal to

∂D and does not belong to $L_1(h)$, it must belong to $\cup_{k \geq 2} L_k$, hence γ is encircled by a loop in $L_2(h)$. Note that the loops of $L_2(h)$ with inner boundary values in $\{-2\lambda, 2\lambda\}$ belong to $\text{CLE}_4(h)$, hence if γ is encircled by such a loop, then we are done. Otherwise, suppose that there exists a loop $\xi \in L_2(h)$ with inner boundary condition equal to 0 such that $O(\gamma) \subsetneq O(\xi)$ (the possibility of $\gamma = \xi$ is ruled out by (7.2)). By Property 3 and Theorem 7.8, we know that the loops in \tilde{A} are obtained from iterations of $H_{2\sqrt{2}\lambda}$, hence they do not cross ξ . Let U be the set of loops in \tilde{A} that are encircled by ξ , then $h|_{O(\xi)}$ and U satisfy the same conditions as h and \tilde{A} as in Lemma 7.11. Therefore, the same argument would imply that any 0-loop in U , in particular γ ,

- is either encircled by a loop in $\text{CLE}_4(h|_{O(\xi)})$, in which case we are done, since $\text{CLE}_4(h|_{O(\xi)})$ is a subset of $\text{CLE}_4(h)$.
- or is strictly encircled by a loop $\xi' \in L_2(h|_{O(\xi)})$ with inner boundary condition 0, in which case we can continue the iteration.

Since γ has non-zero diameter, the above iteration will end up in the first case after finitely many iterations. This will complete the proof of the lemma, given (7.2).

Now, let us prove (7.2). We assume by contradiction that with positive probability, there exists a loop $\gamma \in \tilde{A}^0 \cap L_2(h)$. On this event, let ξ be the loop in $L_1(h)$ that encircles γ and assume without loss of generality that the inner boundary condition of ξ is λ . Note that γ a.s. intersects ξ , hence also intersects some neighboring loop $\hat{\xi}$ of ξ in $\mathcal{L}_{-\lambda, \lambda}(h)$ (i.e., $\hat{\xi}$ and ξ share a positive portion of boundary). Let $z \in \gamma \cap \xi \cap \hat{\xi}$, and let ℓ be the loop in B which encircles γ . By Property 4 of Lemma 7.11, there a.s. exists $\varepsilon > 0$ so that ℓ encircles a small ball $B(z, \varepsilon)$. By Lemma 7.13, $B(z, \varepsilon) \cap O(\xi)$ a.s. intersects at least one loop $\zeta_1 \in \mathcal{L}_{-\lambda, (2\sqrt{2}-1)\lambda}^+(h^0|_{O(\xi)})$. Any such loop ζ_1 in fact belongs to the set of loops in $H_{2\sqrt{2}\lambda}$ that have inner boundary condition $2\sqrt{2}\lambda$. Since A is not equal to the set $\{\partial D\}$ (Property 2 of Lemma 7.11), by Theorem 7.8, we need to do at least one iteration to get \tilde{A} . It follows that ζ_1 belongs to \tilde{A} . More precisely, $\zeta_1 \in \tilde{A}^+$. In the same way, $B(z, \varepsilon) \cap O(\hat{\xi})$ a.s. intersects a loop $\zeta_2 \in \tilde{A}^-$. Since $O(\ell)$ contains $B(z, \varepsilon)$ and ℓ does not cross ζ_1 or ζ_2 (Property 2 of Lemma 7.11), it follows that ℓ encircles both ζ_1 and ζ_2 . This leads to a contradiction, because ℓ cannot encircle loops both from \tilde{A}^- and \tilde{A}^+ , by Property 3 of Lemma 7.11. This completes the proof of (7.2) and also the lemma. \square

Lemma 7.14. *If a loop γ in $\text{CLE}_4(h)$ has inner boundary value 2λ (resp. -2λ), then it has to encircle at least one loop in \tilde{A}^+ (resp. \tilde{A}^-).*

Proof. By applying Lemma 7.9 to $\mu = 2\sqrt{2}\lambda$, we know that every loop in $\tilde{A}^+ \cup \tilde{A}^-$ belongs to $\mathcal{L}_{-2\sqrt{2}, 2\sqrt{2}}(h)$, hence is encircled by a $\text{CLE}_4(h)$ loop. Indeed, $\mathbb{A}_{-2\lambda, 2\lambda}(h) \subseteq \mathbb{A}_{-2\sqrt{2}, 2\sqrt{2}\lambda}(h)$ (by Lemma 6.16) and $\mathcal{L}_{-2\lambda, 2\lambda}(h)$ is equal to $\text{CLE}_4(h)$. Combined with Lemma 7.12, we know that every loop in \tilde{A} is encircled by a $\text{CLE}_4(h)$ loop.

Let γ be a loop in $\text{CLE}_4(h)$ with inner boundary value 2λ . Let U be the set of loops in \tilde{A} which are encircled by γ . By Property 3 of Lemma 7.11, we know that $\text{gask}(\tilde{A})$ is thin, hence $O(\gamma) \setminus \cup_{\eta \in U} O(\eta)$ is again a thin local set of $h|_{O(\gamma)}$. If U does not contain any loop in \tilde{A}^+ , then $O(\gamma) \setminus \cup_{\eta \in U} O(\eta)$ would take boundary values in $\{-2\sqrt{2}\lambda, 0\}$, which is impossible because $h|_{O(\gamma)}$ has boundary value 2λ and $\mathbb{E}[\int_{O(\gamma)} h(x) dx] > 0$. Similarly, we can prove that if a loop γ in $\text{CLE}_4(h)$ has inner boundary value -2λ , then it has to encircle a loop in \tilde{A}^- . \square

Lemma 7.15. *Every loop ℓ in B is a.s. encircled by a loop in $CLE_4(h)$.*

Proof. Let us show that, if $\ell \in B$, then $O(\ell)$ a.s. cannot intersect more than one loop in $CLE_4(h)$. For the sake of contradiction, suppose that with positive probability, $O(\ell)$ intersects two different loops γ_1 and γ_2 in $CLE_4(h)$. On this event, there exists $z \in \gamma_1 \cap O(\ell)$ and $\varepsilon > 0$ such that $B(z, \varepsilon) \subseteq O(\ell)$. There exists $\delta \in (0, \varepsilon)$ such that the union of the loops in $CLE_4(h)$ (apart from γ_1) that intersect $B(z, \delta)$ is contained in $B(z, \varepsilon)$ (because this union converges to the point z as $\delta \rightarrow 0$). Consequently every loop in $CLE_4(h)$ which intersects $B(z, \delta)$ (apart from γ_1) is encircled by ℓ . There are infinitely many loops in $CLE_4(h)$ which intersect $B(z, \delta)$, because none of the loops completely encircle $B(z, \delta)$ and none of the loops intersect each other. Since the loops in $CLE_4(h)$ have inner boundary values $\pm 2\lambda$ for which the signs are distributed as i.i.d. coin tosses given the loops, there a.s. exist loops $\gamma_3 \in CLE_4^+(h)$ and $\gamma_4 \in CLE_4^-(h)$ among the infinitely many loops in $CLE_4(h)$ which intersect $B(z, \delta)$. Moreover, $O(\gamma_3) \subseteq O(\ell)$ and $O(\gamma_4) \subseteq O(\ell)$. By Lemma 7.14, γ_3 a.s. encircles a loop in \tilde{A}^+ and γ_4 a.s. encircles a loop in \tilde{A}^- . This implies that ℓ encircles simultaneously a loop in \tilde{A}^+ and a loop in \tilde{A}^- , which contradicts Property 3 of Lemma 7.11. We have thus proved that $O(\ell)$ a.s. intersects at most one loop in $CLE_4(h)$. In other words, ℓ is a.s. encircled by a loop in $CLE_4(h)$. This completes the proof. \square

Proof of Proposition 7.1 and Theorem 2.2. We know that B is a.s. larger than CLE_4 by Property 5 of Lemma 7.11, so by Lemma 7.15, B must be equal to $CLE_4(h)$. Moreover, for each $\ell \in B$, the inner boundary value of ℓ must be equal to $2\lambda\epsilon(\ell)$. Indeed, if the inner boundary value of ℓ is $-2\lambda\epsilon(\ell)$, then by Lemma 7.14, ℓ must encircle a loop in $\tilde{A}^{-\epsilon(\ell)}$, which contradicts Property 3 of Lemma 7.11.

It follows that the law of \tilde{A} is given by Proposition 7.1. Indeed, Property 3 of Lemma 7.11 ensures that the gasket of $\tilde{A}(\ell)$ in $O(\ell)$ is a thin local set of $h|_{O(\ell)}$, and the loops in $\tilde{A}(\ell)$ have inner boundary conditions 0 or $2\sqrt{2}\lambda\epsilon(\ell)$. This uniquely determines $\tilde{A}(\ell)$ as a two-valued set by Lemma 6.16.

It remains to prove that $\tilde{A} = A$. By Lemma 6.18, we know that for each $\ell \in B$, every loop in $\tilde{A}(\ell)$ can be reached from ℓ via a finite sequence of loops in \tilde{A} . We also know that every loop in A encircles (and does not cross) the loops in \tilde{A} . Therefore every loop in $A(\ell)$ can also be reached from ℓ via a finite sequence of loops in $A(\ell)$. By Property 3 of Proposition 2.3, we deduce that every loop in A has inner boundary value in $\{-2\sqrt{2}, 0, 2\sqrt{2}\}$, hence $\tilde{A} = A$.

Property 3 further implies that a loop in A has inner boundary value 0 if and only if it is the limit of the boundary of an even hole. This completes the proof. \square

7.5 Proofs of Theorems 1.6, 2.4 and 1.7

Proof of Theorem 1.6. Theorem 2.2 identifies the limit of the (inner and outer) boundaries of the outermost clusters in a double random current model with free boundary conditions. By Proposition 5.2, for each loop γ in A , the next layer of outermost clusters in $O(\gamma)$ satisfies the same properties (i.e., Proposition 2.3) as the outermost clusters in D . The same proof as that of Theorem 2.2 then identifies the law of the next layer of outermost clusters in $O(\gamma)$. Iterating, we can deduce Theorem 1.6. \square

Proof of Theorem 2.4. By Proposition 2.5, $\text{gask}(\hat{A})$ is a thin local set of h such that for each $\gamma \in \hat{A}$, h restricted to $O(\gamma)$ is an independent GFF with boundary condition $c(\gamma) \in$

$[-\sqrt{2}\lambda, \sqrt{2}\lambda]$. The gasket of the following set of loops

$$\{\gamma \in \widehat{A} : c(\gamma) = -\sqrt{2}\lambda \text{ or } \sqrt{2}\lambda\} \cup \bigcup_{\gamma \in A : c(\gamma) \in (-\sqrt{2}\lambda, \sqrt{2}\lambda)} \mathcal{L}_{-\sqrt{2}\lambda - c(\gamma), \sqrt{2}\lambda - c(\gamma)}(h^0|_{O(\gamma)}) \quad (7.3)$$

forms a thin local set of h with boundary values in $\{-\sqrt{2}\lambda, \sqrt{2}\lambda\}$. By Lemma 6.16, the set (7.3) is equal to $\mathcal{L}_{-\sqrt{2}\lambda, \sqrt{2}\lambda}(h)$. By Lemma 6.18, we know that every loop γ in $\mathcal{L}_{-\sqrt{2}\lambda, \sqrt{2}\lambda}(h)$ can be reached from ∂D by a finite sequence of loops in $\mathcal{L}_{-\sqrt{2}\lambda, \sqrt{2}\lambda}(h)$. We further know by (7.3) that every loop in \widehat{A} encircles (and does not cross) the loops in $\mathcal{L}_{-\sqrt{2}\lambda, \sqrt{2}\lambda}(h)$. This implies that every loop in \widehat{A} can also be reached from ∂D by a finite sequence of loops in \widehat{A} . This implies that $\widehat{A} = \mathcal{L}_{-\sqrt{2}\lambda, \sqrt{2}\lambda}(h)$. Moreover, the parity of the hole encircled by each loop in \widehat{A} is indicated by its inner boundary value by Property 2. \square

Proof of Theorem 1.7. The first bullet point of Theorem 1.7 is given by Theorem 2.4. Given \widehat{A} , for each loop $\gamma \in \widehat{A}$, we again have the scaling limit of an independent double random current model in $O(\gamma)$ with free boundary conditions (see Proposition 5.3). This Markov property implies the second and third bullet points of Theorem 1.7. \square

8 Scaling limit of the XOR-Ising interfaces

In this section, we will identify the scaling limit of XOR-Ising interfaces with free boundary conditions (Theorem 1.2) and with plus/plus boundary conditions (Theorem 1.5). More concretely, we will focus on proving Theorem 2.8 which implies Theorem 1.2 directly and is the main input for Theorems 2.10 and 1.5.

In Sections 8.1 and 8.2, we deal with the free boundary condition case. We continue to use the setting and notations fixed above Proposition 2.9. There, we defined C^δ , s^δ , S^δ , \widetilde{S}^δ , ϵ^δ , B^δ , A^δ , h^δ for the double random current and XOR-Ising models and their height function, coupled as in Theorem 2.7. In Section 8.1, we will focus on proving the following proposition.

Proposition 8.1. *Almost surely, C is equal to $\mathcal{L}_{-\lambda, \lambda}(h)$. For each $\gamma \in C$, $h|_{O(\gamma)}$ is equal to a GFF with boundary condition $s(\gamma)\lambda$. Moreover, we have*

$$S(\gamma) = \mathcal{L}_{-\lambda, \lambda}^{s(\gamma)}(h^0|_{O(\gamma)}) \quad \text{and} \quad \widetilde{S}(\gamma) = \mathcal{L}_{-\lambda, \lambda}^{-s(\gamma)}(h^0|_{O(\gamma)}).$$

Proposition 8.1 uniquely determines the law of $(C, s, S, \widetilde{S}, h)$. Recall that Theorem 2.2 identifies the law of (ϵ, B, A, h) . Altogether, we have identified the law of $(C, s, S, \widetilde{S}, \epsilon, B, A, h)$.

The main point of Proposition 8.1 is the identification of the set C , which is the scaling limit of the XOR-Ising interfaces between the clusters in Items 1 and 2 in Theorem 2.8. The discrete interfaces C^δ do not satisfy spatial Markov property. The identification of C relies on the sets S and \widetilde{S} which satisfy Property 3 of Proposition 2.9. Recall that for each $\gamma \in C$, $S(\gamma)$ is the collection of loops in B that touch γ , and $\widetilde{S}(\gamma)$ is the collection of outer boundaries of the connected components of $O(\gamma) \setminus \bigcup_{\ell \in S(\gamma)} O(\ell)$. For each $\gamma \in C$, $s(\gamma) \in \{-1, 1\}$ is the spin of the cluster with outer boundary γ . See Fig. 2.4 for an illustration.

In Section 8.2, we complete the proof of Theorem 2.8 (which implies Theorem 1.2). In Section 8.3, we complete the proof of Theorem 2.10 (which implies Theorem 1.5).

8.1 Proof of Proposition 8.1

Introduce $\Omega := \text{gask}(S \cup \tilde{S})$. Property 3 of Proposition 2.9 implies that Ω is a thin local set of h with boundary values in $\{-2\lambda, 0, 2\lambda\}$, such that every loop in \tilde{S} has inner boundary value 0 and every loop in S has inner boundary value -2λ or 2λ (due to $S \subseteq B$ and Theorem 2.2). Theorem 7.8 implies that Ω must be obtained from iterations of $H_{2\lambda}$.

We will first deduce a few geometric properties of $H_{2\lambda}$ and $\mathcal{L}_{-\lambda, \lambda}$ in Lemmata 8.3 and 8.4, and then combine with Proposition 2.9 to identify the law of (C, Ω, h) and complete the proof. Let us first define the adjacency relation between the loops in $H_{2\lambda}$.

Definition 8.2. *We say that two loops in $H_{2\lambda}$ are adjacent if their intersection contains a positive portion of boundary (see Definition 6.9). Two loops $\gamma_1, \gamma_2 \in H_{2\lambda}$ are said to be in the same adjacency class if there is a finite sequence of loops η_1, \dots, η_n so that γ_1 is adjacent to η_1 , η_n is adjacent to γ_2 and η_i is adjacent to η_{i+1} for every $1 \leq i \leq n-1$.*

Lemma 8.3. *Two loops in $H_{2\lambda}$ are in the same adjacency class if and only if they are encircled by the same loop in $\mathcal{L}_{-\lambda, \lambda}(h)$.*

Proof. Note that $H_{2\lambda}$ is obtained via a nested version of $\mathcal{L}_{-\lambda, \lambda}$. For each loop $\gamma \in \mathcal{L}_{-\lambda, \lambda}(h)$, the set of loops in $H_{2\lambda}$ that are encircled by γ is exactly equal to $\mathcal{L}_{-\lambda, \lambda}(h^0|_{O(\gamma)})$. By Lemma 6.18, all the loops in $\mathcal{L}_{-\lambda, \lambda}$ are in the same adjacency class. This implies that for each loop $\gamma \in \mathcal{L}_{-\lambda, \lambda}$, all the loops in $H_{2\lambda}$ that are encircled by γ belong to the same adjacency class.

It remains to prove that for any two different loops $\gamma_1, \gamma_2 \in \mathcal{L}_{-\lambda, \lambda}(h)$ and any two loops $\gamma_3, \gamma_4 \in H_{2\lambda}$ such that $O(\gamma_3) \subseteq O(\gamma_1)$ and $O(\gamma_4) \subseteq O(\gamma_2)$, γ_3 and γ_4 cannot be in the same adjacency class. It is enough to consider the case where γ_1 and γ_2 are adjacent. If γ_3 and γ_4 are in the same adjacency class, then there must exist two adjacent loops γ_5 and γ_6 in $H_{2\lambda}$ such that $O(\gamma_5) \subseteq O(\gamma_1)$ and $O(\gamma_6) \subseteq O(\gamma_2)$. However, neither $\gamma_5 \cap \gamma_1$ nor $\gamma_6 \cap \gamma_2$ contains any positive portion of the loops (see Lemma 6.13). Since $\gamma_5 \cap \gamma_6 \subseteq \gamma_1 \cap \gamma_2$, γ_5 and γ_6 cannot be adjacent, hence γ_3 and γ_4 are not in the same adjacency class. \square

Lemma 8.4. *Almost surely, for each $z \in \partial D$ and $\varepsilon > 0$, $B(z, \varepsilon)$ contains at least one λ -loop and one $-\lambda$ -loop in $\mathcal{L}_{-\lambda, \lambda}(h)$.*

Proof. We put down $N = O(2^{-n})$ points z_1, \dots, z_N on ∂D such that the union of $B(z_i, 2^{-n})$ covers ∂D . We choose these points independently of h . It suffices to show that for each i , $B(z_i, 2^{-n})$ a.s. contains at least one λ -loop and one $-\lambda$ -loop in $\mathcal{L}_{-\lambda, \lambda}(h)$. Indeed, upon showing this, the statement of the lemma holds for $\varepsilon = 2^{-n+3}$, and this is true for all $n \in \mathbb{N}$.

It suffices to show that $B(z_1, 2^{-n})$ a.s. contains at least one λ -loop and one $-\lambda$ -loop in $\mathcal{L}_{-\lambda, \lambda}(h)$. Let ζ be a 0-height level line of h from z_2 targeting z_1 , then ζ is part of $\mathbb{A}_{-\lambda, \lambda}(h)$, and ζ is distributed as a chordal SLE₄(-1, -1) from z_2 to z_1 in D . For $0 < t_1 < t_2$, we say that a subpath $\zeta([t_1, t_2])$ is an arc around z_1 if $\zeta(t_1) \in \partial D, \zeta(t_2) \in \partial D, \zeta([t_1, t_2]) \subseteq D$, and z_1, z_2 are in two different connected components of $D \setminus \zeta([t_1, t_2])$. Then ζ a.s. makes an infinite sequence of arcs around z_1 before reaching z_1 . Any two consecutive arcs that ζ makes around z_1 are of opposite directions, namely one arc encircles z_1 in a clockwise manner and the other arc in a counterclockwise manner. Moreover, since ζ is a continuous curve that goes to z_1 , there a.s. exist $0 < t_1 < t_2$ such that $\zeta([t_1, t_2])$ is an arc contained in $B(z_1, 2^{-n})$ which encircles z_1 in a clockwise manner. Then $\zeta([t_1, t_2])$ is part of a clockwise loop $\xi \in \mathcal{L}_{-\lambda, \lambda}^+(h)$ and $\xi \subseteq B(z_1, 2^{-n})$. Similarly, $B(z_1, 2^{-n})$ also contains at least one $-\lambda$ -loop in $\mathcal{L}_{-\lambda, \lambda}(h)$. \square

We are now ready to prove Proposition 8.1.

Proof of Proposition 8.1. Since $\Omega = \text{gask}(S \cup \tilde{S})$ is a thin local set of h with boundary values in $\{-2\lambda, 0, 2\lambda\}$, by Theorem 7.8, Ω is obtained by iterating $H_{2\lambda}$. Since $\Omega \neq \partial D$ (by Property 1 of Proposition 2.9), one has to do at least the first iteration, i.e., sample $H_{2\lambda}$. The $\pm 2\lambda$ -loops in $H_{2\lambda}$ all belong to $S \cup \tilde{S}$ and each 0-loop in $H_{2\lambda}$ either belongs to $S \cup \tilde{S}$ or is further split. Let γ be a 2λ -loop in $H_{2\lambda}$, and let ξ_1 be the loop in C which encircles γ , i.e., $O(\gamma) \subseteq O(\xi_1)$. Let ξ_2 be the loop in $\mathcal{L}_{-\lambda, \lambda}^+(h)$ which encircles γ . Our goal is to show that $\xi_1 = \xi_2$. Indeed, if this is true for any 2λ -loop (hence also for any -2λ -loop, by symmetry) in $H_{2\lambda}$, then it follows that $C = \mathcal{L}_{-\lambda, \lambda}(h)$. This further implies that $S \cup \tilde{S} = H_{2\lambda}$. Indeed, any 0-loop of $H_{2\lambda}$ cannot be further split, because otherwise the loops in C would encircle both 2λ -loops and -2λ -loops, which contradicts Property 2 of Proposition 2.9. This implies the proposition.

We now prove that $\xi_1 = \xi_2$. Let us first show that ξ_1 a.s. does not cross any 0-loop of $H_{2\lambda}$. For the sake of contradiction, suppose that with positive probability, there exists $\gamma_0 \in H_{2\lambda}$ with zero boundary condition, such that ξ_1 crosses γ_0 . In particular, $O(\gamma_0) \cap O(\xi_1) \neq \emptyset$ and $O(\gamma_0) \not\subseteq O(\xi_1)$. It follows that, in order to get Ω , we have to split γ_0 . Since ξ_1 crosses γ_0 , there exists $z \in \gamma_0$ and $\varepsilon > 0$ such that $B(z, \varepsilon) \subseteq O(\xi_1)$. When we split γ_0 once, we sample $H_{2\lambda}(h|_{O(\gamma_0)})$. The $\pm 2\lambda$ -loops in $\mathcal{L}(H_{2\lambda}(h|_{O(\gamma_0)}))$ belong to $S \cup \tilde{S}$, while the 0-loops can possibly be further split. Note that $H_{2\lambda}(h|_{O(\gamma_0)})$ is obtained by sampling two layers of $\mathcal{L}_{-\lambda, \lambda}$ in $O(\gamma_0)$. By Lemma 8.4, $B(z, \varepsilon)$ must contain at least one λ -loop and one $-\lambda$ -loop of $\mathcal{L}_{-\lambda, \lambda}(h|_{O(\gamma_0)})$. Each λ -loop (resp. $-\lambda$ -loop) of $\mathcal{L}_{-\lambda, \lambda}(h|_{O(\gamma_0)})$ further encircles infinitely many 2λ -loops (resp. -2λ -loop) of $H_{2\lambda}(h|_{O(\gamma_0)})$. Therefore, $B(z, \varepsilon)$ must contain at least one 2λ -loop and one -2λ -loop of S . In particular, ξ_1 must encircle at least one -2λ -loop of S , which is impossible due to Property 2 of Proposition 2.9. Therefore, we have proved that ξ_1 a.s. does not cross any 0-loop of $H_{2\lambda}$.

Recall (see the first paragraph of the proof) that the $\pm 2\lambda$ -loops in $H_{2\lambda}$ all belong to $S \cup \tilde{S}$. Therefore ξ_1 does not cross any $\pm 2\lambda$ -loop of $H_{2\lambda}$. Combined with the previous paragraph, we know that ξ_1 does not cross any loop in $H_{2\lambda}$. Let us further show that ξ_1 also cannot separate two adjacent loops in $H_{2\lambda}$, i.e., the two loops are either both contained in $\overline{O(\xi_1)}$, or are both disjoint from $O(\xi_1)$. Indeed, if ξ_1 separates two adjacent loops, then it must follow the interface between them. For any two adjacent loops in $H_{2\lambda}$, one of them must have inner boundary value $\pm 2\lambda$ and must belong to $S \subseteq B$. This implies that ξ_1 will coincide with a positive portion of a loop in B , which is ruled out by Property 4 of Proposition 2.9. It then follows that ξ_1 also cannot separate any two loops of $H_{2\lambda}$ in the same adjacency class. This implies $O(\xi_2) \subseteq O(\xi_1)$ by Lemma 8.3.

On the other hand, we must have $O(\xi_1) \subseteq O(\xi_2)$. If it is not the case, then there would exist $z \in \xi_2$ and $\varepsilon > 0$ such that $B(z, \varepsilon) \subseteq O(\xi_1)$. Note that $B(z, \varepsilon)$ must intersect $O(\xi_2)$ and another loop $\xi_3 \in \mathcal{L}_{-\lambda, \lambda}(h)$ which is adjacent to ξ_2 . Any two adjacent loops in $\mathcal{L}_{-\lambda, \lambda}(h)$ must have inner boundary conditions with opposite signs. Since ξ_2 is a λ -loop, ξ_3 is a $-\lambda$ -loop. By Lemma 8.4, $B(z, \varepsilon)$ contains at least one loop $\gamma_1 \in \mathcal{L}_{-\lambda, \lambda}^-(h^0|_{O(\xi_3)})$. Note that γ_1 is a -2λ -loop in $H_{2\lambda}$. Therefore $O(\xi_1)$ contains a -2λ -loop in S . This contradicts Property 2 of Proposition 2.9. Therefore, we also have $O(\xi_1) \subseteq O(\xi_2)$, hence $\xi_1 = \xi_2$. This completes the proof of the proposition. \square

8.2 Joint convergence of double random current and XOR-Ising interfaces with free boundary condition

In this section, we prove Theorem 2.8. Our proofs also contain a detailed description of the interactions between the nested XOR-Ising interfaces and the double random current cluster boundaries in the continuum.

Our proof makes use of the spatial Markov property of the so-called renewal loops.

Definition 8.5 (Renewal loop). *We call the loops in A_{nested} and $\tilde{S}_{\text{nested}}$ renewal loops.*

For each renewal loop ξ , the joint scaling limit of the interfaces in $O(\xi)$ and the height function $h^0|_{O(\xi)}$ is independent of the configuration outside of ξ and has the “same law” as the scaling limit of the interfaces in the original domain D . By “same law”, we mean that the former law can be obtained from the latter as the image under a conformal map from D onto $O(\xi)$. Indeed, Proposition 5.2 ensures that inside each renewal loop, the next layer of interfaces satisfies the same discrete properties as the outermost layer of interfaces. In Theorem 2.2 and Proposition 8.1, we have identified the law of the outermost interfaces as being conformally invariant. The same proof can be applied to the interfaces inside each renewal loop.

We point out that for the nested double random current clusters, the relation between their labels and spins is given by (5.9). Proposition 8.1 is stated for only the outermost double random current clusters. When we look at the configuration inside a renewal loop, Proposition 8.1 needs to be adapted according to the parity of the number of odd loops that encircle the renewal loop.

Proof of Theorem 2.8. In D^δ , we sample a double random current model with free boundary conditions, coupled with a XOR-Ising model with free boundary conditions according to Theorem 2.7. By Proposition 8.1, we know that $(C^\delta, s^\delta, S^\delta, \tilde{S}^\delta, \epsilon^\delta, B^\delta, A^\delta, h^\delta)$ converges in distribution to $(C, s, S, \tilde{S}, \epsilon, B, A, h)$.

Our first goal is to determine the outer boundaries of the outermost negative XOR-Ising clusters of Types 1 and 3 in Theorem 2.8. We will achieve this by successively *splitting* the level loops of h , as illustrated in Fig. 8.1. More precisely, we start by letting $U_0 := \{\partial D\}$. In the n -th step, suppose that we have defined U_n . To construct U_{n+1} , we will specify whether and how each loop γ in U_n is split. If γ is the outer boundary of an outermost negative XOR-Ising cluster, then we keep this loop, i.e. we write $V_\gamma := \{\gamma\}$. Otherwise, we split γ into a set $V_\gamma := \mathcal{L}_{-a,b}^-(h^0|_{O(\gamma)})$ for some well-chosen $a, b > 0$. We then let $U_{n+1} := \cup_{\gamma \in U_n} V_\gamma$. One can see by induction that for every $n \in \mathbb{N}$, $\text{gask}(U_n)$ is a thin local set of h , and for every loop γ in U_n , $h|_{O(\gamma)}$ is a GFF with constant boundary conditions.

By Proposition 8.1, the outer boundaries of the clusters of Types 1 and 2 are respectively given by $\mathcal{L}_{-\lambda,\lambda}^+(h)$ and $\mathcal{L}_{-\lambda,\lambda}^-(h)$. We split ∂D into $U_1 := \mathcal{L}_{-\lambda,\lambda}^-(h)$. The set $\mathcal{L}_{-\lambda,\lambda}^-(h)$ of loops are outer boundaries of negative XOR-Ising clusters, hence we will no longer split these loops. Each loop γ_1 in $\mathcal{L}_{-\lambda,\lambda}^+(h)$ is the outer boundary of a positive cluster of Type 1. We split γ_1 into $V_{\gamma_1} := \mathcal{L}_{-\lambda,\lambda}^-(h^0|_{O(\gamma_1)})$. By Proposition 8.1, we know that $\tilde{S}(\gamma_1) = \mathcal{L}_{-\lambda,\lambda}^-(h^0|_{O(\gamma_1)})$ is composed of renewal loops that have inner boundary condition 0. For each loop γ_2 in $\mathcal{L}_{-\lambda,\lambda}^-(h^0|_{O(\gamma_1)})$, the further layers of XOR-Ising and double random current interfaces in $O(\gamma_2)$ as well as their coupling with $h|_{O(\gamma_2)}$ will have the same law as the configuration inside

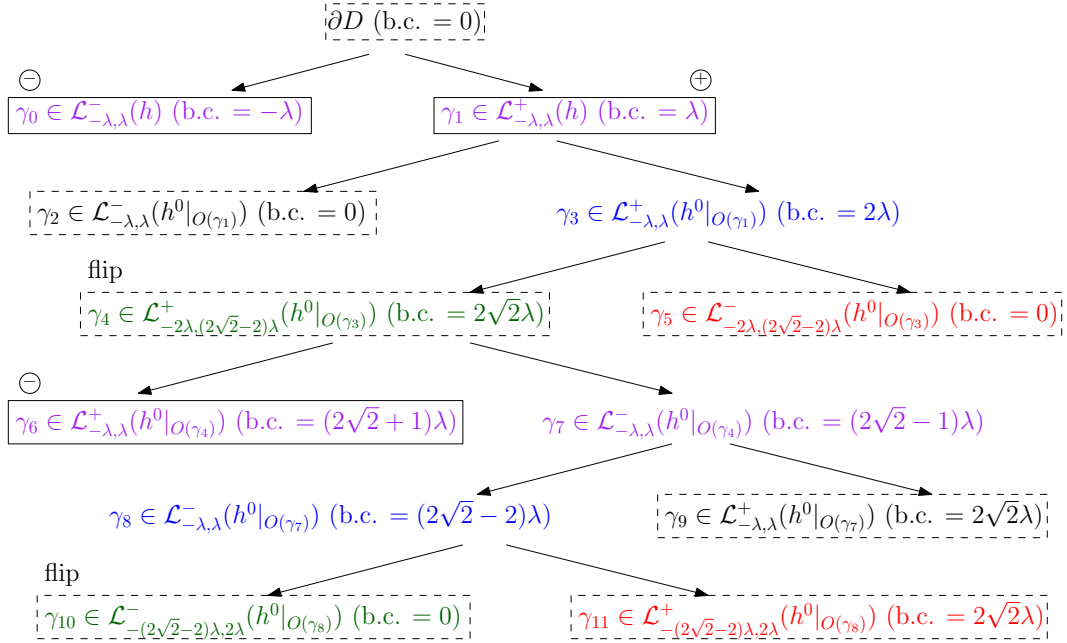


Figure 8.1: Successive splitting of the level loops. The loops inside plain frames are outer boundaries of outermost positive and negative XOR-Ising clusters in D . The purple color is to match the purple interfaces in Fig. 2.4. The blue color corresponds to the outer boundaries of the double random current clusters, as in Figures 2.2 and 2.4. The red and green colors correspond to the two types of holes of the double random current clusters as in Fig. 2.2. Each loop inside a dashed frame is a renewal loop.

D coupled with h (up to a conformal map). Therefore it is enough to understand what happens inside a loop γ_3 in $S(\gamma_3) = \mathcal{L}_{-\lambda,\lambda}^+(h^0|_{O(\gamma_3)})$.

Note that γ_3 represents the outer boundary of a double random current cluster with positive label. By Theorem 2.2, the holes of this double random current cluster are given by $\mathcal{L}_{-2\lambda,(2\sqrt{2}-2)\lambda}^-(h^0|_{O(\gamma_3)})$, and each of these loops are renewal loops. We split γ_3 into $\mathcal{L}_{-2\lambda,(2\sqrt{2}-2)\lambda}^-(h^0|_{O(\gamma_3)})$. The loops in $\mathcal{L}_{-2\lambda,(2\sqrt{2}-2)\lambda}^-(h^0|_{O(\gamma_3)})$ have inner boundary condition 0, hence the configuration of the XOR-Ising interfaces and the corresponding GFF inside it again has the same law as in D . Therefore, it is enough to understand what happens inside a loop γ_4 in $\mathcal{L}_{-2\lambda,(2\sqrt{2}-2)\lambda}^+(h^0|_{O(\gamma_3)})$.

Note that γ_4 is a renewal loop, so that in $O(\gamma_4)$, we have an independent double random current model coupled with a XOR-Ising model, both with free boundary conditions. Moreover, $h|_{O(\gamma_4)}$ is equal to $2\sqrt{2}\lambda$ plus a zero boundary GFF $h^0|_{O(\gamma_4)}$, so γ_4 is the boundary of an odd hole according to Theorem 2.2. Due to (5.9), the labels of the outermost double random current clusters encircled by γ_4 take opposite signs as their spins. Applying Proposition 8.1 by replacing $s(\gamma)$ by $-s(\gamma)$ in the statement, we can split γ_4 into $\mathcal{L}_{-\lambda,\lambda}^+(h^0|_{O(\gamma_4)})$. The outer boundaries of the outermost negative clusters in $O(\gamma_4)$ that are not encircled by any positive cluster in $O(\gamma_4)$ are given by $\mathcal{L}_{-\lambda,\lambda}^-(h^0|_{O(\gamma_4)})$. Each loop in $\mathcal{L}_{-\lambda,\lambda}^+(h^0|_{O(\gamma_4)})$ has inner boundary value $(2\sqrt{2}+1)\lambda$ and is the outer boundary of an outermost negative XOR-Ising cluster (the associated cluster is of Type 4), hence we no longer split these loops. The outer

boundaries of the outermost positive clusters in $O(\gamma_4)$ that are not encircled by any negative cluster in $O(\gamma_4)$ are given by $\mathcal{L}_{-\lambda,\lambda}^-(h^0|_{O(\gamma_4)})$. For each γ_7 in $\mathcal{L}_{-\lambda,\lambda}^-(h^0|_{O(\gamma_4)})$, let us continue to look for the next layer of negative XOR-Ising clusters in $O(\gamma_7)$.

For each γ_7 in $\mathcal{L}_{-\lambda,\lambda}^-(h^0|_{O(\gamma_4)})$, the distribution of the coupled models in $O(\gamma_7)$ is the same as in $O(\gamma_1)$, except that the labels of the double random current clusters in $O(\gamma_7)$ are flipped compared to the picture in $O(\gamma_1)$, since γ_7 is encircled by an odd hole γ_4 . Therefore, we can split γ_7 in the same way as we split γ_1 , but for a GFF with a flipped sign. More precisely, we split γ_7 into $\mathcal{L}_{-\lambda,\lambda}^-(h^0|_{O(\gamma_7)})$.

- The set $\mathcal{L}_{-\lambda,\lambda}^+(h^0|_{O(\gamma_7)})$ of loops all have the renewal property. Each loop γ_9 in the set $\mathcal{L}_{-\lambda,\lambda}^+(h^0|_{O(\gamma_7)})$ has boundary value $2\sqrt{2}\lambda$. The picture in $O(\gamma_9)$ has exactly the same law as that in $O(\gamma_4)$.
- The set $\mathcal{L}_{-\lambda,\lambda}^-(h^0|_{O(\gamma_7)})$ corresponds to the outer boundaries of the double random current clusters in $O(\gamma_7)$ which touch γ_7 . Each loop γ_8 in $\mathcal{L}_{-\lambda,\lambda}^-(h^0|_{O(\gamma_7)})$ is the outer boundary of a double random current cluster with minus label and positive spin.

We can again apply Theorem 2.2, but for a GFF with a flipped sign. The holes of the double random cluster with outer boundary γ_8 are given by $\mathcal{L}_{-(2\sqrt{2}-2)\lambda,2\lambda}(h^0|_{O(\gamma_8)})$. These sets of loops are renewal loops with inner boundary values 0 and $2\sqrt{2}\lambda$. Note that γ_{10} in $\mathcal{L}_{-(2\sqrt{2}-2)\lambda,2\lambda}^-(h^0|_{O(\gamma_8)})$ is again the boundary of an odd hole. By (5.9), the influence on the labels of the two odd holes γ_4 and γ_{10} are cancelled out, and the picture in $O(\gamma_{10})$ is the same as the picture in D . On the other hand, any loop γ_{11} in $\mathcal{L}_{-(2\sqrt{2}-2)\lambda,2\lambda}^-(h^0|_{O(\gamma_8)})$ is the boundary of an even hole so the influence of γ_4 remains. The picture inside γ_{11} is therefore the same as what we see in γ_4 .

By induction, this procedure will allow us to successively split ∂D , until we get a collection U_∞ of outer boundaries of outermost negative XOR-Ising clusters. The previous reasoning guarantees that for each loop γ in U_∞ , $h|_{O(\gamma)}$ has boundary value either $-\lambda$ or $(2\sqrt{2}+1)\lambda$. This implies that $\text{gask}(U_\infty)$ is a local set of h with boundary values in $\{-\lambda, (2\sqrt{2}+1)\lambda\}$, and it remains to prove that $\text{gask}(U_\infty)$ is thin. Note that at each finite step $n \in \mathbb{N}$, $\text{gask}(U_n)$ is a thin local set of h such that each loop in U_n has inner boundary value in $[-\lambda, (2\sqrt{2}+1)\lambda]$. By Lemma 6.17, we know that $\text{gask}(U_n) \subseteq \mathbb{A}_{-\lambda, (2\sqrt{2}+1)\lambda}$. Taking limits, we also have $\text{gask}(U_\infty) \subseteq \mathbb{A}_{-\lambda, (2\sqrt{2}+1)\lambda}$ which implies the thinness of $\text{gask}(U_n)$. Therefore $U_\infty = \mathcal{L}_{-\lambda, (2\sqrt{2}+1)\lambda}(h)$. This also implies that for γ_1 , the outermost negative clusters encircled by γ_1 are given by $\mathcal{L}_{-2\lambda, 2\sqrt{2}\lambda}(h^0|_{O(\gamma_1)})$.

In the above exploration process, we stop whenever we discover the outer boundary of an outermost negative cluster. However, this exploration can in fact be carried on indefinitely, and allows us to describe the nested XOR-Ising and double random current clusters. For example, for each γ_0 in $\mathcal{L}_{-\lambda,\lambda}^-(h)$ which is the outer boundary of a negative cluster, the next layer of outer boundaries of outermost positive clusters encircled by γ_0 is equal to $\mathcal{L}_{-2\sqrt{2}\lambda, 2\lambda}(h^0|_{O(\gamma_0)})$. This can be deduced, by symmetry, from how γ_1 in $\mathcal{L}_{-\lambda,\lambda}^+(h)$ is split. More generally, by induction and symmetry, we can show that

- if γ is the outer boundary of a positive XOR-Ising cluster and γ is surrounded by an even number of odd holes, or if γ is the outer boundary of a negative XOR-Ising cluster

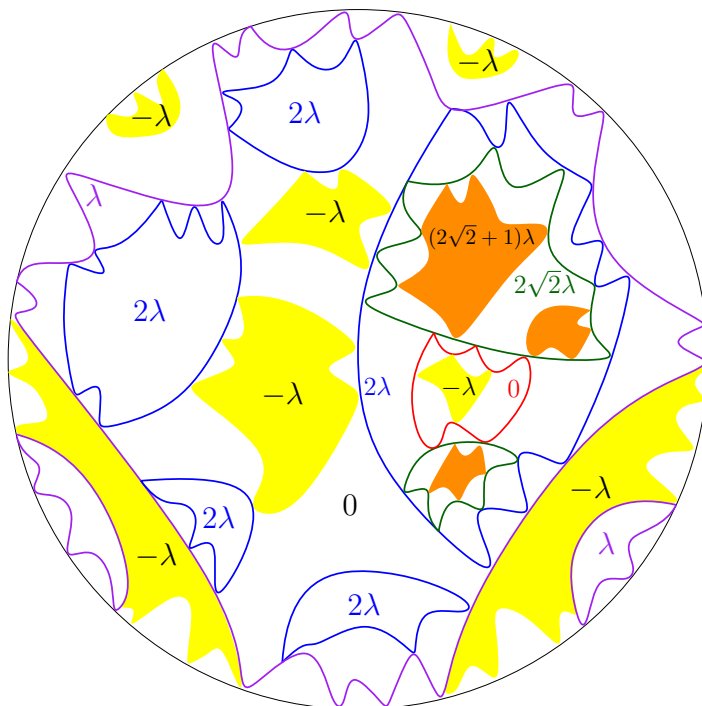


Figure 8.2: This is an illustration of the splitting process depicted in Fig. 8.1. We depict the interfaces of the XOR-Ising and double random current models with free boundary conditions in the same color code as in Figures 2.2 and 2.4. In addition, we also depict a few (filled) outermost negative XOR-Ising clusters (of Types 2 and 4) in yellow and dark orange. The yellow clusters have inner boundary value $-\lambda$ and the dark orange clusters have inner boundary value $(2\sqrt{2} + 1)\lambda$. The purple lines represent the interfaces in C . We depict in detail what happens inside a loop γ in C with λ inner boundary condition. The situation in a loop with $-\lambda$ inner boundary condition is symmetric.

As shown in Fig. 2.4, γ can be split into 2λ -loops and 0 -loops. The 2λ -loops are part of the CLE_4 and are depicted in blue, just as in Fig. 2.2. Inside the 0 -loops, we again have an independent XOR-Ising with free boundary conditions, so that some of its outermost negative clusters are depicted in yellow, and has $-\lambda$ boundary condition. Inside the 2λ -loops, we can carry out the decomposition as described in Fig. 2.2. We depict the $2\sqrt{2}\lambda$ -holes in green, and the 0 -holes in red. Inside a 0 -hole (which is an even hole), we do the same thing as in the original domain, and obtain (among other things) outermost negative clusters with $-\lambda$ boundary condition, also depicted in yellow. Inside a $2\sqrt{2}\lambda$ -hole (which is an odd hole), we again have an independent XOR-Ising model with free boundary conditions, but the labels of the clusters in this hole have an additional -1 factor given their spins. This leads to (filled) outermost negative clusters depicted in dark orange which have $(2\sqrt{2} + 1)\lambda$ inner boundary value.

and γ is surrounded by an odd number of odd holes, then the next layer of outermost positive XOR-Ising clusters in $O(\gamma)$ is distributed as $\mathcal{L}_{-2\lambda, 2\sqrt{2}\lambda}(h^0|_{O(\gamma)})$;

- if γ is the outer boundary of a negative XOR-Ising cluster and γ is surrounded by an even number of odd holes, or if γ is the outer boundary of a positive XOR-Ising cluster and γ is surrounded by an odd number of odd holes, then the next layer of outermost positive XOR-Ising clusters in $O(\gamma)$ is distributed as $\mathcal{L}_{-2\sqrt{2}\lambda, 2\lambda}(h^0|_{O(\gamma)})$.

This completes the proof of Theorem 2.8. \square

8.3 XOR-Ising with plus/plus boundary condition

Let us prove Theorem 2.10 which implies Theorem 1.5.

Proof of Theorem 2.10. We consider the coupling described in Theorem 2.7 and we stay on the dual square lattice throughout the proof. In this coupling, given the double random current model with wired boundary conditions, we can obtain an XOR-Ising model with plus/plus boundary condition by assigning the + spin to the outermost cluster, and then assigning i.i.d. spins to all the other clusters. As a consequence, the outermost negative XOR-Ising clusters are given by the outermost negative XOR-Ising clusters inside each hole of the outermost double random current cluster.

Theorem 2.4 states that the boundaries of the holes of the outermost double random current cluster are distributed as $\mathcal{L}_{-\sqrt{2}\lambda, \sqrt{2}\lambda}(h)$. On the other hand, conditionally on the outermost double random current cluster, in each of its holes, we have an independent double random current model, coupled with an XOR-Ising model, both with free boundary conditions, and a height function, just like on the primal lattice in the original domain. This spatial Markov property in the discrete transforms to the continuum limit (Proposition 5.3). Consequently, for each γ in $\mathcal{L}_{-\sqrt{2}\lambda, \sqrt{2}\lambda}(h)$, we can apply the same proof as that of Theorem 2.8. If γ has inner boundary value $\sqrt{2}\lambda$, then it is the scaling limit of an odd hole, and the outermost negative XOR-Ising clusters in $O(\gamma)$ is distributed as $\mathcal{L}_{-(2\sqrt{2}+1)\lambda, \lambda}(h^0|_{O(\gamma)})$. If γ has inner boundary value $-\sqrt{2}\lambda$, then it is the scaling limit of an even hole, and the outermost negative XOR-Ising clusters in $O(\gamma)$ is distributed as $\mathcal{L}_{-\lambda, (2\sqrt{2}+1)\lambda}(h^0|_{O(\gamma)})$. This implies that the outermost negative XOR-Ising clusters in D is distributed as $\mathcal{L}_{-(\sqrt{2}+1)\lambda, (\sqrt{2}+1)\lambda}(h)$.

The law of the nested layers of interfaces also follows from the spatial Markov property and the proof of Theorem 2.8. In particular, the two bullet points at the end of the proof of Theorem 2.8 also hold for the dual XOR-Ising model (one needs to look at dual clusters and dual holes instead of primal ones). This completes the proof of Theorem 2.10. \square

8.4 Asymptotic behavior of the number of loops

Let us now prove two lemmata which will lead to the asymptotic numbers of loops (or clusters) in the XOR-Ising and double random current models that surround the origin.

Lemma 8.6. *Fix $a, b > 0$ with $a + b \geq 2\lambda$. Let $N(\varepsilon)$ be the number of loops in the nested $\mathcal{L}_{-a, b}$ in the unit disk surrounding 0 whose conformal radii w.r.t. the origin are at least ε . Then*

$$N(\varepsilon)/\log(\varepsilon^{-1}) \xrightarrow{\varepsilon \rightarrow 0} 4\lambda^2/(ab\pi^2) \quad a.s.$$

Proof. Let R be the difference in log conformal radii between two successive $\mathcal{L}_{-a,b}$ loops that encircle the origin. We know by [8, Proposition 20] that R is equal to the exit time of a standard Brownian motion from the interval $[-a\pi/(2\lambda), b\pi/(2\lambda)]$. The n -th loop which encircles the origin has log conformal radius equal to $-S_n$ where $S_n := -(R_1 + \dots + R_n)$ and R_i are i.i.d. random variables distributed like R . Then $N(\varepsilon)$ is the smallest $n \geq 1$ such that $S_{n+1} \geq \log(\varepsilon^{-1})$. By the law of large numbers, we know that S_n/n converges to $\mathbb{E}(R)$ a.s. as $n \rightarrow \infty$. Since $N(\varepsilon) \rightarrow \infty$ as $\varepsilon \rightarrow 0$, we also have that

$$S_{N(\varepsilon)+1}/(N(\varepsilon) + 1) \rightarrow \mathbb{E}(R) \text{ a.s. as } \varepsilon \rightarrow 0.$$

Note that $\log(\varepsilon^{-1}) \leq S_{N(\varepsilon)+1} \leq \log(\varepsilon^{-1}) + R_{N(\varepsilon)}$. It follows that

$$\lim_{\varepsilon \rightarrow 0} \log(\varepsilon^{-1})/N(\varepsilon) = \mathbb{E}(R) = ab\pi^2/(4\lambda^2).$$

The inverse of the above equation proves the lemma. \square

Lemma 8.7. *In the scaling limit of the double random current model in the unit disk (with either the free or wired boundary conditions), let $N(\varepsilon)$ be the number of clusters surrounding the origin such that their outer boundaries have a conformal radius w.r.t. the origin at least ε . Then*

$$N(\varepsilon)/\log(\varepsilon^{-1}) \xrightarrow{\varepsilon \rightarrow 0} 1/(\sqrt{2}\pi^2).$$

Proof. By Theorems 1.6 and 1.7 and [8, Proposition 20], we know that the difference of log conformal radii between the outer boundaries of two successive double random current clusters that encircle the origin is given by $T_1 + T_2$, where T_1 is the first time that a standard Brownian motion exits $[-\pi, (\sqrt{2} - 1)\pi]$ and T_2 is the first time that a standard Brownian motion exits $[-\pi, \pi]$. We have

$$\mathbb{E}(T_1 + T_2) = (\sqrt{2} - 1)\pi^2 + \pi^2 = \sqrt{2}\pi^2.$$

This implies the result of the present lemma, by the same argument as in the proof of the previous lemma. \square

References

- [1] M. Aizenman, *Geometric analysis of φ^4 fields and Ising models. I, II*, Comm. Math. Phys. **86** (1982), no. 1, 1–48.
- [2] M. Aizenman, D. J. Barsky, and R. Fernández, *The phase transition in a general class of Ising-type models is sharp*, J. Statist. Phys. **47** (1987), no. 3-4, 343–374.
- [3] M. Aizenman and A. Burchard, *Hölder regularity and dimension bounds for random curves*, Duke mathematical journal **99** (1999), no. 3, 419–453.
- [4] M. Aizenman and H. Duminil-Copin, *Marginal triviality of the scaling limits of critical 4D Ising and ϕ_4^4 models*, Annals of Mathematics **194** (2021), 163–235.
- [5] M. Aizenman, H. Duminil-Copin, and V. Sidoravicius, *Random Currents and Continuity of Ising Model’s Spontaneous Magnetization*, Communications in Mathematical Physics **334** (2015), 719–742.
- [6] M. Aizenman, H. Duminil-Copin, V. Tassion, and S. Warzel, *Emergent planarity in two-dimensional ising models with finite-range interactions*, Inventiones mathematicae **216** (2019), no. 3, 661–743.

- [7] J. Aru and A. Sepúlveda, *Two-valued local sets of the 2D continuum Gaussian free field: connectivity, labels, and induced metrics*, Electron. J. Probab. **23** (2018), Paper No. 61, 35.
- [8] J. Aru, A. Sepúlveda, and W. Werner, *On bounded-type thin local sets of the two-dimensional Gaussian Free Field*, J. Inst. Math. Jussieu **18** (2019), no. 3, 591–618.
- [9] M. Basok and D. Chelkak, *Tau-functions a la Dubédat and probabilities of cylindrical events for double-dimers and CLE (4)*, arXiv:1809.00690 (2018).
- [10] S. Benoist and C. Hongler, *The scaling limit of critical Ising interfaces is CLE_3* , The Annals of Probability **47** (2019), no. 4, 2049–2086.
- [11] C. Boutillier and B. de Tilière, *Height representation of XOR-Ising loops via bipartite dimers*, Electron. J. Probab. **19** (2014), no. 80, 33.
- [12] T. van de Brug, F. Camia, and M. Lis, *Random walk loop soups and conformal loop ensembles*, Probability Theory and Related Fields **166** (2016), no. 1, 553–584.
- [13] D. Chelkak, *Planar Ising model at criticality: state-of-the-art and perspectives*, Proceedings of the International Congress of Mathematicians (ICM 2018), 2019, pp. 2801–2828.
- [14] D. Chelkak, H. Duminil-Copin, and C. Hongler, *Crossing probabilities in topological rectangles for the critical planar FK-Ising model*, Electronic Journal of Probability **21** (2016).
- [15] D. Chelkak, H. Duminil-Copin, C. Hongler, A. Kemppainen, and S. Smirnov, *Convergence of Ising interfaces to Schramm’s SLE curves*, Comptes Rendus Mathématique **352** (2014), no. 2, 157–161.
- [16] D. Chelkak, *Ising model and s -embeddings of planar graphs*, arXiv:2006.14559 (2020).
- [17] D. Chelkak, D. Cimasoni, and A. Kassel, *Revisiting the combinatorics of the 2D Ising model*, 2015. to appear in Ann. Inst. Henri Poincaré Comb. Phys. Interact.
- [18] D. Chelkak, C. Hongler, and K. Izyurov, *Conformal invariance of spin correlations in the planar Ising model*, Ann. of Math. (2) **181** (2015), no. 3, 1087–1138.
- [19] D. Chelkak and S. Smirnov, *Universality in the 2D Ising model and conformal invariance of fermionic observables*, Invent. Math. **189** (2012), no. 3, 515–580.
- [20] D. Cimasoni and H. Duminil-Copin, *The critical temperature for the Ising model on planar doubly periodic graphs*, Electron. J. Probab **18** (2013), no. 44, 1–18.
- [21] B. de Tilière, *Scaling limit of isoradial dimer models and the case of triangular quadri-tilings*, Annales de l’Institut Henri Poincaré (B) Probability and Statistics **43** (2007), no. 6, 729–750.
- [22] J. Dubédat, *Exact bosonization of the Ising model*, 2011. arXiv:1112.4399.
- [23] J. Dubédat, *Double dimers, conformal loop ensembles and isomonodromic deformations*, Journal of the European Mathematical Society **21** (2018), no. 1, 1–54.
- [24] J. Dubédat, *SLE and the free field: partition functions and couplings*, J. Amer. Math. Soc. **22** (2009), no. 4, 995–1054.
- [25] H. Duminil-Copin, *Lectures on the Ising and Potts models on the hypercubic lattice*. arXiv:1707.00520.
- [26] H. Duminil-Copin, *Random currents expansion of the Ising model*, 2016. arXiv:1607:06933.
- [27] H. Duminil-Copin and M. Lis, *On the double random current nesting field*, Probability Theory and Related Fields **175** (2019), no. 3-4, 937–955.
- [28] H. Duminil-Copin, M. Lis, and W. Qian, *Conformal invariance of double random currents and the XOR-Ising model II: tightness and properties in the discrete* (2021). preprint.
- [29] H. Duminil-Copin, S. Goswami, and A. Raoufi, *Exponential decay of truncated correlations for the Ising model in any dimension for all but the critical temperature*, Communications in Mathematical Physics **374** (2020), no. 2, 891–921.
- [30] H. Duminil-Copin, C. Hongler, and P. Nolin, *Connection probabilities and RSW-type bounds for the two-dimensional FK Ising model*, Communications on pure and applied mathematics **64** (2011), no. 9, 1165–1198.
- [31] H. Duminil-Copin, V. Sidoravicius, and V. Tassion, *Continuity of the Phase Transition for Planar Random-Cluster and Potts Models with $1 \leq q \leq 4$* , Communications in Mathematical Physics **349** (2017), no. 1, 47–107.

- [32] H. Duminil-Copin, I. Manolescu, and V. Tassion, *Planar random-cluster model: fractal properties of the critical phase*, arXiv:2007.14707 (2020).
- [33] H. Duminil-Copin and V. Tassion, *A new proof of the sharpness of the phase transition for Bernoulli percolation and the Ising model*, Communications in Mathematical Physics **343** (2016), no. 2, 725–745.
- [34] R. G. Edwards and A. D. Sokal, *Generalization of the Fortuin-Kasteleyn-Swendsen-Wang representation and Monte Carlo algorithm*, Phys. Rev. D **38** (1988), 2009–2012, DOI 10.1103/PhysRevD.38.2009.
- [35] A. Giuliani, V. Mastropietro, and F. Toninelli, *Height fluctuations in non-integrable classical dimers*, EPL (Europhysics Letters) **109** (2015), no. 6, 60004.
- [36] R. B. Griffiths, C. A. Hurst, and S. Sherman, *Concavity of Magnetization of an Ising Ferromagnet in a Positive External Field*, Journal of Mathematical Physics **11** (1970), no. 3, 790–795.
- [37] C. Hongler, *Conformal Invariance of Ising Model Correlations*, Ph.D. Thesis, 2010.
- [38] C. Hongler and S. Smirnov, *The energy density in the planar Ising model*, Acta Math. **211** (2013), no. 2, 191–225.
- [39] L. P. Kadanoff and H. Ceva, *Determination of an operator algebra for the two-dimensional Ising model*, Physical Review B **3** (1971), no. 11, 3918.
- [40] P. Kasteleyn, *The statistics of dimers on a lattice. I. The number of dimer arrangements on a quadratic lattice*, Physica **27** (1961), 1209–1225.
- [41] A. Kemppainen and S. Smirnov, *Random curves, scaling limits and Loewner evolutions*, The Annals of Probability **45** (2017), no. 2, 698–779.
- [42] A. Kemppainen and W. Werner, *The nested simple conformal loop ensembles in the Riemann sphere*, Probab. Theory Related Fields **165** (2016), no. 3–4, 835–866, DOI 10.1007/s00440-015-0647-3.
- [43] R. Kenyon, *Conformal invariance of domino tiling*, Ann. Probab. **28** (2000), no. 2, 759–795.
- [44] ———, *Dominos and the Gaussian free field*, Ann. Probab. **29** (2001), no. 3, 1128–1137.
- [45] ———, *The Laplacian and Dirac operators on critical planar graphs*, Inventiones mathematicae **150** (2002), no. 2, 409–439.
- [46] ———, *Conformal Invariance of Loops in the Double-Dimer Model*, Communications in Mathematical Physics **326** (2014Mar), no. 2, 477–497.
- [47] R. W. Kenyon, J. G. Propp, and D. B. Wilson, *Trees and matchings*, Electron. J. Combin. **7** (2000), Research Paper 25, 34. MR1756162
- [48] R. W. Kenyon and S. Sheffield, *Dimers, tilings and trees*, Journal of Combinatorial Theory, Series B **92** (2004), no. 2, 295–317. Special Issue Dedicated to Professor W.T. Tutte.
- [49] G. F. Lawler, O. Schramm, and W. Werner, *Conformal invariance of planar loop-erased random walks and uniform spanning trees*, Ann. Probab. **32** (2004), no. 1B, 939–995.
- [50] G. F. Lawler, O. Schramm, and W. Werner, *Conformal restriction: the chordal case*, J. Amer. Math. Soc. **16** (2003), no. 4, 917–955 (electronic).
- [51] M. Lis, *On Boundary Correlations in Planar Ashkin–Teller Models*, International Mathematics Research Notices, posted on 2021, DOI 10.1093/imrn/rnaa380. rnaa380.
- [52] M. Lis, *Spins, percolation and height functions*, 2019. arXiv:1909.07351.
- [53] M. Lis, *The planar Ising model and total positivity*, J. Stat. Phys. **166** (2017), no. 1, 72–89.
- [54] T. Lupu, *Convergence of the two-dimensional random walk loop-soup clusters to CLE*, Journal of the European Mathematical Society **21** (2018), no. 4, 1201–1227.
- [55] T. Lupu and W. Werner, *A note on Ising random currents, Ising-FK, loop-soups and the Gaussian free field*, Electron. Commun. Probab. **21** (2016), 7 pp.
- [56] J. Miller and S. Sheffield, *CLE(4) and the Gaussian Free Field*, In preparation.
- [57] ———, *Imaginary geometry I: interacting SLEs*, Probab. Theory Related Fields **164** (2016), no. 3–4, 553–705.
- [58] ———, *Imaginary geometry II: Reversibility of SLE $_{\kappa}(\rho_1; \rho_2)$ for $\kappa \in (0, 4)$* , Ann. Probab. **44** (2016), no. 3, 1647–1722.

- [59] ———, *Imaginary geometry III: reversibility of SLE_κ for $\kappa \in (4, 8)$* , *Ann. of Math. (2)* **184** (2016), no. 2, 455–486.
- [60] ———, *Imaginary geometry IV: interior rays, whole-plane reversibility, and space-filling trees*, *Probab. Theory Related Fields* **169** (2017), no. 3-4, 729–869.
- [61] J. Miller, S. Sheffield, and W. Werner, *CLE percolations*, *Forum Math. Pi* **5** (2017), e4, 102.
- [62] J. Miller, S. Watson, and D. B. Wilson, *Extreme nesting in the conformal loop ensemble*, *Ann. Probab.* **44** (2016), no. 2, 1013–1052.
- [63] E. Powell and H. Wu, *Level lines of the Gaussian free field with general boundary data*, *Ann. Inst. Henri Poincaré Probab. Stat.* **53** (2017), no. 4, 2229–2259.
- [64] W. Qian and W. Werner, *Coupling the Gaussian free fields with free and with zero boundary conditions via common level lines*, *Comm. Math. Phys.* **361** (2018), no. 1, 53–80.
- [65] A. Raoufi, *Translation-invariant Gibbs states of the Ising model: General setting*, *The Annals of Probability* **48** (2020), no. 2, 760 – 777.
- [66] M. Russkikh, *Dominos in hedgehog domains*, *Annales de l’Institut Henri Poincaré D* **8** (2020), no. 1, 1–33.
- [67] L. Schoug, A. Sepúlveda, and F. Viklund, *Dimensions of Two-Valued Sets via Imaginary Chaos*, *International Mathematics Research Notices*, posted on 2020, DOI 10.1093/imrn/rnaa250. rnaa250.
- [68] O. Schramm, *Scaling limits of loop-erased random walks and uniform spanning trees*, *Israel J. Math.* **118** (2000), 221–288.
- [69] O. Schramm and S. Sheffield, *Contour lines of the two-dimensional discrete Gaussian free field*, *Acta Math.* **202** (2009), no. 1, 21–137.
- [70] ———, *A contour line of the continuum Gaussian free field*, *Probab. Theory Related Fields* **157** (2013), no. 1-2, 47–80.
- [71] A. Sepúlveda, *On thin local sets of the Gaussian free field*, *Ann. Inst. Henri Poincaré Probab. Stat.* **55** (2019), no. 3, 1797–1813.
- [72] O. Schramm and S. Sheffield, *Harmonic explorer and its convergence to SLE_4* , *The Annals of Probability* **33** (2005), no. 6, 2127–2148.
- [73] O. Schramm and D. B. Wilson, *SLE coordinate changes*, *New York J. Math.* **11** (2005), 659–669.
- [74] S. Sheffield, *Exploration trees and conformal loop ensembles*, *Duke Math. J.* **147** (2009), no. 1, 79–129.
- [75] S. Sheffield and W. Werner, *Conformal loop ensembles: the Markovian characterization and the loop-soup construction*, *Ann. of Math. (2)* **176** (2012), no. 3, 1827–1917.
- [76] S. Smirnov, *Critical percolation in the plane: conformal invariance, Cardy’s formula, scaling limits*, *Comptes Rendus de l’Académie des Sciences-Series I-Mathematics* **333** (2001), no. 3, 239–244.
- [77] ———, *Conformal invariance in random cluster models. I. Holomorphic fermions in the Ising model*, *Ann. of Math. (2)* **172** (2010), no. 2, 1435–1467.
- [78] S. Rohde and O. Schramm, *Basic properties of SLE* , *Ann. of Math. (2)* **161** (2005), no. 2, 883–924.
- [79] H. N. V. Temperley, *Combinatorics: Being the proceedings of the conference on combinatorial mathematics held at the mathematical institute, 1972*, pp. 356–357.
- [80] H. Whitney, *On regular closed curves in the plane*, *Compositio Mathematica* **4** (1937), 276–284.
- [81] D. B. Wilson, *XOR-Ising loops and the Gaussian free field*, arXiv:1102.3782.